

MONSOONAL NORTH
CLUSTER REPORT



PROJECTIONS
FOR AUSTRALIA'S NRM REGIONS



Australian Government
Department of the Environment
Bureau of Meteorology

-20° -10° 0° 10° 20° 30° 40° 50°



-20° -10° 0° 10° 20° 30° 40° 50°



MONSOONAL NORTH
CLUSTER REPORT



PROJECTIONS
FOR AUSTRALIA'S NRM REGIONS

-20° -10° 0° 10° 20° 30° 40° 50°

© CSIRO 2015

CLIMATE CHANGE IN AUSTRALIA PROJECTIONS CLUSTER REPORT – MONSOONAL NORTH

ISBN

Print: 978-1-4863-0422-6

Online: 978-1-4863-0423-3

CITATION

Moise, A. *et al.* 2015, *Monsoonal North Cluster Report*, Climate Change in Australia Projections for Australia's Natural Resource Management Regions: Cluster Reports, eds. Ekström, M. *et al.*, CSIRO and Bureau of Meteorology, Australia.

CONTACTS

E: enquiries@csiro.au

T: 1300 363 400

ACKNOWLEDGEMENTS

Lead Author – Aurel Moise.

Contributing Authors – Debbie Abbs, Jonas Bhend, Francis Chiew, John Church, Marie Ekström, Dewi Kirono, Andrew Lenton, Chris Lucas, Kathleen McInnes, Didier Monselesan, Freddie Mpelasoka, Leanne Webb and Penny Whetton.

Editors – Marie Ekström, Penny Whetton, Chris Gerbing, Michael Grose, Leanne Webb and James Risbey.

Additional acknowledgements – Janice Bathols, Tim Bedin, John Clarke, Clement Davis, Tim Erwin, Craig Heady, Peter Hoffman, Jack Katzfey, Julian O'Grady, Tony Rafter, Surendra Rauniyar, Rob Smalley, Bertrand Timbal, Yang Wang, Ian Watterson, and Louise Wilson.

Project coordinators – Kevin Hennessy, Paul Holper and Mandy Hopkins.

Design and editorial support – Alicia Annable, Siobhan Duffy, Liz Butler, and Peter Van Der Merwe.

We gratefully acknowledge the assistance of Andrew Tait, Michael Hutchinson and David Karoly.

We acknowledge the World Climate Research Programme's Working Group on Coupled Modelling, which is responsible for CMIP, and we thank the climate modelling groups for producing and making available their model output. For CMIP the U.S. Department of Energy's Program for Climate Model Diagnosis and Intercomparison provides coordinating support and led development of software infrastructure in partnership with the Global Organization for Earth System Science Portals.

COPYRIGHT AND DISCLAIMER

© 2015 CSIRO and the Bureau of Meteorology. To the extent permitted by law, all rights are reserved and no part of this publication covered by copyright may be reproduced or copied in any form or by any means except with the written permission of CSIRO and the Bureau of Meteorology.

IMPORTANT DISCLAIMER

CSIRO and the Bureau of Meteorology advise that the information contained in this publication comprises general statements based on scientific research. The reader is advised and needs to be aware that such information may be incomplete or unable to be used in any specific situation. No reliance or actions must therefore be made on that information without seeking prior expert professional, scientific and technical advice. To the extent permitted by law, CSIRO and the Bureau of Meteorology (including their employees and consultants) exclude all liability to any person for any consequences, including but not limited to all losses, damages, costs, expenses and any other compensation, arising directly or indirectly from using this publication (in part or in whole) and any information or material contained in it.

This report has been printed on ecoStar, a recycled paper made from 100% post-consumer waste.



TABLE OF CONTENTS

PREFACE	2
EXECUTIVE SUMMARY	4
1 THE MONSOONAL NORTH CLUSTER	7
2 CLIMATE OF MONSOONAL NORTH.....	8
3 SIMULATING REGIONAL CLIMATE	11
4 THE CHANGING CLIMATE OF THE MONSOONAL NORTH	13
4.1 Ranges of projected climate change and confidence in projections.....	14
4.2 Temperature.....	15
4.2.1 Extremes	21
4.3 Rainfall	23
4.3.1 Heavy rainfall events	26
4.3.2 Drought	26
4.4 Winds, storms and weather systems	27
4.4.1 Mean winds.....	27
4.4.2 Extreme winds	28
4.4.3 Tropical cyclones.....	28
4.5 Solar radiation	29
4.6 Relative humidity.....	29
4.7 Potential evapotranspiration	29
4.8 Soil moisture and runoff	30
4.9 Fire weather	30
4.10 Marine Projections	32
4.10.1 Sea Level	32
4.10.2 Sea surface temperatures, salinity and acidification.....	33
4.11 Other projection material for the cluster	34
5 APPLYING THE REGIONAL PROJECTIONS IN ADAPTATION PLANNING.....	35
5.1 Identifying future climate scenarios	35
5.2 Developing climate scenarios using the Climate Futures tool.....	36
REFERENCES.....	39
APPENDIX.....	42
ABBREVIATIONS	47
NRM GLOSSARY OF TERMS	48

PREFACE

Australia's changing climate represents a significant challenge to individuals, communities, governments, businesses and the environment. Australia has already experienced increasing temperatures, shifting rainfall patterns and rising oceans.

The Intergovernmental Panel on Climate Change (IPCC) *Fifth Assessment Report* (IPCC, 2013) rigorously assessed the current state and future of the global climate system. The report concluded that:

- greenhouse gas emissions have markedly increased as a result of human activities
- human influence has been detected in warming of the atmosphere and the ocean, in changes in the global water cycle, in reductions in snow and ice, in global mean sea level rise, and in changes in some climate extremes
- it is extremely likely that human influence has been the dominant cause of the observed warming since the mid-20th century
- continued emissions of greenhouse gases will cause further warming and changes in all components of the climate system.

In recognition of the impact of climate change on the management of Australia's natural resources, the Australian Government developed the Regional Natural Resource Management Planning for Climate Change Fund. This fund has enabled significant research into the impact of the future climate on Australia's natural resources, as well as adaptation opportunities for protecting and managing our land, soil, water, plants and animals.

Australia has 54 natural resource management (NRM) regions, which are defined by catchments and bioregions. Many activities of organisations and ecosystem services within the NRM regions are vulnerable to impacts of climate change.

For this report, these NRM regions are grouped into 'clusters', which largely correspond to the broad-scale climate and biophysical regions of Australia (Figure A). The clusters are diverse in their history, population, resource base, geography and climate. Therefore, each cluster has a unique set of priorities for responding to climate change.

CSIRO and the Australian Bureau of Meteorology have prepared tailored climate change projection reports for each NRM cluster. These projections provide guidance on the changes in climate that need to be considered in planning.

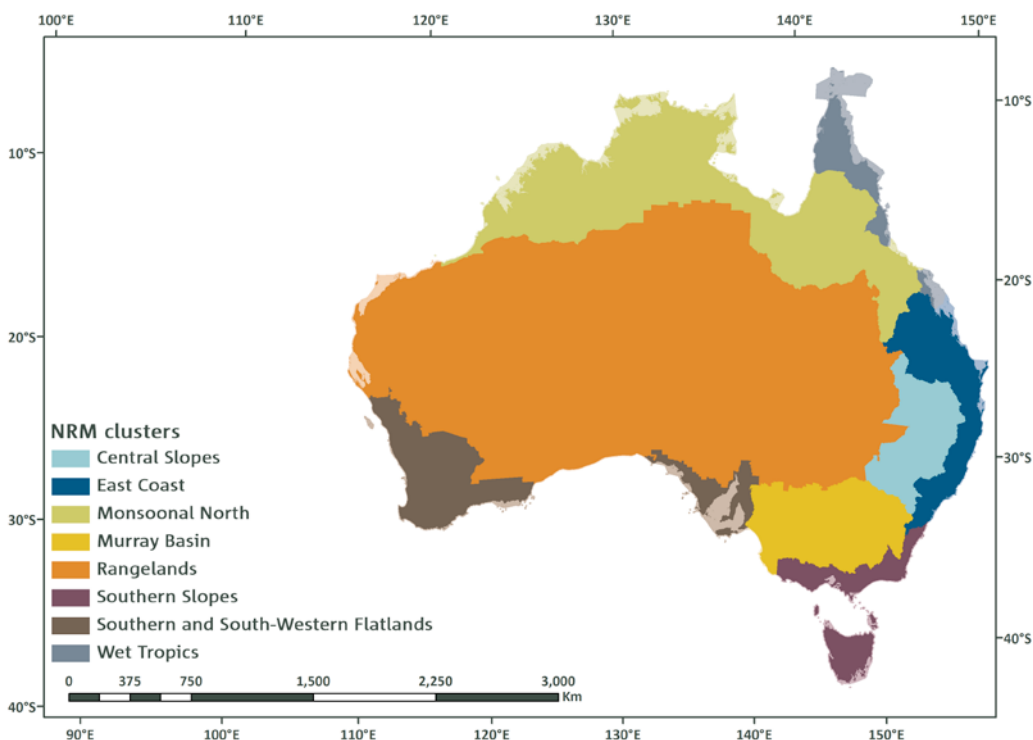


FIGURE A: THE EIGHT NATURAL RESOURCE MANAGEMENT (NRM) CLUSTERS

This is the regional projections report for the Monsoonal North cluster. This document provides projections in a straightforward and concise format with information about the cluster as a whole, as well as additional information at finer scales where appropriate.

This cluster report is part of a suite of products. These include a brochure for each cluster that provides the key projection statements in a brief format. There is also the Australian climate change projections Technical Report, which describes the underlying scientific basis for the climate change projections. Box 1 describes all supporting products.

This report provides the most up to date, comprehensive and robust information available for this part of Australia, and draws on both international and national data resources and published peer-reviewed literature.

The projections in this report are based on the outputs of sophisticated global climate models (GCMs). GCMs are based on the laws of physics, and have been developed over many years in numerous centres around the world. These models are rigorously tested for their ability to reproduce past climate. The projections in this report primarily use output from the ensemble of model simulations brought together for the Coupled Model Inter-comparison Project phase 5 (CMIP5) (Taylor *et al.*, 2012), where phase 5 is the most recent comparison of model simulations addressing, amongst other things, projections of future climates. In this report, outputs from GCMs in the CMIP5 archive are complemented by regional climate modelling and statistical downscaling.

BOX 1: CLIMATE CHANGE IN AUSTRALIA – PRODUCTS

This report is part of a suite of Climate Change in Australia (CCIA) products prepared as part of the Australian Government's Regional Natural Resource Management Planning for Climate Change Fund. These products provide information on climate change projections and their application.

CLUSTER BROCHURES

Purpose: Key regional messages for everyone

A set of brochures that summarise key climate change projections for each of the eight clusters. The brochures are a useful tool for community engagement.

CLUSTER REPORTS

Purpose: Regional detail for planners and decision makers

The cluster reports are to assist regional decision-makers in understanding the important messages deduced from climate change projection modelling. The cluster reports present a range of emissions scenarios across multiple variables and years. They also include relevant sub-cluster level information in cases where distinct messages are evident in the projections.

TECHNICAL REPORT

Purpose: Technical information for researchers and decision-makers

A comprehensive report outlining the key climate change projection messages for Australia across a range of variables. The report underpins all information found in other products. It contains an extensive set of figures and descriptions on recent Australian climate trends, global climate change science, climate model evaluation processes, modelling methodologies and downscaling approaches. The report includes a chapter describing how to use climate change data in risk assessment and adaptation planning.

WEBSITE

URL: www.climatechangeinaustralia.gov.au

Purpose: One stop shop for products, data and learning

The CCIA website is for Australians to find comprehensive information about the future climate. This includes some information on the impacts of climate change that communities, including the natural resource management sector, can use as a basis for future adaptation planning. Users can interactively explore a range of variables and their changes to the end of the 21st century. A 'Climate Campus' educational section is also available. This explains the science of climate change and how climate change projections are created.

Information about climate observations can be found on the Bureau of Meteorology website (www.bom.gov.au/climate). Observations of past climate are used as a baseline for climate projections, and also in evaluating model performance.

EXECUTIVE SUMMARY

INTRODUCTION

This report presents projections of future climate for Monsoonal North based on our current understanding of the climate system, historical trends and model simulations of the climate response to changing greenhouse gas and decreasing aerosol emissions. Sub-clusters – Monsoonal North West (MNW) and Monsoonal North East (MNE) (Figure 1.1) – will be reported on when their climate differs from the cluster mean. The simulated climate response is that of the CMIP5 model archive, which also underpins the projections science of the *Fifth Assessment Report* of the Intergovernmental Panel on Climate Change (IPCC, 2013).

The global climate model (GCM) simulations presented here represent the full range of emission scenarios, as defined by the Representative Concentration Pathways (RCPs) used by the IPCC, with a particular focus on RCP4.5 and RCP8.5. The former represents a pathway consistent with low-level emissions, which stabilise the carbon dioxide concentration at about 540 ppm by the end of the 21st century. The latter is representative of a high-emission scenario, for which the carbon dioxide concentration reaches about 940 ppm by the end of the 21st century.

Projections are generally given for two 20-year time periods: the near future 2020–2039 (herein referred to as 2030) and late in the century 2080–2099 (herein referred to as 2090). The spread of model results are presented as the range between the 10th and 90th percentile in the CMIP5 ensemble output. For each time period, the model spread can be attributed to three sources of uncertainty: the range of future emissions, the climate response of the models, and natural variability. Climate projections do not make a forecast of the exact sequence of natural variability, so they are not ‘predictions’. They do however show a plausible range of climate system responses to a given emission scenario and also show the range of natural variability for a given climate. Greenhouse gas concentrations are similar amongst different RCPs for the near future, and for some variables, such as rainfall, the largest range in that period stems from natural variability. Later in the century, the differences between RCPs are more pronounced, and climate responses may be larger than natural variability.

For each variable, the projected change is accompanied by a confidence rating. This rating follows the method used by the IPCC in the *Fifth Assessment Report*, whereby the confidence in a projected change is assessed based on the type, amount, quality and consistency of evidence (which can be process understanding, theory, model output, or expert judgment) and the degree of agreement amongst the different lines of evidence (IPCC, 2013). The confidence ratings used here are set as *low*, *medium*, *high* or *very high*.

HIGHER TEMPERATURES

Temperatures in the cluster have been increasing since national records began in 1910. From 1910 to 2013, mean surface air temperature increased by 1.0 °C and 0.9 °C for Monsoonal North-East (MNE) and Monsoonal North-West (MNW) sub-clusters respectively using a linear trend. For the same period, daytime maximum temperatures have increased by 0.7 °C and 1.0 °C for MNE and MNW while overnight minimum temperatures have increased by 1.3 °C and 0.9 °C for MNE and MNW. This is in spite of the more recent cooling seen over north-western areas due to increased clouds.

Future substantial warming for the Monsoonal North cluster for mean, maximum and minimum temperature is projected with *very high confidence*, taking into consideration the robust understanding of the driving mechanisms of warming as well as strong agreement on direction and magnitude of change among GCMs, and downscaling results.

For the near future (2030), the mean warming is around 0.5 to 1.3 °C above the climate of 1986–2005, with only minor differences between RCPs. For late in the century (2090) the warming is 1.3 to 2.7 °C for RCP4.5 and 2.8 to 5.1 °C for RCP8.5.

HOTTER AND MORE FREQUENT HOT DAYS

A substantial increase in the temperature reached on the hottest days, the frequency of hot days and the duration of warm spells is projected with *very high confidence*, based on model results and physical understanding. For example, for Broome, the number of days above 35 °C by 2090 more than doubles under RCP4.5 and median warming, and the number of days over 40 °C nearly triples.



RAINFALL CHANGES MAY UNDERGO LARGE INCREASES OR DECREASES



The cluster experienced an overall slight increase in rainfall during the 20th century.

This includes prolonged periods of drying as well as above average rainfall. The strongest increases have been across the north-western regions during recent decades.

We have *high confidence* that natural climate variability will remain the major driver of annual mean rainfall changes by 2030 (20-year mean differences of +/- 10 % annually), as it has been in the recent past.

There is generally *low confidence* in projected rainfall changes for later in the century (2090) in this cluster. This is because of the differing simulations of the GCMs, but also because different processes, such as monsoon onset, Madden-Julian Oscillation (MJO) and tropical circulation can have opposite impacts on model projected rainfall changes. Also, there is large spread in the skill of models in simulating these processes. Additionally, GCMs may not adequately represent the influence of Eastern Australian orography on rainfall.

In the near future (2030) the magnitude of possible summer rainfall changes is around +/-10 %. Late in the century (2090) it is around -15 to +10 % under RCP4.5 and around -25 to +20 % under RCP8.5. There is an indication of a slight decline in spring by 2090 (model range from around -45 to +30 % under RCP8.5). The magnitude of possible differences in spring and autumn is around -25 to +20 % in 2030, and in 2090 around +/-30 % under RCP4.5 and -45 to +30 % under RCP8.5 (Figure 4.3.5 and Appendix Table 1).

INCREASED INTENSITY OF HEAVY RAINFALL EVENTS. CHANGES TO DROUGHT ARE LESS CLEAR



Understanding of physical processes and high model agreement gives us *high confidence* that the intensity of heavy rainfall events will increase. The magnitude of change, and the time when any change may be evident against natural variability, cannot be reliably projected.

We have *low confidence* in projecting changes in the frequency and duration of extreme meteorological drought.

SOME INCREASE IN SUMMER AND SPRING WIND SPEED, FEWER BUT POSSIBLY MORE INTENSE TROPICAL CYCLONES



Small changes in mean surface wind speed are projected with *high confidence* under all RCPs by 2030. By 2090 little change is projected with *medium confidence*. However, substantial changes are present in some models, seasons and parts of the cluster (particularly with increases in spring and decreases in autumn wind speed under RCP8.5).

Based on global and regional studies, tropical cyclones are projected with *medium confidence* to become less frequent, but with increases in the proportion of the most intense storms.

MOSTLY SMALL CHANGES TO SOLAR RADIATION AND HUMIDITY



Little change is projected for solar radiation by 2030 with *high confidence*. By 2090 under RCP8.5, larger changes in radiation are projected by some models, and with some agreement on a decrease. The causes of these changes are not well understood. Consequently we have *low confidence* in these projections.

There is *high confidence* in little change in relative humidity by 2030. There is *medium confidence* in a decrease in relative humidity by 2090 under RCP8.5 based on model results and physical understanding.

INCREASED EVAPORATION RATES AND REDUCED SOIL MOISTURE. CHANGES TO RUNOFF ARE LESS CLEAR



Projections for potential evapotranspiration indicate increases in all seasons with *high confidence*, with the largest absolute rates in summer by 2090. However, despite high model agreement we have only *medium confidence* in the magnitude of these projections due to shortcomings in the simulation of historical changes.

Soil moisture projections indicate overall seasonal decreases with *medium confidence* by 2090, but predominately in winter and spring. These changes in soil moisture are strongly influenced by changes in rainfall, but tend to be more negative because they are reinforced by increases in potential evapotranspiration. For similar reasons, runoff is projected to decrease, but only with *low confidence*. More detailed hydrological modelling is needed to confidently assess changes to runoff.

CHANGES TO FIRE CONDITIONS NOT CLEAR



The primary determinant of bushfire in the Monsoonal North is fuel availability (e.g. Williams *et al.*, 2009), which varies mainly with rainfall. In northern regions of the cluster such as the Top End and the Kimberley, where abundant rainfall and bushfire are common, the projected changes in rainfall are not expected to have a significant impact. There is *high confidence* in projections of little change to fire frequency. However, further south where rainfall is less reliable, there is only *medium confidence* in projections of little change to fire frequency. Here, change to fire frequency depends on the spatial variability of future rainfall. Across the cluster, when and where fire does occur, there is *high confidence* that fire behaviour will be more extreme.

HIGHER SEA LEVELS AND MORE FREQUENT SEA LEVEL EXTREMES



Relative sea level has risen around Australia at an average rate of 1.4 mm per year between 1966 and 2009, and 1.6 mm per year after the influence of the El Niño Southern Oscillation (ENSO) on sea level is removed.

There is *very high confidence* that sea level will continue to rise during the 21st century. By 2030, the projected range of sea-level rise for the cluster coastline is 0.06 to 0.17 m above the 1986–2005 level, with only minor differences between emission scenarios. As the century progresses, projections are sensitive to RCPs. By 2090, RCP4.5 gives a rise of 0.28 to 0.64 m and RCP8.5 gives a rise of 0.38 to 0.85 m. These ranges of sea level rise are considered likely (at least 66 % probability). However, if a collapse in the marine based sectors of the Antarctic ice sheet were initiated, these projections could be several tenths of a metre higher by late in the century.

Taking into account the nature of extreme sea levels along the Monsoonal North coastlines and the uncertainty in the sea level rise projections, an indicative extreme sea level ‘allowance’ is provided. This allowance is the minimum distance required to raise an asset to maintain current frequency of breaches under projected sea level rise. For the Monsoonal North in 2030 the vertical allowances along the cluster coastline are in the range of 11 to 14 cm for all RCPs, and by 2090 are 46 to 54 cm for RCP4.5, and 63 to 75 cm for RCP8.5.

WARMER AND MORE ACIDIC OCEANS IN THE FUTURE



Sea surface temperature (SST) has risen significantly across the globe over recent decades and warming is projected to continue with *very high confidence*. Across the coastal waters of the Monsoonal North in 2090, warming is projected in the range of 2.2 to 4.1 °C for RCP8.5.

About 30 % of the anthropogenic carbon dioxide emitted into the atmosphere over the past 200 years has been absorbed by the oceans. This has led to a 0.1 pH fall in the ocean’s surface water pH (a 26 % rise in acidity). Continued acidification will compromise the ability of calcifying marine organisms such as corals, oysters and some plankton to form their shells or skeletons. There is *very high confidence* that the ocean around Australia will become more acidic and also *high confidence* that the rate of ocean acidification will be proportional to carbon dioxide emissions. By 2030 pH is projected to fall by an additional 0.07 units in the coastal waters of the cluster. By 2090, a decrease of up to 0.14 is projected under RCP4.5 and up to 0.3 under RCP8.5. These values would represent a 40 and 100 % increase in acidity respectively.

MAKING USE OF THESE PROJECTIONS FOR CLIMATE ADAPTATION PLANNING



These regional projections provide the best available science to support impact assessment and adaptation planning in the Monsoonal North cluster. This report provides some guidance on how to use these projections, including the Australian Climate Futures web tool, available from the Climate Change in Australia website. The tool allows users to investigate the range of climate model outcomes for their region across timescales and RCPs of interest, and to select and use data from models that represent a particular change of interest (e.g. warmer and drier conditions).



1 THE MONSOONAL NORTH CLUSTER

This report describes climate change projections for the Monsoonal North cluster, which is comprised of NRM regions of Western Australia (northern section of Rangelands NRM region; north of latitude 20 °South), Northern Territory (north of latitude 16 °South) and Queensland (Burdekin, Southern Gulf, and Northern Gulf NRM regions) (Figure 1.1).

Because of the large east-west extent of this cluster, some of the results have been divided into those for the Monsoonal North West (MNW) and the Monsoonal North East (MNE) regions. These two NRM sub-clusters extend over much of tropical northern Australia.

The MNW sub-cluster covers the Kimberley region of Western Australia and the northern part of the Northern Territory. The Kimberley consists of many steep mountain ranges and two main river systems: the Ord River and Fitzroy River. The former feeds Lake Argyle, Australia's largest artificial lake. Across the top end of the Northern Territory, tropical rainforests, wetlands and arid rangelands dominate. Bordering along the north is the Timor Sea, while the Gulf of Carpentaria lies along the eastern edges. There is an extensive series of river systems in this cluster, including the Liverpool, Alligator, Daly, Finke, McArthur, Roper, Todd and Victoria Rivers.

The MNE sub-cluster contains the Northern and Southern Gulf regions as well as the Burdekin region. The Northern Gulf region consists of the Mitchell, Gilbert, Norman and Staaten River catchments, all of which flow into the Gulf of Carpentaria. Much of the sub-cluster is covered by

savannah woodland but also includes important rainforest areas in the western fall of the Great Dividing Range and associated tablelands (bordering the Wet Tropics cluster). The Southern Gulf region comprises eight river catchments, which drain into the southern part of the Gulf of Carpentaria. It also comprises major grasslands (Gulf Plains and Mitchell Grass Downs), highlands (North-West Highlands) and wetlands. Located in the drier part of the tropics on Queensland's east coast, the Burdekin region encompasses a diversity of landscapes including wet tropical rainforests (Eungella and the Paluma Range), drier sub-catchment areas (Belyando and Burdekin Rivers) and the very wet coastal plains of the lower Burdekin River. The delta of the Burdekin River supplies irrigation, mainly for sugar cane farming.

A range of climate change impacts and adaptation challenges have been identified by the NRM organisations across this cluster. Broad acre cropping and intensive agriculture, invasive species and biodiversity management, water security and availability, and tourism are priorities for the cluster's natural resource management community.

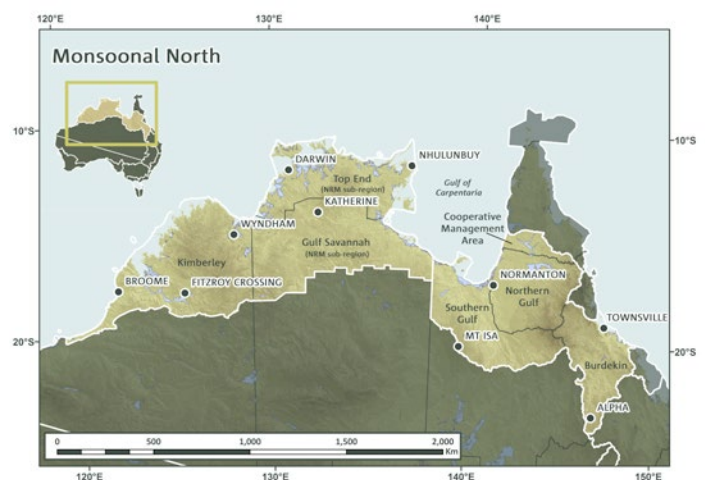


FIGURE 1.1: THE MONSOONAL NORTH CLUSTER AND MAIN LOCALITIES WITH RESPECT TO THE AUSTRALIAN CONTINENT. THE STATE BOUNDARY BETWEEN QUEENSLAND AND NORTHERN TERRITORY IS ALSO THE SEPARATION BETWEEN THE WESTERN AND EASTERN SUB-CLUSTERS.

2 CLIMATE OF MONSOONAL NORTH

The Monsoonal North (MN) cluster comprises five NRM regions and is further divided into two sub-clusters, Monsoonal North West (MNW) and Monsoonal North East (MNE). Situated mostly within the global tropical belt (*i.e.* north of the Tropic of Capricorn), this cluster is strongly affected by the seasonal migration of the monsoon back and forth across the equator. These seasonal characteristics result in two distinct climates: very wet during summer and dry during winter. There are multiple additional influences on this basic monsoonal climate: tropical cyclones, the impact of the El Niño-Southern Oscillation (ENSO), and variability in the south-east trade winds along the tropical east coast. In the sections below, the current climate of Monsoonal North is presented for the period 1986–2005 (Box 3.1 presents the observational data sets used in this report).

The climate in the MNW sub-cluster is generally very hot and humid with a distinct summer monsoon season (late December to March) during which it receives most of its rainfall. This season overlaps with the tropical cyclone season (November to April). Thus, rainfall in the north is strongly influenced by the intensity of the wet season and monsoon, and by tropical cyclones. The climate in the MNE sub-cluster is generally hot to very hot and humid with a distinct ‘wet’ season (December to March). Rainfall is associated with moist onshore south-east trade winds, monsoonal lows or tropical cyclones.

Daily mean temperatures are fairly evenly distributed in summer across the MN cluster, ranging mostly between

27 °C and 33 °C, dropping to below 27 °C for coastal areas along and east of the Great Dividing Range (Figure 2.1a). In winter, there is a stronger north-south gradient with 24 to 27 °C in coastal areas along the north and 18 to 21 °C in the south with somewhat lower temperatures in the elevated areas of the Great Dividing Range (Figure 2.1b). The highest temperatures are experienced in January, with an average daily maximum temperature of 33 to 36 °C for large parts of the MN cluster, increasing further inland and decreasing towards the northern and eastern coasts (Figure 2.1c). Lowest temperatures occur most commonly in July with average minimum temperatures of 12 to 18 °C, dropping below 12 °C further south and along the Great Dividing Range (Figure 2.1d).

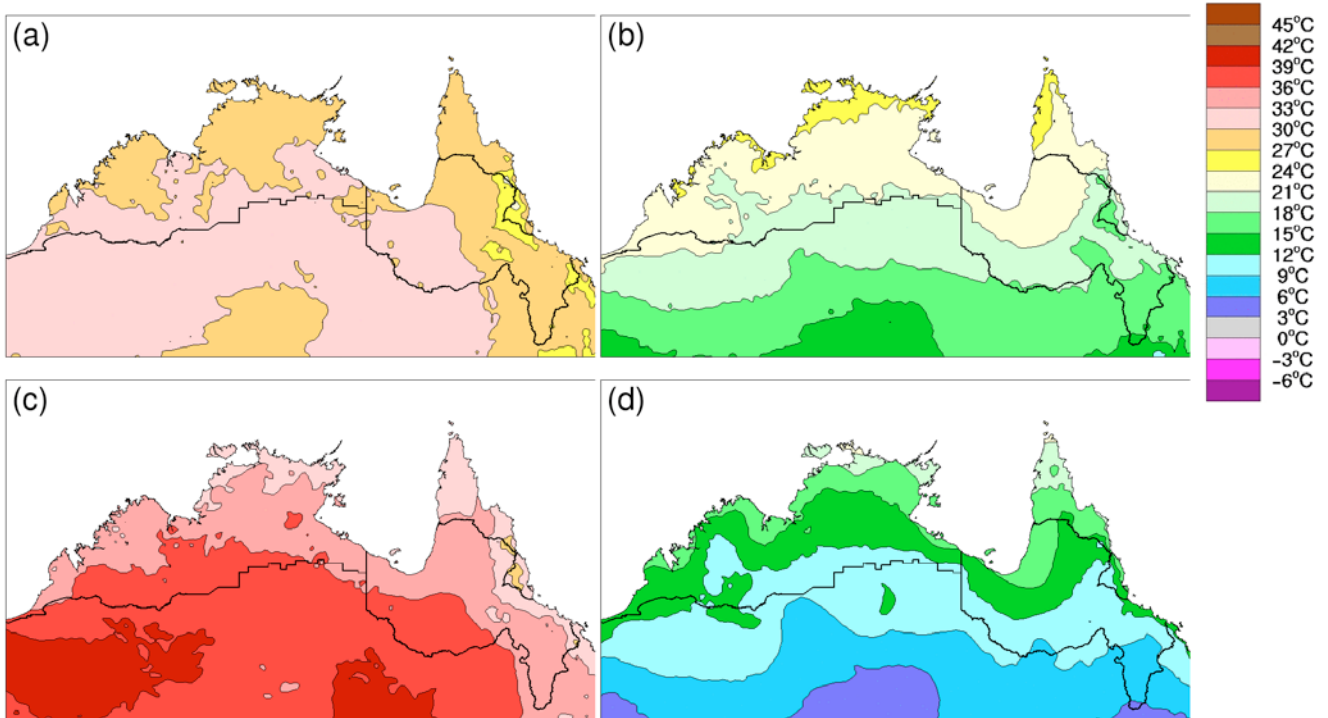


FIGURE 2.1: MAPS OF (A) AVERAGE SUMMER (DECEMBER TO JANUARY) DAILY MEAN TEMPERATURE, (B) AVERAGE WINTER (JUNE-AUGUST) DAILY MEAN TEMPERATURE, (C) AVERAGE JANUARY MAXIMUM DAILY TEMPERATURE AND (D) AVERAGE JULY MINIMUM DAILY TEMPERATURE FOR THE PERIOD 1986–2005.



As a whole, the cluster exhibits a clear seasonal cycle in temperature with daily mean temperatures ranging from about 30 °C in summer (January) to about 22 °C in winter (July). The maximum value for the cluster (about 37 °C) occurs during the monsoon build-up in November. The minimum value of about 14°C occurs in July (Figure 2.2). The annual cycle of temperature is very similar for MNW and MNE.

The annual cycle of rainfall shows the typical monsoonal pattern of wet (December to March) and dry (June to September) seasons (Figure 2.2), whereby the MNW experiences higher rainfall totals during the wet season compared to the MNE sub-cluster¹. The MNE sub-cluster also shows significantly more winter rainfall originating

mainly from south-east trade winds. The total annual rainfall is 890 mm for MNW and 665 mm for MNE, of which 90 % occurs during the wet season in MNW and 85 % occurs during the wet season in MNE.

The wet season rainfall pattern for the cluster is characterised by a spatial rainfall gradient from the north to the south, with average annual rainfall ranging from about 1600 mm in northern and eastern coastal regions, to about 600 mm further inland and in the south (Figure 2.3a). During the dry season, rainfall totals are very low with large parts of the Monsoonal North sub-cluster receiving less than 50 mm for the entire six month period (Figure 2.3b).

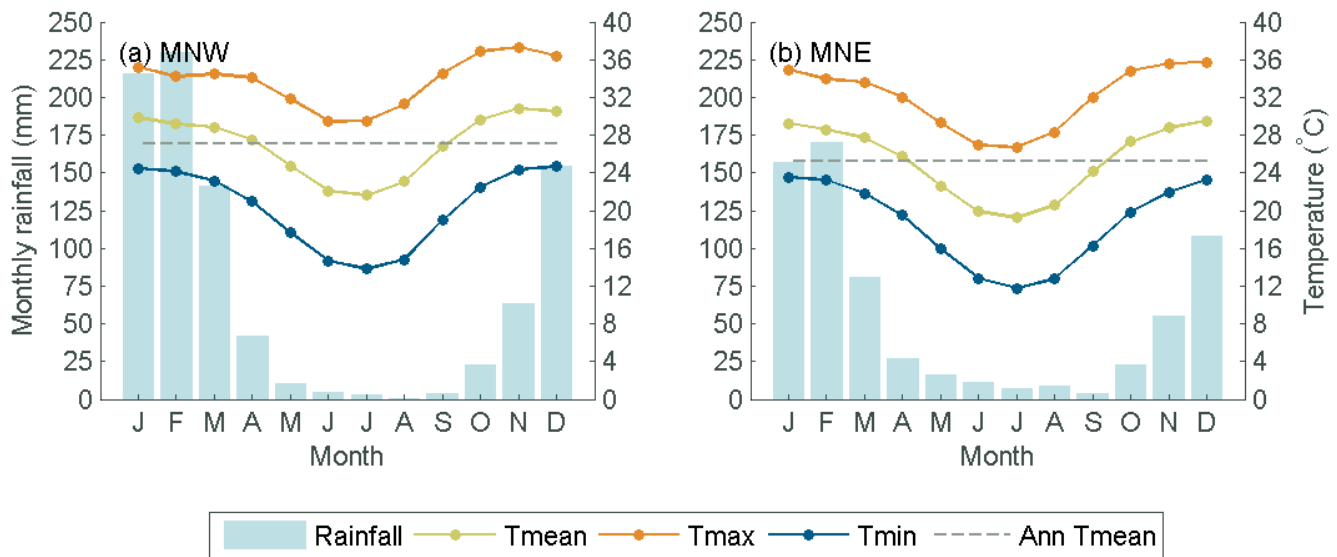


FIGURE 2.2: MONTHLY RAINFALL (BLUE BARS) AND TEMPERATURE CHARACTERISTICS FOR THE MONSOONAL NORTH CLUSTER WEST (A) AND EAST (B) (1986–2005). TMEAN IS MONTHLY MEAN TEMPERATURE (GREEN LINE), TMAX IS MONTHLY MEAN MAXIMUM TEMPERATURE (ORANGE LINE), TMIN IS MONTHLY MEAN MINIMUM TEMPERATURE (BLUE LINE) AND ANN TMEAN IS THE ANNUAL AVERAGE OF MEAN TEMPERATURE (GREY LINE) (27.3 °C FOR MNW AND 25.5 °C FOR MNE). TEMPERATURE AND RAINFALL DATA ARE FROM AWAP.

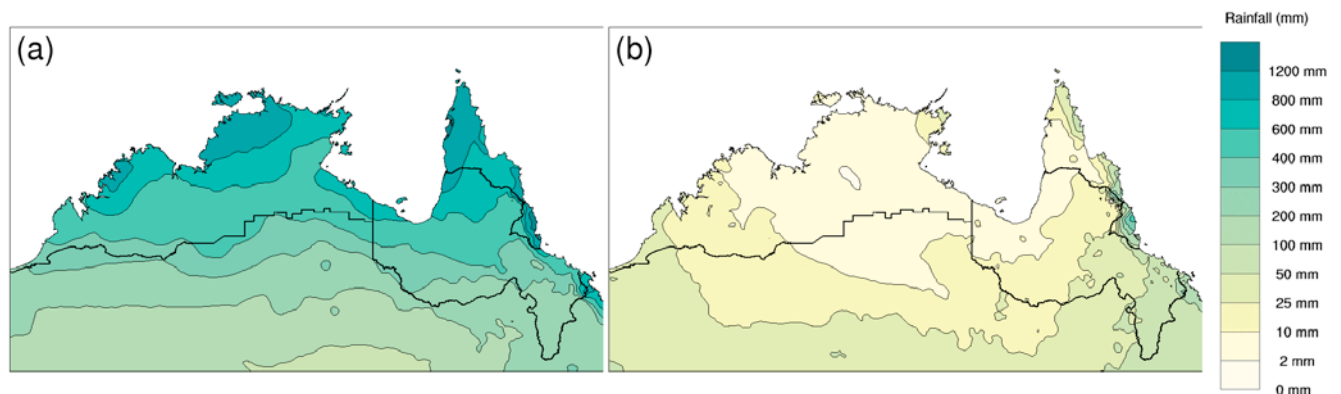


FIGURE 2.3: FOR THE 1986–2005 PERIOD, AVERAGE RAINFALL FOR (A) SUMMER (DECEMBER TO FEBRUARY) AND (B) WINTER (JUNE TO AUGUST).

¹ Note that MNE excludes the Wet Tropics of Queensland which shows some of the highest rainfall totals across the entire continent.



During the baseline period 1986–2005, rainfall in the Monsoonal North cluster experienced moderate to strong year to year variability relative to other parts of Australia, mainly due to the phases of the El Niño Southern Oscillation (ENSO). El Niño years tend to be drier than average while La Niña years tend to be wetter than average. Seasonal rainfall characteristics in the Monsoonal North cluster are determined by complex interactions of several rainfall drivers that influence this region. The term ‘driver’ is used to signify a system’s role in the generation of rainfall and includes a range of large-scale and synoptic weather features. For this cluster, most drivers influence rainfall during a particular time of the year. These drivers include local factors such as topography, and properties of large-scale climate features such as the strength (onset, duration and retreat) of the monsoon season; the phase of ENSO; the occurrence of tropical cyclones; and the strength of the south-eastern trade winds.

The impact of ENSO on the monsoon season depends on the phase of ENSO; while during El Niño only eastern and central parts of tropical Australia are affected, leading to slightly lower wet season rainfall totals. La Niña can lead to an early wet season onset with significant rainfall during the usual build-up season.

The pre-monsoon season build-up creates the large-scale environment upon which a ‘trigger’ can initiate the actual monsoon onset. This trigger can be the Madden-Julian Oscillation (MJO, see Sections 3.5 and 4.1 in the Technical Report) or an extra-tropical disturbance (Davidson *et al.*, 2007). The active phase of the MJO in the Australian region often coincides with monsoon onset. The MJO also strongly modulates active and break phases during the monsoon as well as tropical cyclone activity (Hendon *et al.*, 2007, Wheeler *et al.*, 2009). Variations in the warmth of the sea surface temperatures in the ocean surrounding tropical Australia are also part of this system.

The heaviest rainfall events usually occur in summer across the monsoonal trough and/or from land-falling tropical cyclones. Monthly 90th percentile values can reach around 600 to 800 mm (based on the 1986–2005 reference period), especially for the month of February.



3 SIMULATING REGIONAL CLIMATE

Researchers use climate models to examine future global and regional climate change. These models have a foundation in well-established physical principles and are closely related to the models used successfully in weather forecasting. Climate modelling groups from around the world produce their own simulations of the future climate, which may be analysed and compared to assess climate change in any region. For this report, projections are based on historical and future climate simulations from the CMIP5 model archive that holds the most recent simulations, as submitted by approximately 20 modelling groups (Taylor *et al.*, 2012). The number of models used in these projections varies by RCP and variable depending on availability, *e.g.* for monthly temperature and rainfall, data are available for 39 models for RCP8.5 but only 28 models for RCP2.6 (see Chapter 3 in the Technical Report).

The skill of a climate model is assessed by comparing model simulations of the current climate with observational data sets (see Box 3.1 for details on the observed data used for model evaluation for the Monsoonal North cluster). Accurate simulation of key aspects of the regional climate provides a basis for placing

some confidence in the model's projections. However, models are not perfect representations of the real world. Some differences in model output relative to the observations are to be expected. The measure of model skill can also vary depending on the scoring measure used and regions being assessed.

BOX 3.1: COMPARING MODELS AND OBSERVATIONS: EVALUATION PERIOD, OBSERVED DATA SETS, AND SPATIAL RESOLUTION

Model skill is assessed by running simulations over historical time periods and comparing simulations with observed climate data. Projections presented here are assessed using the 1986–2005 baseline period, which conforms to the *Fifth Assessment Report* (IPCC, 2013). The period is also the baseline for projected changes, as presented in bar plots and tabled values in the Appendix. An exception is the time series projection plots, which use a baseline of 1950–2005, as explained in Section 6.2.2 of the Technical Report.

Several data sets are used to evaluate model simulations of the current climate. For assessment of rainfall and temperature, the observed data are derived from the Australian Water Availability Project

(AWAP) (Jones *et al.*, 2009) and from the Australian Climate Observations Reference Network – Surface Air Temperature (ACORN-SAT), a data set developed for the study of long-term changes in monthly and seasonal climate (Fawcett *et al.*, 2012).

The spatial resolution of climate model data (around 200 km between the edges of grid cells) is much coarser than observations, and for the Monsoonal North cluster, approximately half of the CMIP5 models provide coverage by partial grid cells only (*i.e.* partially included within the cluster boundaries). This means that simulation of past and future climates should be interpreted as representative of a region, which could include areas of adjacent clusters.

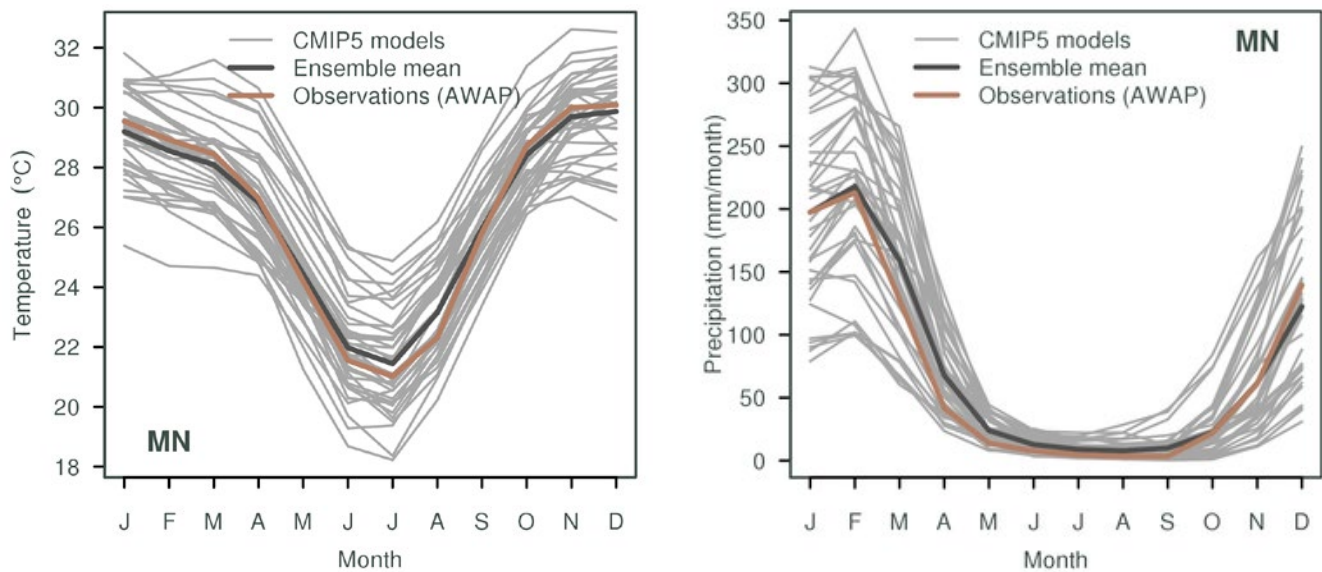


FIGURE 3.1: THE ANNUAL CYCLE OF (LEFT) TEMPERATURE AND (RIGHT) RAINFALL IN THE MONSOONAL NORTH CLUSTER SIMULATED BY CMIP5 MODELS (GREY LINES) WITH MODEL ENSEMBLE MEAN (BLACK LINE) AND OBSERVATIONS BASED ON AWAP (BROWN LINES) FOR THE BASELINE PERIOD 1986–2005.

For Monsoonal North, models performed well in terms of simulating the timing and magnitude of the seasonal cycle of temperature (Figure 3.1). Some models show a systematic departure from the observed seasonal cycle with a 2 °C cold or warm bias. Evaluation results for rainfall show a more mixed picture; while overall models also show good skill in simulating the timing of the seasonal rainfall patterns, there is a very large spread in the intensity of the simulated rainfall during the wet season (Figure 3.1). Some models simulate too much rain during the monsoon season, others not enough. In some models these deficiencies relate to systematic errors in the southward extent of the monsoon system. To see how the models performed across different parts of Australia, refer to Chapter 5 in the Technical Report.

The majority of models, however, show good skill in simulating the timing of the seasonal rainfall patterns (Figure 3.1), even if temporal variability (as represented by the time series' standard deviation) is somewhat underestimated by a large proportion of CMIP5 models relative to the AWAP climatology. It is worth noting, however, that many historical re-analysis data sets show similarly low values for standard deviation when compared to AWAP.

Evaluation of CMIP5 models also extends to some of the key drivers for rainfall variability in the Monsoonal North cluster. In spring and summer, ENSO is a main driver for rainfall, together with MJO and the surrounding Indian Ocean sea surface temperatures. Significantly, the connection between El Niño variations and rainfall is reasonably well simulated and improved over the previous generation of climate models. However, all models have at least some significant shortcomings across a range

of other tests (see Chapter 5 of the Technical Report). Some of these shortcomings are noted in the context of interpreting specific projection results in the Chapter that follows. No single or small number of models performed considerably better than others for the Monsoonal North cluster.

In addition to the CMIP5 model results, downscaling can be used to derive finer spatial information in the regional projections, thus potentially capturing processes occurring on a finer scale. While downscaling can provide added value on finer scale processes, it increases the uncertainty in the projections since there is no single best downscaling method, but a range of methods that are more or less appropriate depending on the application. It is advisable to consider more than one technique, as different downscaling techniques have different strengths and weaknesses.

For the regional projections we consider downscaled projections from two techniques: outputs from a dynamical downscaling model, the Conformal Cubic Atmospheric Model (CCAM) (McGregor and Dix, 2008) using six CMIP5 GCMs as input; and the Bureau of Meteorology analogue-based statistical downscaling model with 22 CMIP5 GCMs as input for rainfall and 21 CMIP5 GCMs as input for temperature (Timbal and McAvaney, 2001). Where relevant, projections from these methods are compared to those from GCMs (the primary source of climate change projections in this report). The downscaled results are only emphasised if there are strong reasons for giving the downscaled data more credibility than the GCM data (see Section 6.3 in the Technical Report for further details on downscaling).

4 THE CHANGING CLIMATE OF THE MONSOONAL NORTH

This Section presents projections of climate change to the end of the 21st century for a range of climate variables, including average and extreme conditions, for the Monsoonal North cluster. Where there is relevant observational data available, the report shows historical trends.

As outlined in the *Fifth Assessment Report* (IPCC, 2013), greenhouse gases, such as carbon dioxide, have a warming effect on global climate. Greenhouse gases absorb heat that would otherwise be lost to space, and re-radiate it back into the atmosphere and to the Earth's surface. The IPCC concluded that it was *extremely likely* that more than half of the observed increase in global average surface air temperature from 1951–2010 has been caused by the anthropogenic increase in greenhouse gas emissions and other anthropogenic forcings. Further increases in greenhouse gas concentrations, resulting primarily from burning fossil fuel, will lead to further warming, as well as other physical and chemical changes in the atmosphere, ocean and land surface.

The CMIP5 simulations give the climate response to a set of greenhouse gas, aerosol and land-use scenarios that are consistent with socio-economic assumptions of how the future may evolve. These scenarios are known as the Representative Concentration Pathways (RCPs) (Moss *et al.*, 2010; van Vuuren *et al.*, 2011). Box 4.1 presents a brief introduction to the RCPs.

In its *Fifth Assessment Report* (IPCC, 2013), the IPCC concluded that global mean surface air temperatures for 2081–2100 relative to 1986–2005 are likely to be in the following ranges: 0.3 to 1.7 °C warmer for RCP2.6 (representing low emissions); 1.1 to 2.6 °C and 1.4 to 3.1 °C warmer for RCP4.5 and RCP6.0 respectively (representing intermediate emissions); and 2.6 to 4.8 °C warmer for RCP8.5 (representing high emissions).

The projections for the climate of the Monsoonal North cluster consider model ranges of change, as simulated by the CMIP5 ensemble. However, the projections should be viewed in the context of the confidence ratings that are provided, which consider a broader range of evidence than just the model outputs. The projected change is assessed for two 20-year periods: a near future 2020–2039 (herein referred to as 2030) and a period late in the 21st century, 2080–2099 (herein referred to as 2090) following RCPs 2.6, 4.5 and 8.5 (Box 4.1)².

The spread of model results is presented in graphical form (Box 4.2) and provided as tabulated percentiles in Table 1 (10th, 50th and 90th) and Table 3 (5th, 50th and 95th, for sea level rise) in the Appendix. CMIP5 results for additional time periods between 2030 and 2090 are provided through the Climate Change in Australia website (Box 1).

Unless otherwise stated, users of these projections should consider the ranges of projected change, as indicated by the different plots and tabulated values, as applicable to each location within the cluster.

² For sea level rise and sea allowance, the future averaging periods are 2020–2040 and 2080–2100. In the report, these are referred to as 2030 and 2090 respectively.

BOX 4.1: REPRESENTATIVE CONCENTRATION PATHWAYS (RCPs)

The climate projections presented in this report are based on climate model simulations following a set of greenhouse gas, aerosol and land-use scenarios that are consistent with socio-economic assumptions of how the future may evolve. The well mixed concentrations of greenhouse gases and aerosols in the atmosphere are affected by emissions as well as absorption through land and ocean sinks.

There are four Representative Concentration Pathways (RCPs) underpinned by different emissions. They represent a plausible range of radiative forcing (in W/m^2) during the 21st century relative to pre-industrial levels. Radiative forcing is a measure of the energy absorbed and retained in the lower atmosphere. The RCPs are:

- RCP8.5: high radiative forcing (high emissions)
- RCP4.5 and 6.0: intermediate radiative forcing (intermediate emissions)
- RCP2.6: low radiative forcing (low emissions).

RCP8.5, represents a future with little curbing of emissions, with carbon dioxide concentrations reaching 940 ppm by 2100. The higher of the two intermediate concentration pathways (RCP6.0) assumes implementation of some mitigation strategies, with carbon dioxide reaching 670 ppm by 2100. RCP4.5 describes somewhat higher emissions than RCP6.0 in

the early part of the century, with emissions peaking earlier then declining, and stabilisation of the carbon dioxide concentration at about 540 ppm by 2100. RCP2.6 describes emissions that peak around 2020 and then rapidly decline, with the carbon dioxide concentration at about 420 ppm by 2100. It is likely that later in the century active removal of carbon dioxide from the atmosphere would be required for this scenario to be achieved. For further details on all RCPs refer to Section 3.2 and Figure 3.2.2 in the Technical Report.

The previous generation of climate model experiments that underpins the science of the IPCC's *Fourth Assessment Report* used a different set of scenarios. These are described in the IPCC's Special Report on Emissions Scenarios (SRES) (Nakićenović and Swart, 2000). The RCPs and SRES scenarios do not correspond directly to each other, though carbon dioxide concentrations under RCP4.5 and RCP8.5 are similar to those of SRES scenarios B1 and A1FI respectively.

In the Technical and Cluster Reports, RCP6.0 is not included due to a smaller sample of model simulations available compared to the other RCPs. Remaining RCPs are included in most graphical and tabulated material of the Cluster Reports, with the text focusing foremost on results following RCP4.5 and RCP8.5.

4.1 RANGES OF PROJECTED CLIMATE CHANGE AND CONFIDENCE IN PROJECTIONS

Quantitative projections of future climate change in the Monsoonal North are presented as ranges. This allows for differences in how future climate may evolve due to three factors – greenhouse gas and aerosol emissions, the climate response and natural variability – that are not known precisely:

- Future emissions cannot be known precisely and are dealt with here by examining several different RCPs described in Box 4.1. There is no 'correct' scenario, so the choice of how many and which scenarios to examine is dependent on the decision-making context.
- The response of the climate system to emissions is well known in some respects, but less well known in others. The thermodynamic response (direct warming) of the atmosphere to greenhouse gases is well understood, although the global climate sensitivity varies. However, changes to atmospheric circulation in a warmer climate are one of the biggest uncertainties regarding the climate response. The range between different climate

models (and downscaled models) gives some indication of the possible responses. However, the range of model results is not a systematic or quantitative assessment of the full range of possibilities, and models have some known regional biases that affect confidence.

- Natural variability (or natural 'internal variability' within the climate system) can dominate over the 'forced' climate change in some instances, particularly over shorter time frames and smaller geographic areas. The precise evolution of climate due to natural variability (e.g. the sequence of wet years and dry years) cannot be predicted (IPCC, 2013, see Chapter 11). However, the projections presented here allow for a range of outcomes due to natural variability, based on the different evolutions of natural climatic variability contained within each of the climate model simulations.

The relative importance of each of these factors differs for each variable, different timeframes and spatial scale. For some variables with large natural variability, such as rainfall, the predominant reason for differing projections in the early period is likely to be natural variability rather than differences in emission scenarios (the influence of which becomes relatively more important as greenhouse



gas concentrations increase). In addition, unpredictable events, such as large volcanic eruptions, and processes not included in models, could influence climate over the century. See the IPCC's *Fifth Assessment Report* (IPCC, 2013) Chapter 11 for further discussion of these issues.

The projections presented are accompanied by a confidence rating that follows that used by the IPCC in the *Fifth Assessment Report* (Mastrandrea *et al.*, 2010), whereby the confidence in a projected change is assessed based on the type, amount, quality and consistency of evidence (which can be process understanding, theory, model output, or expert judgment) and the extent of agreement amongst the different lines of evidence. Hence, this confidence rating does not equate precisely to probabilistic confidence. The levels of confidence used here are set as *low*, *medium*, *high* or *very high*. Note that although confidence may be high in the direction of change, in some cases confidence in magnitude of change may be medium or low (*e.g.* due to some known model deficiency). When confidence is low, only qualitative assessments are given. More information on the method used to assess confidence in the projections is provided in Section 6.4 of the Technical Report.

4.2 TEMPERATURE

Surface air temperatures in the cluster have been increasing since national records began in 1910 (Figure 4.2.1, 4.2.2). By 2013, mean temperature had risen by 1.0 °C and 0.9 °C since 1910 for MNE and MNW respectively using a linear trend. The trend in mean temperature since 1960 is negative in a region of north-west Australia (Figure 4.2.2). For the same period, daytime maximum temperatures have risen by 0.7 °C and 1.0 °C for MNE and MNW while overnight minimum temperatures have increased by 1.3 °C and 0.9 °C for MNE and MNW using a linear trend.

However, as shown in Figure 4.2.1, this increase is not strictly linear in past decades with alternating periods of increases and slight decreases. The recent period of some cooling is mainly driven by increases in convection and rainfall over the same period and is especially pronounced in summer/autumn for MNW and autumn/winter for MNE. Minimum and maximum temperatures have also changed since the early 20th century, showing similar decadal variability to the mean temperature (Figure 4.2.3).

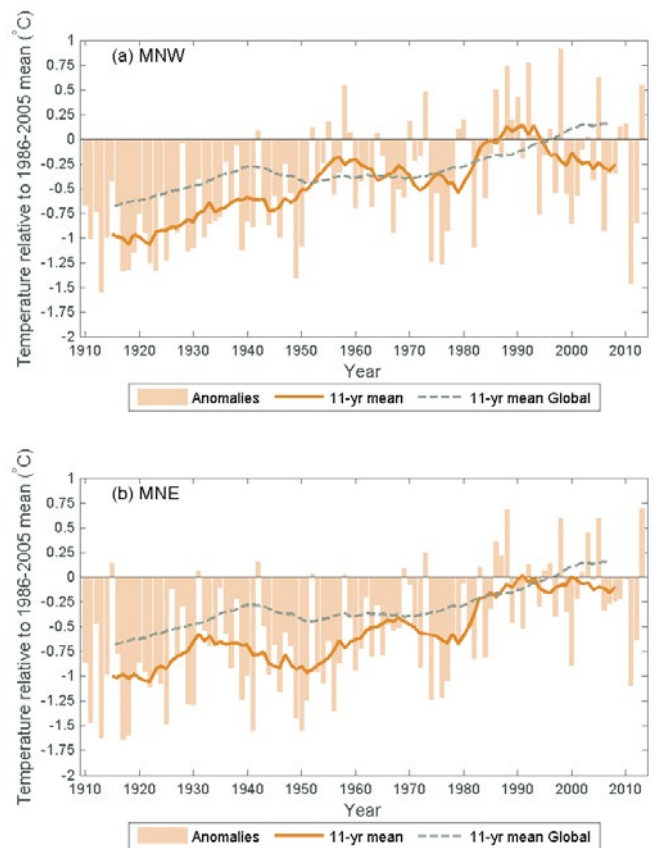


FIGURE 4.2.1: OBSERVED ANNUAL MEAN TEMPERATURE ANOMALIES (°C) FOR 1910–2013 COMPARED TO THE BASELINE 1986–2005 FOR (A) MONSOONAL NORTH WEST AND (B) MONSOONAL NORTH EAST. CLUSTER AVERAGE DATA ARE FROM ACORN-SAT AND GLOBAL DATA ARE FROM HADCRUT3V (BROHAN *ET AL.*, 2006).

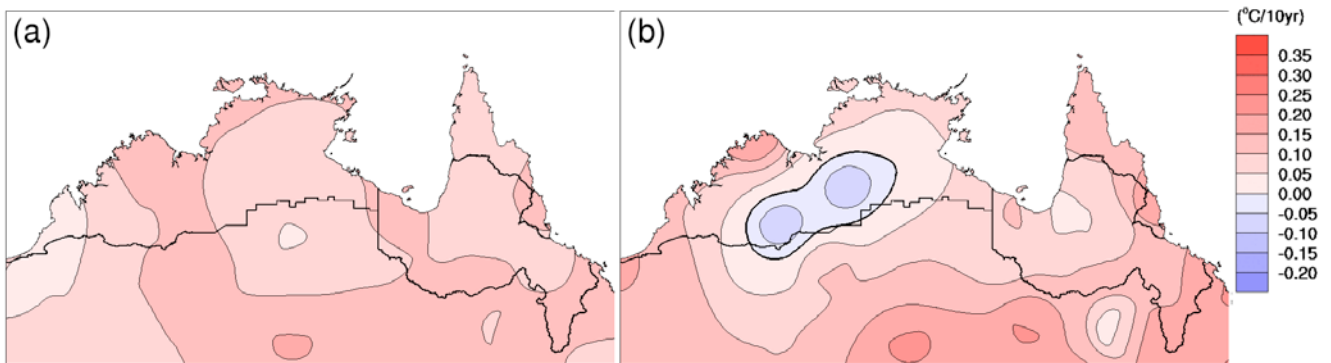


FIGURE 4.2.2: MAPS OF TREND IN MEAN TEMPERATURE ($^{\circ}\text{C}/10$ YEARS) FOR A) 1910–2013 AND B) 1960–2013 (ACORN-SAT).

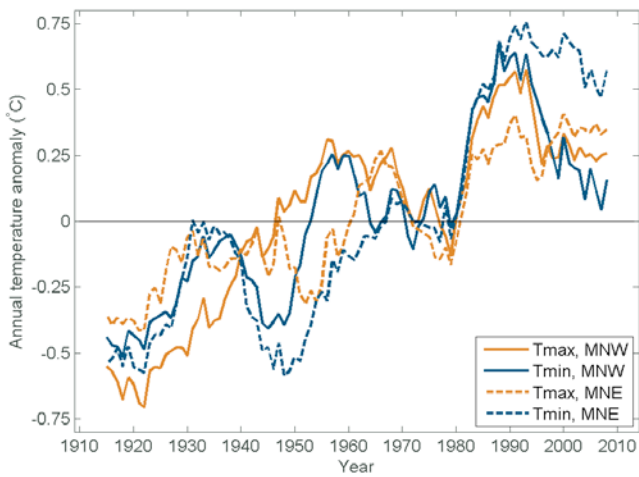
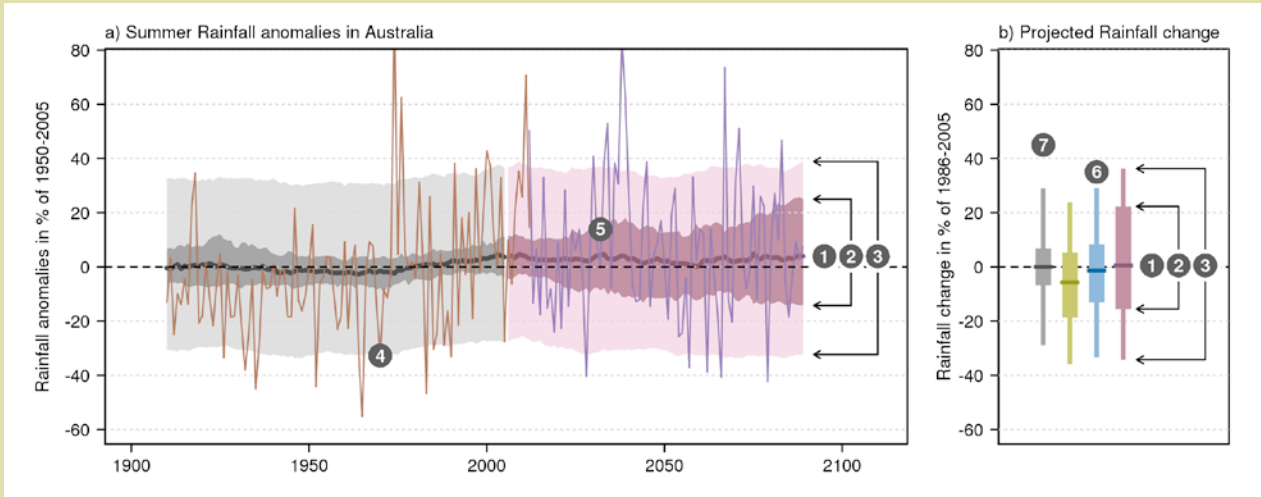


FIGURE 4.2.3: OBSERVED ANNUAL MEAN OF DAILY MAXIMUM (ORANGE LINE) AND MINIMUM (BLUE LINE) TEMPERATURE ($^{\circ}\text{C}$, 11-YEAR RUNNING MEAN) FOR MNW (SOLID LINES) AND MNE (DASHED LINES) SUB-CLUSTERS, PRESENTED AS ANOMALIES RELATIVE TO THEIR RESPECTIVE 1910–2013 MEAN VALUE (ACORN-SAT).

BOX 4.2: UNDERSTANDING PROJECTION PLOTS



Projections based on climate model results are illustrated using time series (a) and bar plots (b). The model data are expressed as anomalies from a reference climate. For the time series (a), anomalies are calculated as relative to 1950–2005, and for the bar plots (b) anomalies are calculated as the change between 1986–2005 and 2080–2099 (referred to elsewhere as ‘2090’). The graphs can be summarised as follows:

1. The middle (bold) line in both (a) and (b) is the median value of the model simulations (20-year moving average); half the model results fall above and half below this line.
2. The bars in (b) and dark shaded areas in (a) show the range (10th to 90th percentile) of model simulations of 20-year average climate.
3. Line segments in (b) and light shaded areas in (a) represent the projected range (10th to 90th

percentile) of individual years taking into account year to year variability in addition to the long-term response (20-year moving average).

In the time series (a), where available, an observed time series (4) is overlaid to enable comparison between observed variability and simulated model spread. A time series of the future climate from one model is shown to illustrate what a possible future may look like (5). ACCESS1-0 was used for RCP4.5 and 8.5, and BCC-CSM-1 was used for RCP2.6, as ACCESS1-0 was not available.

In both (a) and (b), different RCPs are shown in different colours (6). Throughout this document, green is used for RCP2.6, blue for RCP4.5 and purple for RCP8.5, with grey bars used in bar plots (b) to illustrate the expected range of change due to natural internal climate variability alone (7).

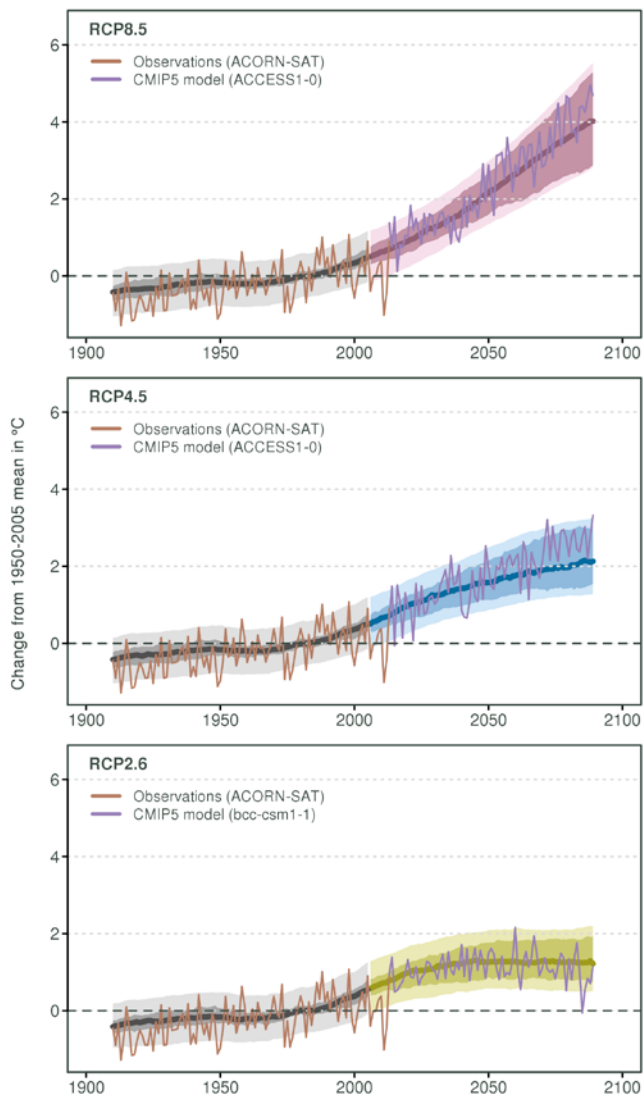


FIGURE 4.2.4: TIME SERIES FOR MONSOONAL NORTH ANNUAL AVERAGE SURFACE AIR TEMPERATURE (°C) FOR 1910–2090, AS SIMULATED IN CMIP5 RELATIVE TO THE 1950–2005 MEAN. THE CENTRAL LINE IS THE MEDIAN VALUE. THE SHADING IS THE 10TH AND 90TH PERCENTILE RANGE OF 20-YEAR MEANS (INNER) AND SINGLE YEAR VALUES (OUTER). THE GREY SHADING INDICATES THE PERIOD OF THE HISTORICAL SIMULATION, WHILE THREE FUTURE SCENARIOS ARE SHOWN WITH COLOUR-CODED SHADING: RCP8.5 (PURPLE), RCP4.5 (BLUE) AND RCP2.6 (GREEN). ACORN-SAT OBSERVATIONS AND PROJECTED VALUES FROM A TYPICAL MODEL ARE SHOWN. TIME SERIES PLOTS ARE EXPLAINED IN BOX 4.2.

In CMIP5 simulations, the Monsoonal North cluster is projected to continue to warm throughout the 21st century, at a rate that strongly follows the increase in global greenhouse gases (Figure 4.2.4). Tabulated warming for various time slices and RCPs are given in Table 1 in the Appendix. For 2030, the warming is 0.5 to 1.3 °C (10th and 90th percentile), with only minor differences between the scenarios. The projected temperature range for 2090 shows larger differences between emission scenarios with 1.3 to 2.7 °C for RCP4.5, and 2.8 to 5.1 °C following RCP8.5.

The warming is large compared to natural year to year variability in the cluster. For example, cold years become warmer than warm years in the current climate by 2050 under RCP8.5 and warmer than most current warm years under RCP4.5. This is illustrated in Figure 4.2.4 by overlaying the simulated year to year variability in one model's simulation and comparing this to the historical variability. This comparison also illustrates that individual model runs produce temporal variability much similar to that of observed temperature, as well as a warming trend. Overall there is good agreement between model and observed data on decadal scales. When comparing the trajectory of warming to the spread of natural variability, the warming signal in regional temperature due to increased emissions appears to emerge from the natural variability around the 2050s for most RCPs. Here, 'emergence' means when the range of temperatures in the future moves beyond that of the current climate.

Overall, the warming rates of the Monsoonal North cluster are in line with the majority of other regions of Australia; with somewhat higher rates being projected for western Australia and somewhat lower overall rates for the south-east and Tasmania (see Figure 7.1.4 in the Technical Report).

Changes to the spatial pattern of temperature in the cluster can be illustrated by adding the projected change in annual mean temperature onto a mapped observed climatology. Figure 4.2.5 gives an example of this for the 2090 period following the high emission scenario RCP8.5 and the median warming from the CMIP5 models. This case, which corresponds to a global warming of 3.7 °C, shows regional temperatures increasing from within the range of about 27 to 29 °C for the current climate up to a range of about 31 to 33 °C for the future climate. Also evident in this figure is the spatial expansion of the 'above 27 °C' area between current and future climate, covering most of northern Australia.

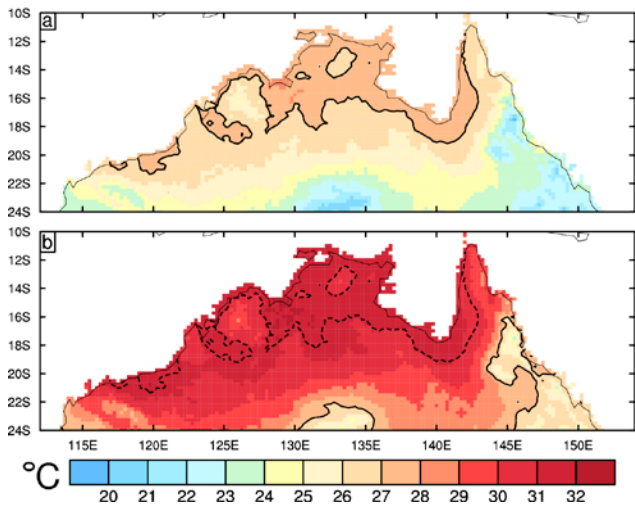


FIGURE 4.2.5: ANNUAL MEAN SURFACE AIR TEMPERATURE (IN °C), FOR THE PRESENT CLIMATE (A), FOR MEDIAN WARMING IN 2090 UNDER RCP8.5 (B). THE PRESENT IS USING AWAP FOR 1986–2005 (BASED ON A 0.25 DEGREE GRID). FOR CLARITY, 27 °C IS SHOWN WITH A SOLID BLACK LINE. IN (B) THE SAME CONTOUR FROM THE ORIGINAL CLIMATE IS PLOTTED AS DOTTED LINE.

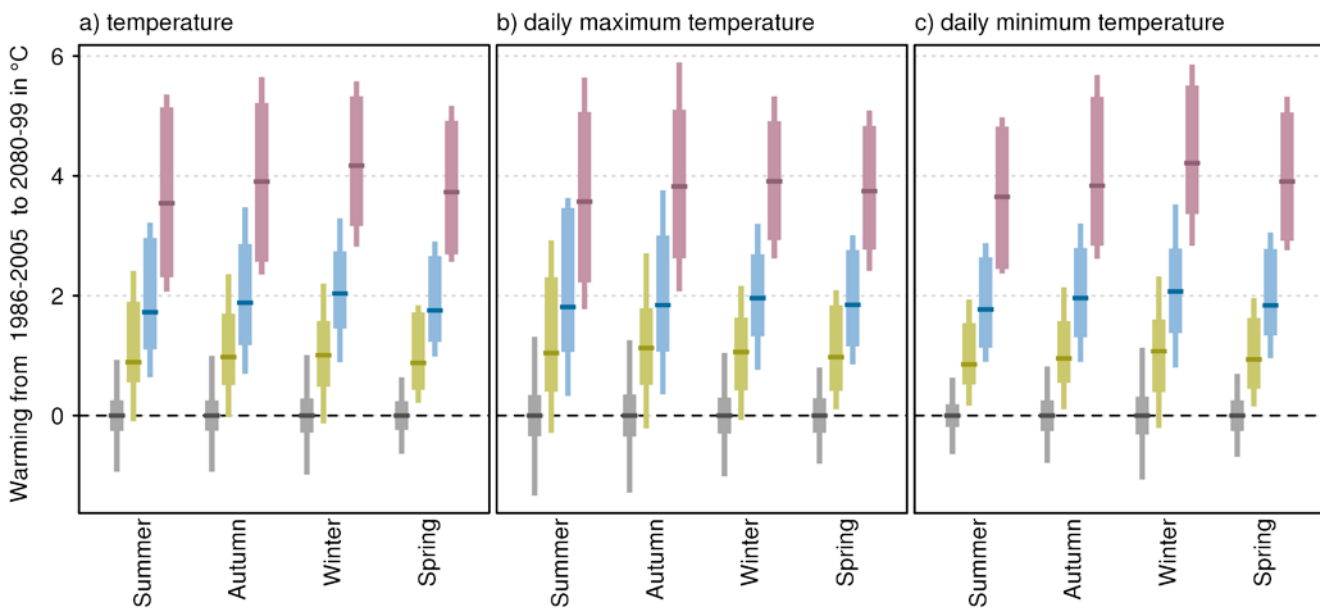


FIGURE 4.2.6: PROJECTED SEASONAL SURFACE AIR TEMPERATURE CHANGES FOR 2090. GRAPHS SHOW CHANGES TO THE (A) MEAN, (B) DAILY MAXIMUM AND (C) DAILY MINIMUM TEMPERATURE. TEMPERATURE ANOMALIES ARE GIVEN IN °C WITH RESPECT TO 1986–2005 UNDER RCP2.6 (GREEN), RCP4.5 (BLUE) AND RCP8.5 (PURPLE). NATURAL CLIMATE VARIABILITY IS REPRESENTED BY THE GREY BAR. BAR PLOTS ARE EXPLAINED IN BOX 4.2.



Projected warming in the CMIP5 models is similar across the four standard seasons in the Monsoonal North, with some models simulating somewhat larger warming in winter than in other seasons. Warming is also broadly similar if maximum or minimum temperatures are considered rather than mean temperatures (Figure 4.2.6 and Appendix Table 1).

Downscaling methods generally do not lead to projected warming ranges that differ from those simulated by the CMIP5 GCM ensemble. No significantly different trends are seen for the dynamical downscaling method (CCAM), with strong overlap in model ensemble spread for downscaled results and GCM results for each season. For the statistical downscaling method (SDM), the seasonal warming in maximum temperature is around half a degree less than in the CMIP5 models (except in winter where it is slightly higher). The ensemble spread is also reduced in all cases (except winter). Figure 4.2.7 presents a comparison of downscaling results and GCM results, and shows simulated change in 2090 following RCP8.5 (which gives the strongest climate change response, and hence best illustrates the differences between methods).

Taking into consideration the strong agreement on the direction and magnitude of change among GCMs and downscaling results, and the robust understanding of the driving mechanisms of warming and its seasonal variation, there is *very high confidence* in substantial increase in temperature for the Monsoonal North cluster for the annual and seasonal projections for mean, maximum and minimum surface air temperature.

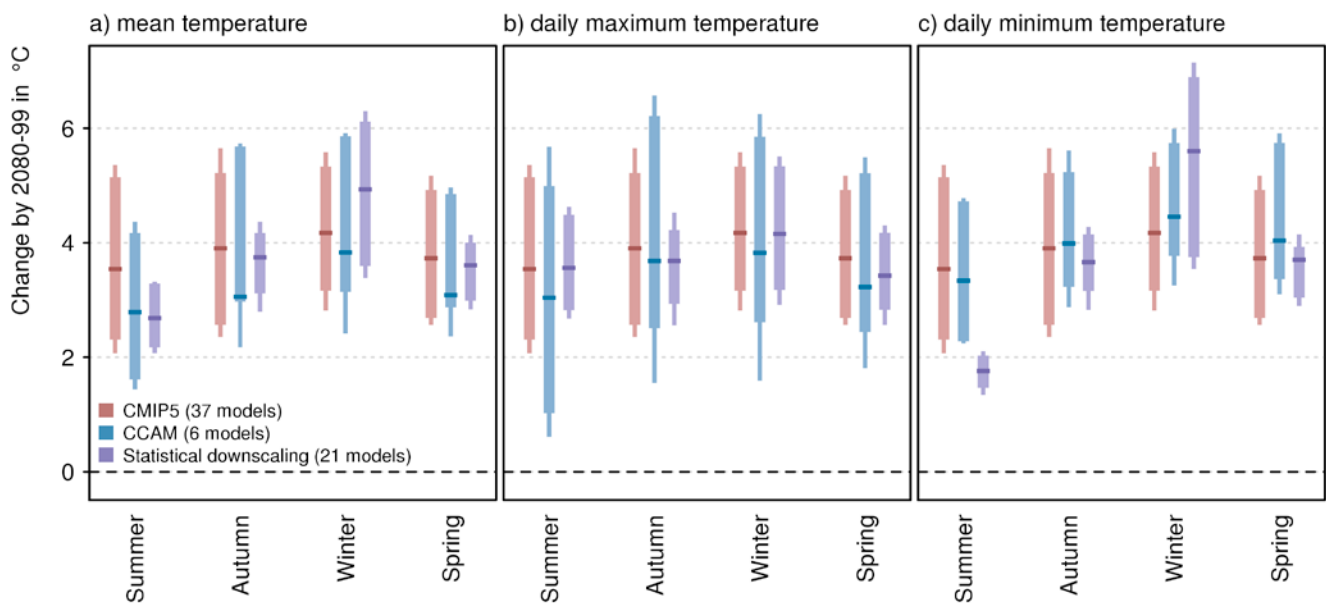


FIGURE 4.2.7: PROJECTED CHANGE IN MONSOONAL NORTH SEASONAL SURFACE AIR TEMPERATURE FOR 2090 USING CMIP5 GCMs AND TWO DOWNSCALING METHODS (CCAM AND SDM) UNDER RCP8.5 FOR THE (A) MEAN, (B) DAILY MAXIMUM AND (C) DAILY MINIMUM. TEMPERATURE ANOMALIES ARE GIVEN IN °C WITH RESPECT TO THE 1986–2005 MEAN. BAR PLOTS ARE EXPLAINED IN BOX 4.2.

4.2.1 EXTREMES

Changes to temperature extremes often lead to greater impacts than changes to the mean. To assess impact on extremes, researchers examine CMIP5 projected changes in measures of warm spell duration (see definition below) and the warmest day in the year.

Heat-related extremes are projected to increase at the same rate as projected mean temperatures with a substantial increase in the number of warm spell days. Figure 4.2.8 (2090 case only) gives the CMIP5 model simulated warming on the hottest day of the year averaged across the cluster, and the corresponding warming for the hottest day in 20 years (20-year return value, equal to a 5 % chance of occurrence within any one year). The rate of warming for these hot days is similar to that for all days (*i.e.* the average warming in the previous section). The GCM projections also indicate a marked increase in a warm spell index, which is defined as the annual count of days for events with at least six consecutive days with a cluster average temperature maximum above the 90th percentile (as an example, the 90th percentile for daily temperature maximum for Darwin is 34°C based on BOM historical data for January 1910 to June 2014).

Given the similarity in projected warming for the mean and annual daily maximum temperature, an indication of the change in frequency of hot days locally can be obtained by applying the projected changes for maximum temperature for selected time slices and RCPs to the historical daily record at selected sites. This is illustrated in Box 4.3 for Broome, where it can be seen that the number of days above 35 °C by 2090 more than doubles under RCP4.5 and median model warming, and the number of days over 40 °C nearly triples.

Strong model agreement and understanding of physical mechanisms of warming lead to *very high confidence* in a projected substantial increase in temperature of the hottest days, the frequency of hot days and in warm spell duration.

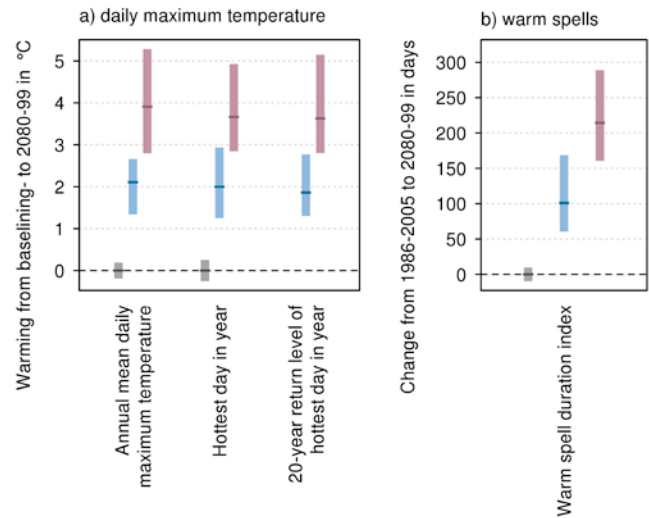


FIGURE 4.2.8: PROJECTED CHANGES IN SURFACE AIR TEMPERATURE EXTREMES BY 2090 IN (A) MEAN DAILY MAXIMUM TEMPERATURE, HOTTEST DAY OF THE YEAR AND THE 20-YEAR RETURN VALUE OF THE HOTTEST DAY OF THE YEAR (°C); AND (B) CHANGE IN THE NUMBER OF DAYS IN WARM SPELLS FOR MONSOONAL NORTH (SEE TEXT FOR DEFINITION OF VARIABLES). RESULTS ARE SHOWN FOR EMISSION SCENARIOS RCP4.5 (BLUE) AND RCP8.5 (PURPLE) RELATIVE TO THE 1986–2005 MEAN. NATURAL CLIMATE VARIABILITY IS REPRESENTED BY THE GREY BAR. BAR PLOTS ARE EXPLAINED IN BOX 4.2.

BOX 4.3: HOW WILL THE FREQUENCY OF HOT DAYS CHANGE IN DARWIN, BROOME AND CAIRNS?

To illustrate what the CMIP5 projected warming implies for changes to the occurrence of hot days at a station in Monsoonal North, a simple downscaling example is conducted for Darwin, Broome and Cairns. Although from an adjacent cluster, results from Cairns are given as indicative of sites in the far east of the Monsoonal North.

The type of downscaling used here is commonly referred to as 'change factor approach' (see Section 6.3.1. in the

Technical Report), whereby a change (calculated from the simulated model change) is applied to an observed time series. In doing so, it is possible to estimate the frequency of extreme days under different emission scenarios.

In Table B4.3, days with maximum temperatures above 35 and 40 °C are provided for a number of locations for a 30-year period (1981–2010), and for downscaled data using seasonal change factors for maximum temperature for 2030 and 2090 under different RCPs.

TABLE B4.3: CURRENT AVERAGE ANNUAL NUMBER OF DAYS (FOR THE 30-YEAR PERIOD 1981–2010) ABOVE 35 AND 40 °C FOR DARWIN AIRPORT (NT), BROOME AIRPORT (WA) AND CAIRNS AIRPORT (QLD) BASED ON ACORN-SAT. ESTIMATES FOR THE FUTURE ARE CALCULATED USING THE MEDIAN CMIP5 WARMING FOR 2030 AND 2090, AND WITHIN BRACKETS THE 10TH AND 90TH PERCENTILE CMIP5 WARMING FOR THESE PERIODS, APPLIED TO THE 30-YEAR ACORN-SAT STATION SERIES. NUMBERS ARE TAKEN FROM TABLE 7.1.2 AND TABLE 7.1.3 IN THE TECHNICAL REPORT.

THRESHOLD	CURRENT	DARWIN FUTURE PROJECTED DAYS WITH TMAX GREATER THAN THRESHOLD			
		2030 RCP4.5	2090 RCP2.6	2090 RCP4.5	2090 RCP8.5
Over 35 °C	11	43 (25 to 74)	52 (24 to 118)	111 (54 to 211)	265 (180 to 322)
Over 40 °C	0	0.0 (0.0 to 0.0)	0.0 (0.0 to 0.0)	0.0 (0.0 to 0.2)	1.3 (0.2 to 11)

THRESHOLD	CURRENT	BROOME FUTURE PROJECTED DAYS WITH TMAX GREATER THAN THRESHOLD			
		2030 RCP4.5	2090 RCP2.6	2090 RCP4.5	2090 RCP8.5
Over 35 °C	56	87 (72 to 111)	95 (70 to 154)	133 (94 to 204)	231 (173 to 282)
Over 40 °C	4	7.2 (6.0 to 9.3)	7.7 (5.7 to 13)	11 (7.7 to 22)	30 (17 to 61)

THRESHOLD	CURRENT	CAIRNS FUTURE PROJECTED DAYS WITH TMAX GREATER THAN THRESHOLD			
		2030 RCP4.5	2090 RCP2.6	2090 RCP4.5	2090 RCP8.5
Over 35 °C	3	5.5 (4.4 to 7.9)	5.5 (4.4 to 14)	11 (7.4 to 22)	48 (24 to 105)
Over 40 °C	0	0.1 (0.1 to 0.2)	0.1 (0.1 to 0.3)	0.3 (0.2 to 0.4)	0.7 (0.5 to 2.0)

4.3 RAINFALL

The linear trend in annual rainfall for 1900–2012 (Figure 4.3.1) suggests an overall slight increase of about 20 mm/decade (MNW) and 10 mm/decade (MNE) respectively. As is shown in Figure 4.3.1, this increase is non-linear with alternating decades of wetter and drier conditions throughout the 20th century.

During much of the early part of the 20th century, the cluster experienced drier conditions, particularly in the north-west. This included the Australia-wide Federation drought at the start of the century and the World War II drought a few decades later (Figure 4.3.1). The latter part of the 20th century saw more variable conditions with individual years of very high rainfall, and sequences of years with below average rainfall (late 1980s and early 1990s) and above average rainfall (since the mid-1990s in the MNW). The recent increases in annual rainfall are at a rate of 82 mm/decade (MNW) and 84 mm/decade (MNE; Figure 4.3.2).

The largest increases in rainfall since the 1980s are found in summer (increased monsoonal rainfall) and autumn (possible extension of wet season rainfall). The impact of tropical cyclones on total annual rainfall is clearly visible in Figure 4.3.1 with some of the largest interannual variability originating from these years. Similarly, strong La Niña

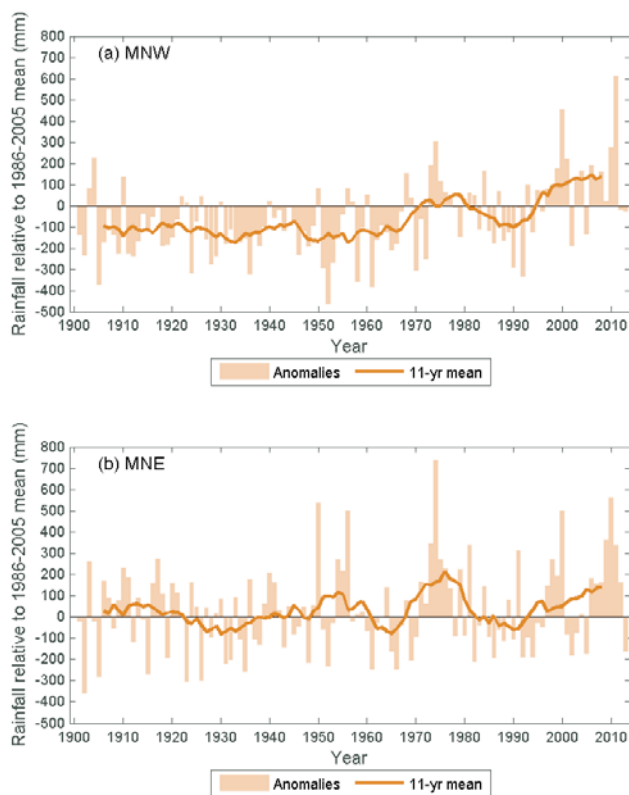


FIGURE 4.3.1: OBSERVED ANNUAL RAINFALL ANOMALIES (MM) FOR 1901-2013, COMPARED TO THE BASELINE 1986–2005 FOR (A) MONSOONAL NORTH WEST AND (B) MONSOONAL NORTH EAST. DATA ARE FROM AWAP.

events also contributed to this large variability. Despite these recent increases across most of tropical Australia, coastal regions of the tropical east coast have experienced decreases (Figure 4.3.2).

Spatial trend patterns for the full duration of the rainfall record (1901–2012) show minor increases in summer and autumn (about 5–10 mm/decade) over the western parts of Monsoonal North cluster (Figure 4.3.2a and b). Coastal eastern Monsoonal North regions show minor decreases. Winter trends are very small and occur against the backdrop of very low climatological rainfall totals. Somewhat stronger trends are seen in the more recent period (1960–2012), especially during summer (Figure 4.3.2e) where some MNW regions show increases above 40 mm/decade. Increases are also observable at the Gulf of Carpentaria and along the east coast of tropical Queensland. The MNW regions and Gulf of Carpentaria also show these increasing trends extended into the autumn season (Figure 4.3.2f; possibly hinting at longer wet seasons over the recent decades), but not along the tropical east coast where areas of decreasing trends expand.

This feature is somewhat reversed during the monsoon build-up season (spring; Figure 4.3.2h) where recent trends are mostly positive along the east coast and slightly negative across the Top End. The statistical significance of trends in monsoonal rainfall is difficult to determine due to high intrinsic variability in the summer monsoon, but the increase in monsoonal rainfall has been large enough to increase total Australian rainfall (averaged over the entire continent). Additionally, more recent rainfall during the monsoon season from 2000 to 2012 was very much above average over large parts of the continent. The period 2010 – 2012 recorded the highest 24-month rainfall totals for Australia as a whole, in conjunction with two strong La Niña events.

The projected changes for the future provide minimal guidance in terms of the direction of change, as some CMIP5 models simulate increases while others simulate decreases (Figure 4.3.3). Simulated annual rainfall changes for the 21st century are also small compared to natural variability under RCP2.6 and RCP4.5, but changes become evident in some models under RCP8.5 by 2090 (see also Table 1 in Appendix). By 2030, natural climate variability will remain the major driver of rainfall changes (changes of around +/- 10%). For late this century (2090) the magnitude of possible annual differences from the climate of 1986–2005 indicated by GCM results range up to -25 to +25% under RCP8.5.

Changes to the spatial distribution of rainfall in the cluster can be illustrated by adding the CMIP5 projected change in annual mean rainfall onto the observed climatology. Figure 4.3.4 gives an example of this for 2090 under RCP8.5. The figure displays the dry (10th percentile) and wet (90th percentile) case of the simulated model range relative to the observed climatology. For the drier case, characteristic rainfall rates decrease from about 1 to 2 mm/day to 0.7 to 1.5 mm/day, while for the wetter case, rates increase to about 1.5 to 2.5 mm/day. More substantial increases are seen along the tropical east coast, Cape York and the tip of the Northern Territory.

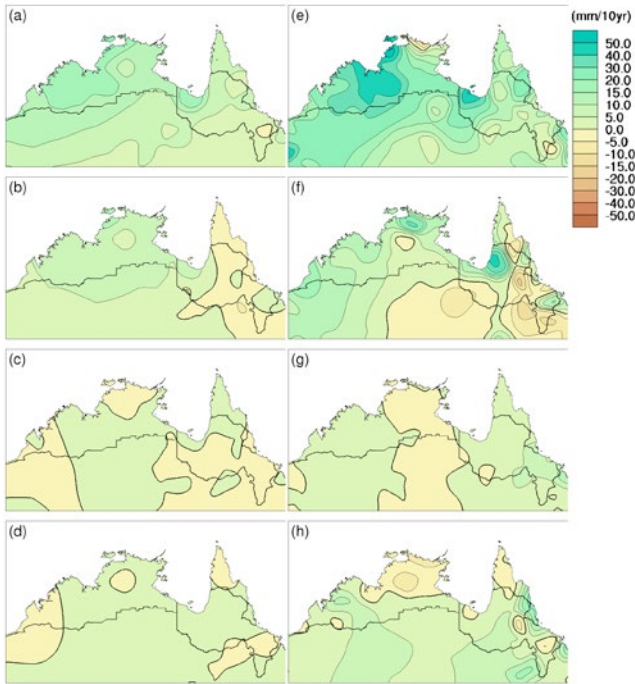


FIGURE 4.3.2: MAPS OF SEASONAL RAINFALL TRENDS (MM/DECADE). THE LEFT COLUMN OF MAPS SHOWS TRENDS FOR (A) SUMMER, (B) AUTUMN, (C) WINTER AND (D) SPRING FOR 1901–2013. THE RIGHT COLUMN SHOWS TRENDS FOR (E) SUMMER, (F) AUTUMN, (G) WINTER AND (H) SPRING FOR 1960–2013.

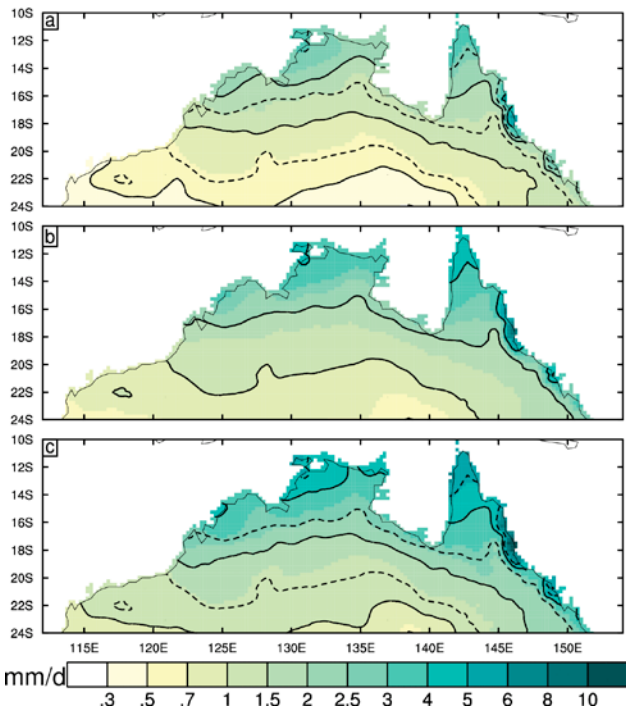


FIGURE 4.3.4: ANNUAL MEAN RAINFALL (MM/DAY), FOR THE PRESENT CLIMATE (B), AND FOR DRIER CONDITIONS (A) OR WETTER CONDITIONS (C). THE PRESENT IS USING THE AWAP DATA SET FOR 1986–2005 (BASED ON A 0.25 DEGREE LONGITUDE-LATITUDE GRID). THE DRIER AND WETTER CASES USE THE 10TH AND 90TH PERCENTILES AT 2090 FOR RCP8.5 (UNDER A GLOBAL WARMING OF 3.7 °C CASE). FOR CLARITY, THE 0.5, 1, 2 AND 4 MM/DAY CONTOURS ARE PLOTTED WITH SOLID BLACK LINES. IN (A) AND (C) THE SAME CONTOURS FROM THE ORIGINAL CLIMATE (B) ARE PLOTTED AS DOTTED LINES.

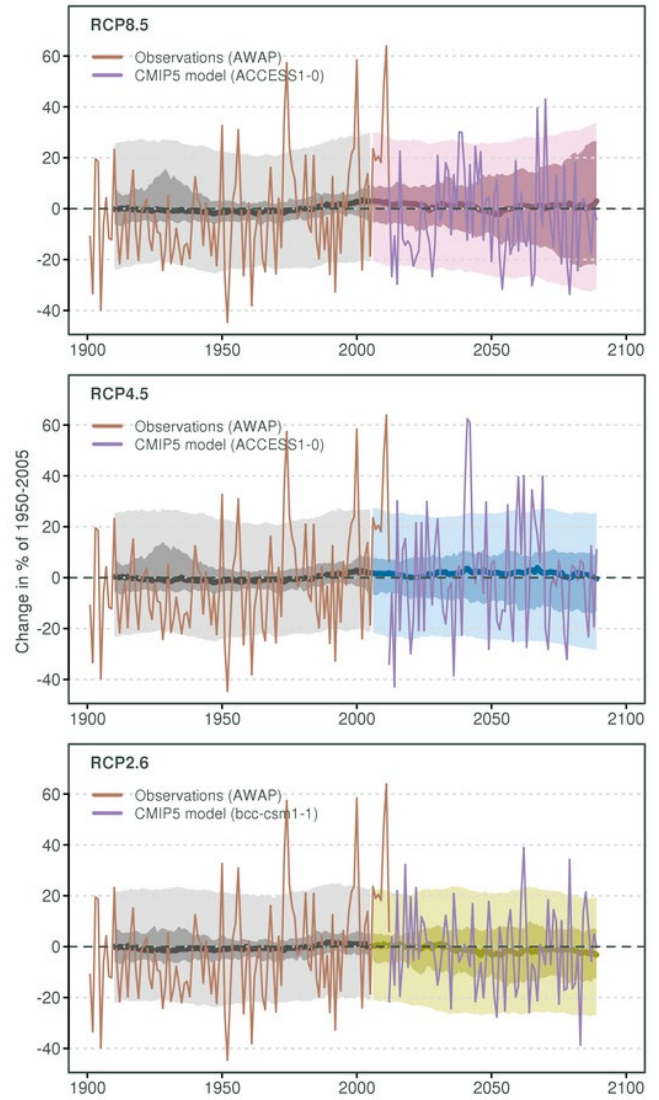


FIGURE 4.3.3: TIME SERIES FOR MONSOONAL NORTH ANNUAL RAINFALL FOR 1910–2090, AS SIMULATED IN CMIP5 EXPRESSED AS A PERCENTAGE RELATIVE TO THE 1950–2005 MEAN. THE CENTRAL LINE IS THE MEDIAN VALUE, AND THE SHADING IS THE 10TH AND 90TH PERCENTILE RANGE OF 20-YEAR MEANS (INNER) AND SINGLE YEAR VALUES (OUTER). THE GREY SHADING INDICATES THE PERIOD OF THE HISTORICAL SIMULATION, WHILE THREE FUTURE SCENARIOS ARE SHOWN WITH COLOUR-CODED SHADING: RCP8.5 (PURPLE), RCP4.5 (BLUE) AND RCP2.6 (GREEN). AWAP OBSERVATIONS (BEGINNING 1901) AND PROJECTED VALUES FROM A TYPICAL MODEL ARE SHOWN. TIME SERIES PLOTS ARE EXPLAINED IN BOX 4.2.

In summer most (but not all) models show changes that are not clearly different to that of natural variability, even in 2090 (Figure 4.3.5 and Appendix Table 1). In the near future (2030), the magnitude of possible summer differences from the climate of 1986–2005 is around +/-10 %, and late in the century is around -15 to +10 % under RCP4.5 and from -25 to +20 % under RCP8.5. The widening of the model envelope for the 20-year averages (the dark band) under higher emission scenarios, suggests an increase in model spread (Figure 4.3.3a). That is, the signal of individual models (of either direction) becomes increasingly stronger under higher emission concentrations. Such contrasting model simulations highlight the need to consider the possibility of both drier and wetter conditions in impact assessments in this cluster.

Among the other seasons, there is an indication of a slight decline in spring by 2090 (model range from around -45 to +30 % under RCP8.5). Overall, the magnitude of possible differences for these other seasons from the climate of 1986–2005 is around -25 to +25 % in 2030, and around -30 to +30 % under RCP4.5 in 2090 and -45 to +45 % under RCP8.5 in 2090 (Figure 4.3.5 and Appendix Table 1).

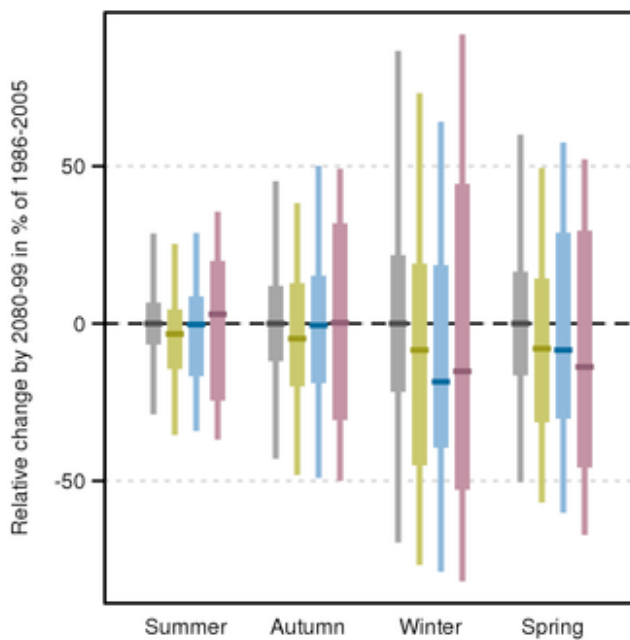


FIGURE 4.3.5: PROJECTED SEASONAL RAINFALL CHANGES FOR MONSOONAL NORTH. RAINFALL ANOMALIES ARE GIVEN IN PER CENT WITH RESPECT TO THE 1986–2005 MEAN UNDER RCP2.6 (GREEN), RCP4.5 (BLUE) AND RCP8.5 (PURPLE) FOR 2090. NATURAL CLIMATE VARIABILITY IS REPRESENTED BY THE GREY BAR. BAR PLOTS ARE EXPLAINED IN BOX 4.2.

Downscaled rainfall projections from the statistical downscaling method for the Monsoonal North cluster (Figure 4.3.6) are broadly similar to the GCM results, with similar median changes for all seasons and a similar ensemble spread. The CCAM dynamical downscaling gives a more unclear picture. While the summer and autumn rainfall projections are very similar to the GCM projections both in median and spread, the winter and spring projections show significant increases in the dynamical downscaling compared to the GCM’s decreases or no change. One possible explanation is the uneven sampling: only six models were used in the dynamical downscaling method, while 22 models were used in the statistical downscaling method.

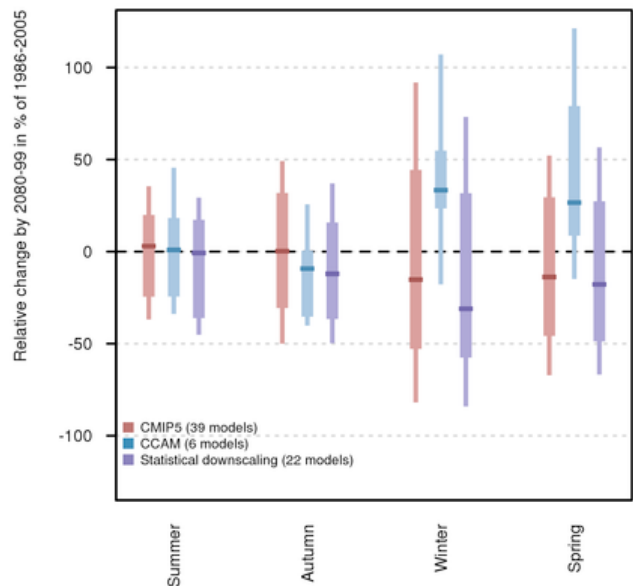


FIGURE 4.3.6: PROJECTED CHANGE IN MONSOONAL NORTH SEASONAL RAINFALL FOR 2090 USING CMIP5 GCMs AND TWO DOWNSCALING METHODS (CCAM AND STATISTICAL) UNDER RCP8.5. RAINFALL ANOMALIES ARE GIVEN IN PER CENT WITH RESPECT TO 1986–2005. BAR PLOTS ARE EXPLAINED IN BOX 4.2.

In summary, there is *high confidence* that natural climate variability will remain the major driver of rainfall changes in the next few decades in this cluster. There is generally *low confidence* in projected rainfall changes in this cluster for later in the century for all seasons except for a slight decrease in spring. This is because of the large differences between GCM projections, and because different processes, such as monsoon onset, MJO and tropical circulation, can have opposite impacts on model-projected rainfall changes. Furthermore, there is a large spread in the skill of models in simulating these processes, and GCMs may not adequately represent the influence of eastern seaboard orography on rainfall. While there is some evidence for a rainfall decrease during spring, there is *low confidence* in this particular projection.

4.3.1 HEAVY RAINFALL EVENTS

In a warming climate, heavy rainfall events are expected to increase in magnitude mainly due to a warmer atmosphere being able to hold more moisture (Sherwood *et al.*, 2010).

For the Monsoonal North, the CMIP5 models also simulate an increase in the magnitude of the annual maximum 1-day rainfall and the magnitude of the 20-year return value of maximum 1-day rainfall for 2090 (Figure 4.3.7 for RCP8.5); where a 20-year return value is equivalent to a 5 % chance of occurrence within any one year. Comparing the trend in the two extreme indices with that of the annual mean rainfall (Figure 4.3.7) clearly shows that while the projection for mean rainfall is showing no tendency for increases in the cluster, the extremes are projected to increase. This pattern (change in mean relative to extremes) is found in all other NRM clusters, and is also supported by results from other studies (see Technical Report, section 7.2.2)

The magnitudes of the simulated changes in extreme rainfall indices are strongly dependent on emission scenario and time in the future. Furthermore, magnitude of changes simulated by GCMs is less certain because many of the smaller scale systems that generate extreme rainfall are not well resolved by GCMs (Fowler and Ekstroem, 2009). In summary, there is *high confidence* that the intensity of heavy rainfall events will increase in the cluster, but there is *low confidence* in the magnitude of change, and thus the time when any change may be evident against natural fluctuations, cannot be reliably projected.

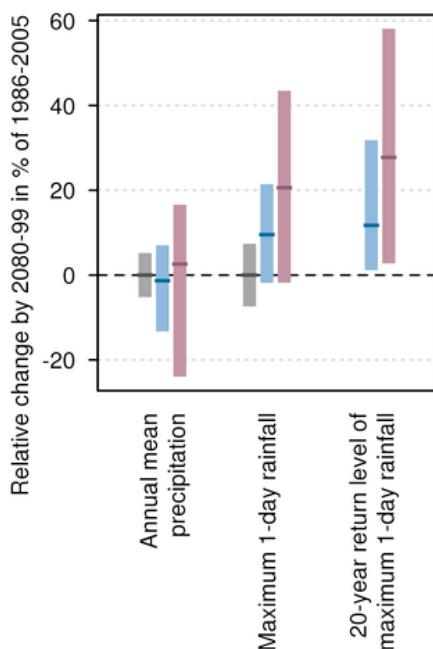


FIGURE 4.3.7: PROJECTED CHANGES IN MEAN RAINFALL, INTENSITY OF ANNUAL MAXIMUM 1-DAY RAINFALL AND INTENSITY OF THE 20-YEAR RETURN VALUE FOR THE 1-DAY RAINFALL FOR THE SOUTHERN SLOPES CLUSTER (SEE TEXT FOR DEFINITION OF VARIABLES). CHANGES ARE GIVEN IN % WITH RESPECT TO THE 1986-2005 MEAN FOR RCP4.5 (BLUE) AND RCP8.5 (PURPLE). NATURAL CLIMATE VARIABILITY IS REPRESENTED BY THE GREY BAR. BAR PLOTS ARE EXPLAINED IN BOX 4.2.

4.3.2 DROUGHT

The Monsoonal North cluster was clearly affected by the Federation drought and the World War II drought in the early part of the 20th century (Figure 4.2.1). However, the Millennium drought was not as pronounced in the Monsoonal North as it was in the clusters further south and east – regions that display positive trends for both drought events and duration, but negative trends in intensity for the 1960–2009 period (Gallant *et al.*, 2007). Because of the persistent droughts foremost in the early part of the 20th century, linear trends of drought characteristics in the Monsoonal North cluster over the historical record (1911–2009) are largely negative in terms of the number of events and duration, but positive with respect to intensity (Gallant *et al.*, 2013).

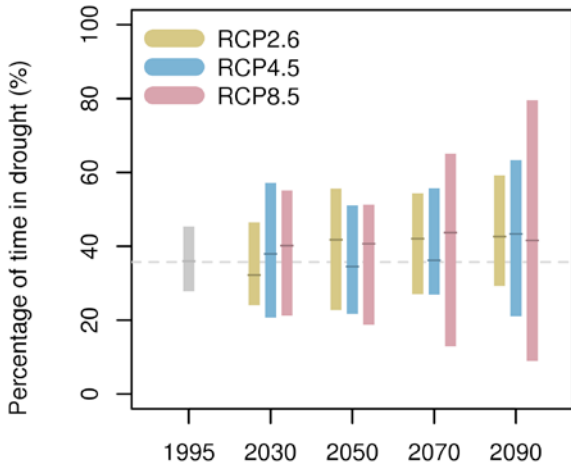
To assess the implications of projections for drought occurrence, researchers selected a measure of meteorological drought, the Standardised Precipitation Index (SPI). Total time spent in drought and changes to the duration and frequency of individual droughts were calculated. Section 7.2.3 of the Technical Report presents details on calculation of the SPI, as well as further information on drought.

Projected changes to drought share much of the uncertainty of mean rainfall change, so there is not a clear indication on changes to drought conditions in the cluster (Figure 4.3.8). Under RCP8.5, there is an increase in the proportion of time spent in drought through the century; however the picture is less clear for RCP4.5. Projections of extreme drought duration generally show little change for the first half of the century for all emission scenarios. The 90th percentiles of the model range under RCP8.5 suggest that extreme drought duration could increase in some models with not much change to their frequency, but other models (see 10th percentile) show change in the opposite direction for the change in duration.

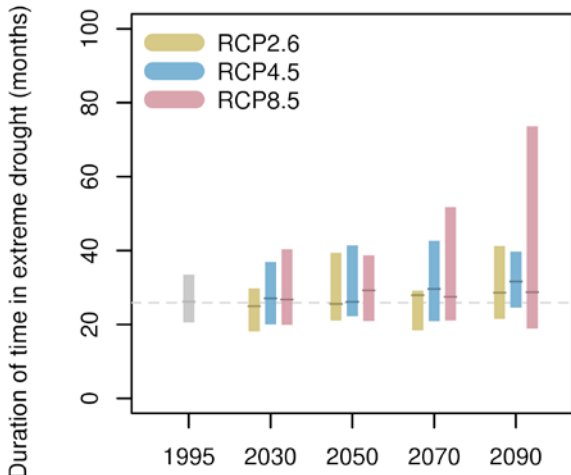
This is also supported by projections of increases in rainfall variability both on inter-annual and intra-seasonal scales which could lead to increased drought duration and frequency. Given the importance of the ENSO for rainfall in the Monsoonal North cluster, it is worth noting that there is some indication that these events will intensify under global warming, which would lead to an intensification of El-Niño driven drying in this cluster (Power *et al.*, 2013).

Meteorological drought will continue to be a regular feature of regional climate. It may change its characteristics as the climate warms, but there is *low confidence* in projections of how the frequency and duration of extreme drought may change.

Projections of time spent in drought (SPI<-1) for Monsoonal North



Projections of extreme drought duration for Monsoonal North



Projections of extreme drought frequency for Monsoonal North

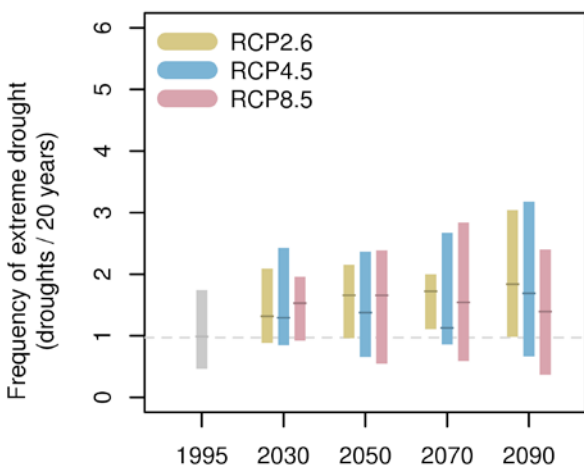


FIGURE 4.3.8: BAR GRAPHS OF THE STANDARDISED PRECIPITATION INDEX (SPI); THE OUTLINE OF THE BAR INDICATING THE EXTENT OF THE 10TH TO 90TH PERCENTILE RANGE, THE THICK CENTRE LINE THE MEDIAN. THE TOP PANEL SHOWS THE MULTI-MODEL ENSEMBLE OF PERCENTAGE TIME IN DROUGHT FOR FIVE DIFFERENT 20-YEARS TIME PERIODS FOLLOWING RCP2.6 (GREEN), RCP4.5 (BLUE) AND RCP8.5 (PURPLE). THE GREY BAR SHOWS AN ESTIMATE OF NATURAL VARIABILITY AS SIMULATED BY THE MODELS. THE MIDDLE AND BOTTOM PANEL SHOW, RESPECTIVELY, PROJECTED DURATION AND FREQUENCY OF EXTREME DROUGHT. BAR PLOTS ARE EXPLAINED IN BOX 4.2.

4.4 WINDS, STORMS AND WEATHER SYSTEMS

4.4.1 MEAN WINDS

The surface wind climate is driven by the large-scale circulation pattern of the atmosphere: when pressure gradients are strong, winds are strong. For the Monsoonal North cluster, mean surface winds over most of the year are dominated by easterly and south-easterly winds associated with the south-east trade winds. During spring they become more easterly. However, over the wet season, north-westerly winds associated with the north-west monsoon are more prevalent. The southward extent of the monsoon trough often determines how far inland the monsoon westerly wind domain reaches. Any trends in observed winds are difficult to establish due to sparse coverage of wind observations and difficulties with instruments and the changing circumstances of anemometer sites (Jakob, 2010). McVicar *et al.* (2012) and Troccoli *et al.* (2012) have reported weak and conflicting trends across Australia (although they considered winds at different altitudes).

Projected changes to seasonal surface winds for Monsoonal North are small (about -4 to +3 % seasonally) for 2030 under all RCPs (Appendix Table 1). For 2090, changes are still small under RCP4.5 with medium to high agreement amongst models on little change. For RCP8.5 there is high agreement amongst models on an increase in spring (0 to 8%) and whilst there is medium agreement on little change in both summer and autumn (see Appendix Table 1), some models suggest the potential for a substantial increase in summer and a decrease in autumn (Figure 4.4.1). The spring increases for the high emission scenario could be related to a stronger easterly flow in the trade wind regime and are present in projections for MNE and the Wet Tropics clusters (see corresponding Regional Report).

Taking this into account, there is *high confidence* in little change for the near future (2030) in all seasons. For later in the century (2090), there is only *medium confidence* in little change. Substantial changes are present in some models, seasons and part of the cluster (particularly increase in spring and decreases in autumn under RCP8.5).



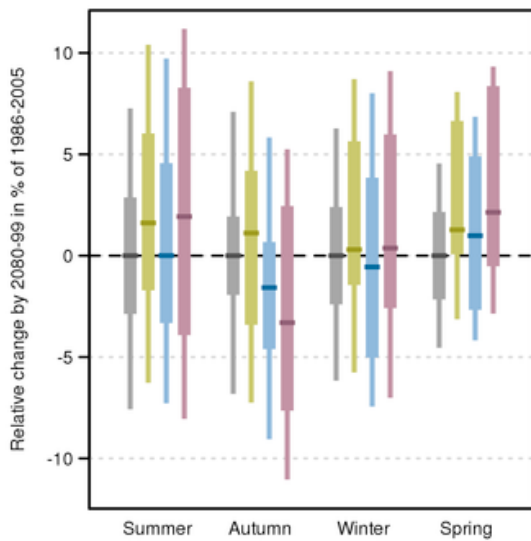


FIGURE 4.4.1: PROJECTED NEAR-SURFACE WIND SPEED CHANGES FOR 2090 FOR MONSOONAL NORTH. ANOMALIES ARE GIVEN IN PERCENT WITH RESPECT TO THE 1986–2005 MEAN FOR RCP2.6 (GREEN), RCP4.5 (BLUE) AND RCP8.5 (PURPLE), WITH GREY BARS SHOWING THE EXTENT OF NATURAL CLIMATE VARIABILITY. BAR PLOTS ARE EXPLAINED IN BOX 4.2.

EXTREME WINDS

Extreme winds create hazardous conditions for marine and terrestrial based activities and infrastructure and may change with climate change. Figure 4.4.2 compares the change in annual wind speed by 2090 with the changes projected for two extreme wind metrics. For the high emission scenario the extreme wind metrics follow the trend for mean winds. That is, an increase in annual maximum daily wind speed and 20-year return values (equivalent to a 5% chance occurrence within any one year), although the range of change shows a large spread across the models with some showing strong decrease. For RCP4.5, there is little change in the 20-year return level whereas the median change in annual maximum daily wind speed is for a decrease. Because of the various shortcomings associated with modelling extremes in near-surface winds, including the inability of GCMs to resolve small scale meteorological systems that contribute to extreme winds such as tropical cyclones (see further details in the Technical Report Chapter 7.3) there is generally *low confidence* in wind projections in the Monsoonal North.

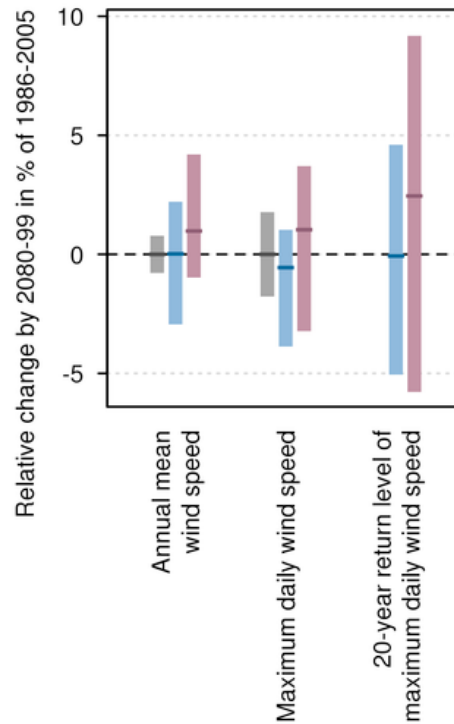


FIGURE 4.4.2: PROJECTED NEAR-SURFACE ANNUAL MEAN WIND SPEED, ANNUAL MAXIMUM DAILY WIND SPEED AND THE 20-YEAR RETURN VALUE FOR THE ANNUAL MAXIMUM DAILY WIND SPEED FOR 2090 FOR MONSOONAL NORTH. ANOMALIES ARE GIVEN IN PER CENT WITH RESPECT TO THE 1986–2005 MEAN FOR RCP2.6 (GREEN), RCP4.5 (BLUE) AND RCP8.5 (PURPLE) WITH GREY BARS SHOWING THE EXTENT OF NATURAL CLIMATE VARIABILITY. BAR PLOTS ARE EXPLAINED IN BOX 4.2.

TROPICAL CYCLONES

Tropical cyclones and associated severe winds can directly impact the entire Monsoonal North coastline and associated heavy rain can extend to areas further inland. Projected changes of tropical cyclone frequency have been assessed in the current generation of GCMs over the Australian north-east and north-west regions, from both the large-scale environmental conditions that promote cyclones and from direct simulation of cyclone-like synoptic features (see Section 7.3.3 of the Technical Report). Results in both the north-east and north-west regions generally indicate a decrease in the formation of tropical cyclones. These results are broadly consistent with current projections of cyclones over the globe (IPCC, 2013; section 14.6.1), which indicate little change through to substantial decreases in frequency. It is also anticipated that the proportion of the most intense storms will increase over the century while the intensity of associated rainfall may increase further, as can be anticipated from section 4.3.1 of this report. In summary, based on global and regional studies, tropical cyclones are projected with *medium confidence* to become less frequent with increases in the proportion of the most intense storms.

4.5 SOLAR RADIATION

Projected changes to solar radiation in the Monsoonal North cluster are summarised for a range of time periods and two emission scenarios in Table 1 (Appendix) and results for 2090 are shown in Figure 4.7.1.

By 2030, the CMIP5 models overall simulate little change in radiation (about -2 to +2 %) for both RCP4.5 and RCP8.5, and for 2090, projected seasonal changes are generally less than +/- 5 %, with some tendency for decrease (Appendix Table 1, Figure 4.7.1). However, an Australian model evaluation suggested some models are not able to adequately reproduce the climatology of solar radiation (Watterson *et al.*, 2013). Globally, CMIP3 and CMIP5 models appear to underestimate the observed trends in some regions due to underestimation of aerosol direct radiative forcing and/or deficient aerosol emission inventories (Allen *et al.*, 2013). Taking this into account, there is *high confidence* in little change for 2030, whereas by 2090 under RCP8.5, larger changes in radiation are present in some models (mainly decreases), but the causes of these changes are not well understood and these projections are of *low confidence*.

4.6 RELATIVE HUMIDITY

CMIP5 projections of relative humidity in Monsoonal North indicate an overall tendency for decrease (Figure 4.7.1). For 2030, seasonal reductions for both RCP4.5 and 8.5 are generally smaller than -3 % and projected increases less than 2 %, for both scenarios, and there is medium or high model agreement on little change. For 2090, reductions are more marked, particularly in autumn and winter with projected ranges of -6 to +1 % under RCP4.5 and -8 to +3 % under RCP8.5 (Appendix Table 1). A decrease in relative humidity away from coasts is expected because of an increase in the moisture holding capacity of a warming atmosphere and the greater warming of land compared

to sea. This would lead to increases in relative humidity over ocean and decreases over continents. This general tendency for decrease can be counteracted by a strong rainfall increase. Taking this and the CMIP5 projections into account, there is *high confidence* in little change for the near future (2030), and there is *medium confidence* in a decrease in relative humidity by 2090.

4.7 POTENTIAL EVAPOTRANSPIRATION

Projected changes for potential evapotranspiration using Morton’s wet-environmental potential evapotranspiration (McMahon *et al.*, (2013) and Technical Report section 7.6) suggest increases for all seasons in Monsoonal North (*high confidence*, Figure 4.7.1). In relative terms, there are somewhat larger increases in autumn and winter relative to summer and spring. Projected changes for autumn, winter and spring for 2030 are around 2 to 6 % (about 1 to 5 % for summer) and for 2090 are about 5 to 10 % (about 2 to 10 % for summer) for RCP4.5 and 10 to 20% (about 5 to 15 % for summer) for RCP8.5 (Table 1 in Appendix).

As described in section 7.6 in the Technical Report, despite having *high confidence* in an increase, as supported by very high model agreement, there is only *medium confidence* about the magnitude of the increase. The method is able to reproduce the spatial pattern and the annual cycle of the observed climatology and there is theoretical understanding around increases as a response to increasing temperatures and an intensified hydrological cycle (Huntington, 2006), which adds to confidence. However, there has been no clear increase in observed Pan Evaporation across Australia from data available since 1970 (see Technical Report, Chapter 4). Also, earlier GCMs were not able to reproduce the historical linear trends found in Morton’s potential evapotranspiration (Kirono and Kent 2011).

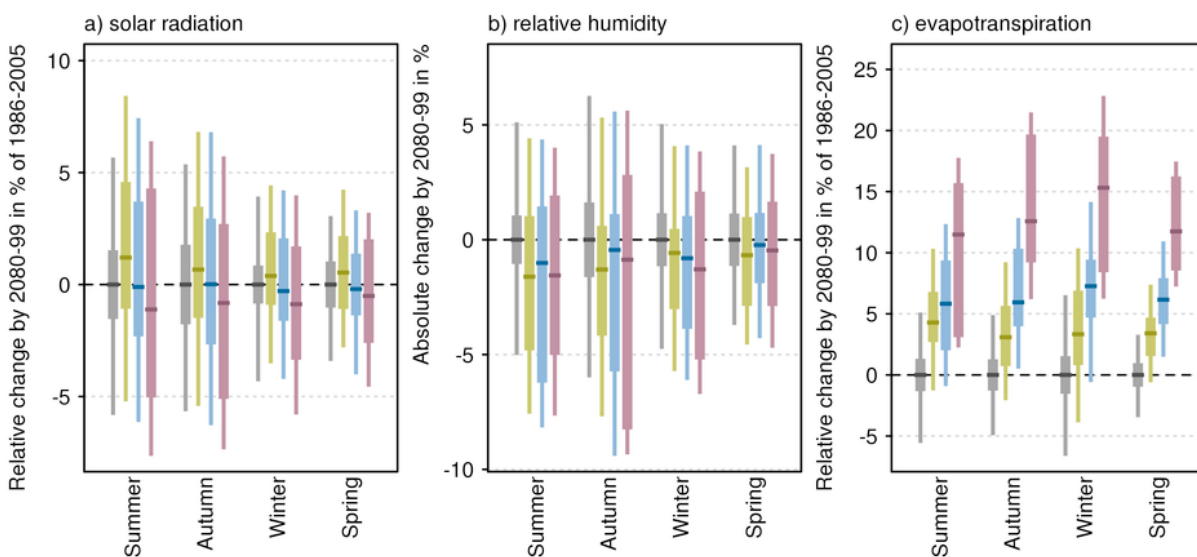


FIGURE 4.7.1: PROJECTED CHANGES IN (A) SOLAR RADIATION (%), (B) RELATIVE HUMIDITY (%), (ABSOLUTE CHANGE) AND (C) WET-ENVIRONMENTAL POTENTIAL EVAPOTRANSPIRATION (%) FOR MONSOONAL NORTH IN 2090. THE BAR PLOTS SHOW SEASONAL PROJECTIONS WITH RESPECT TO THE 1986–2005 MEAN FOR RCP2.6 (GREEN), RCP4.5 (BLUE) AND RCP8.5 (PURPLE), AND THE EXTENT OF NATURAL CLIMATE VARIABILITY IS SHOWN IN GREY. BAR CHARTS ARE EXPLAINED IN BOX 4.2.

SOIL MOISTURE AND RUNOFF

Increases in evaporation rates (Figure 4.7.1) combined with (less certain) changes in rainfall (Figure 4.3.3) will have implications for soil moisture and runoff. However, soil moisture and runoff are difficult to simulate. This is particularly true in GCMs where, due to their relatively coarse resolution, the models cannot simulate much of the rainfall detail that is important to many hydrological processes, such as the intensity of rainfall. For these reasons, and in line with many previous studies, this study does not present directly simulated GCM runoff and soil moisture. Instead, the results of hydrological models forced by CMIP5 simulated rainfall and potential evapotranspiration are presented. Soil moisture is estimated using a dynamic hydrological model based on an extension of the Budyko framework (Zhang *et al.*, 2008), and runoff is estimated by the long-term annual water and energy balance Budyko framework (Teng *et al.*, 2012). Runoff is presented as change in 20-year averages, derived from output of a water balance model. The latter uses input from CMIP5 models as smoothed time series (30-year running means), the reason being that 30 years is the minimum required for dynamic water balance to attain equilibrium using the Budyko framework. For further details on methods (including limitations) see Section 7.7 of the Technical Report.

Some decreases in soil moisture are projected (Figure 4.8.1), with the largest decreases evident in autumn. The annual changes for RCP8.5 by 2090 range from around -13% to +4% with medium model agreement on substantial decrease (Table 1 in Appendix). The percentage changes in soil moisture are strongly influenced by those in rainfall, but tend to be more negative due to the strong increase in potential evapotranspiration. Given the potential limitations of this method, there is only *medium confidence* that soil moisture will decline.

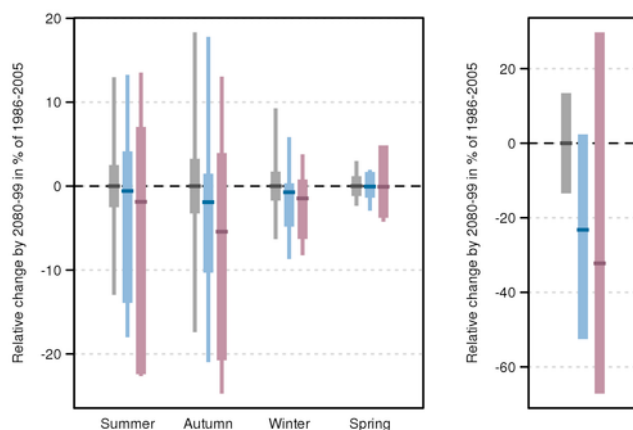


FIGURE 4.8.1: PROJECTED CHANGE (%) IN SEASONAL SOIL MOISTURE (LEFT) AND ANNUAL RUNOFF (RIGHT) FOR 2080-99 WITH RESPECT TO 1986-2005 FOR NATURAL CLIMATE VARIABILITY ONLY (GREY), RCP4.5 (BLUE) AND RCP8.5 (PURPLE). BAR CHARTS ARE EXPLAINED IN BOX 4.2.

For Monsoonal North, runoff could increase or decrease under RCP4.5 and RCP8.5 in 2090, though the majority of models suggest decrease, as indicated by the negative multi-model ensemble median (Figure 4.8.1). The confidence in these projections is *low* because the method used is not able to consider changes to rainfall intensity, seasonality and changes in vegetation characteristics – factors that each could impact future runoff. Further hydrological modelling with appropriate climate scenarios (*e.g.* Chiew *et al.*, 2009) could provide further insights into impacts on future runoff and soil moisture characteristics that may be needed in detailed climate change impact assessment studies.

4.8 FIRE WEATHER

Bushfire occurrence at a given place depends on four ‘switches’: 1) ignition, either human-caused or from natural sources such as lightning; 2) fuel abundance or load (a sufficient amount of fuel must be present); 3) fuel dryness, where lower moisture contents are required for fire, and 4) suitable weather conditions for fire spread, generally hot, dry and windy (Bradstock, 2010). The settings of the switches depend on meteorological conditions across a variety of time scales, particularly the fuel conditions. Given this strong dependency on the weather, climate change will have a significant impact on future fire weather (*e.g.* Hennessy *et al.*, 2005; Lucas *et al.*, 2007; Williams *et al.*, 2009; Clarke *et al.*, 2011; Grose *et al.*, 2014). The study of Clarke *et al.* (2013) shows few significant trends over 1973 to 2010 in observed fire weather across the Monsoonal North cluster.

Fire weather is estimated here using the McArthur Forest Fire Danger Index (FFDI) (McArthur, 1967), which captures two of the four switches (note that it excludes ignition). The fuel dryness is summarised by the drought factor (DF) component of FFDI, which depends on both long-term and short-term rainfall. The FFDI also estimates the ability of a fire to spread, as the temperature, relative humidity and wind speed are direct inputs into the calculation. Fuel abundance is not measured by FFDI, but does depend largely on rainfall, with higher rainfall totals generally resulting in a larger fuel load, particularly in regions dominated by grasslands. However, the relationship between fuel abundance and climate change in Australia is complex and only poorly understood. Fire weather is considered ‘severe’ when FFDI exceeds 50 – bushfires have potentially greater human impacts at this level (Blanchi *et al.*, 2010).

Here, estimates of future fire weather using FFDI are derived from three CMIP5 models (GFDL-ESM2M, MIROC5 and CESM-CAM5), chosen to provide a spread of results across all clusters. Using a method similar to that of Hennessy *et al.* (2005), monthly-mean changes to maximum temperature, rainfall, relative humidity and wind speed from these models are applied to observation-based high-quality historical fire weather records (Lucas, 2010). A period centred on 1995 (*i.e.* 1981–2010) serves as the baseline; these records

are modified using the changes from the three models for four 30-year time slices (centred on 2030, 2050, 2070 and 2090) and the RCP4.5 and RCP8.5 emission scenarios. In the Monsoonal North cluster, the weather conditions are often conducive to fire activity, and the limiting switch in these regions is fuel availability. Following wet periods, fuel is abundant and fires are more frequent; dry periods see less fuel and fire activity. Four stations are used in the analysis for this cluster: Darwin, Broome, Mt. Isa and Townsville.

Focusing on the 2030 and 2090 time slices, the results indicate a tendency towards increased fire weather in the future (Table 4.9.1). On average, both temperature and rainfall increase, although in the 2030 RCP4.5 scenario rainfall slightly declines. The drought factor (DF) remains about the same. The sum of all daily FFDI values over a year (Σ FFDI from July to June) is broadly indicative of general fire weather danger and increases by 5 % by 2030 and by 8 % under RCP4.5, and 17 % under RCP8.5, by 2090. The number of days with a 'severe' fire danger rating is generally low in the current climate, but increases by around 25 % under RCP4.5, to 40 % under RCP8.5 by 2030, and 45 % under RCP4.5 by 2090 to 120 % under RCP8.5 by 2090.

Across much of the cluster, bushfire is frequent, occurring annually in some areas, particularly in the Top End and the Kimberley regions. As noted above, the primary determinant of bushfires in this cluster is fuel availability, which varies according to rainfall. Land use (e.g. grazing) is also an important determinant of fuel availability. In this cluster, rainfall primarily occurs during the period from October to March. After the wet season ends, fuel dries and eventually burns, with fire activity and intensity peaking just before the onset of the next wet season. The extent of the area affected by bushfire activity depends primarily on the amount and location of the rain.

Table 2 in the Appendix shows the same results for individual stations and models. Rainfall varies across most of the cluster, loosely following a north-south gradient. In the northern portions (e.g. Darwin), rainfall totals are higher and fire is more frequent. Further south (e.g. Mt Isa), the active monsoon may not be observed every year, rainfall is less reliable and fire activity is less frequent (perhaps every few years). Differences between the east and west sub-clusters are also relevant. Interannual variability of the monsoon and tropical cyclone activity are two of the key factors influencing rainfall.

Table 2 in the Appendix also depicts large differences in future rainfall projections between the three models. Most simulations using the GFDL-ESM2M model indicate a drying climate, with rainfall reductions of up to 30 to 40 % in MNE and 5 to 10 % in the MNW. In most scenarios, the CESM-CAM and MIROC5 simulations suggest a wetter future, with increases in rainfall of up to 15 %. These increases are smaller in MNW. Not all model/scenario combinations follow this pattern; the GFDL-ESM2M 2090 RCP4.5 shows increasing rainfall, while the MIROC5 2090 RCP8.5 shows a decrease.

Projecting changes in future fire frequency from this information is difficult. In areas where copious amounts of rain already fall, the projected changes in the rainfall amount are not expected to have a significant impact on fire frequency; even in the drier GFDL model (a reduction of 10 % in MNW, 30 % in MNE), there is still a 'wet season' that results in significant rainfall and the growth of vegetation, leading to bushfire. In the southern and inland regions of the cluster, the fire frequency in the future is less clear and depends on how the rainfall changes. If rainfall-producing weather events occur more often (i.e. a change in the frequency of wet years), then more frequent fire activity could be expected. With higher temperatures, greater fuel loads from enhanced rainfall and a greater number of severe fire weather days, fire behaviour will possibly become more extreme when and where fire occurs.

In northern regions of the cluster such as the Top End and the Kimberley where there is abundant rainfall and bushfire is common, the projected changes in rainfall are not expected to significantly interrupt the current cycle, and there is *high confidence* in projections of little change to fire frequency. However, further south where rainfall is more variable from year to year, there is only *medium confidence* in projections of little change in fire frequency, as the methodology used to make the projections does not incorporate any changes to interannual variability (see Technical Summary for more details). Across the cluster, when and where fire does occur, there is *high confidence* that fire behaviour will be more extreme. Additional changes to the fuel characteristics for bushfire not considered here include changes to land use, the introduction of exotic species and the effects of higher CO₂ levels in the atmosphere.

TABLE 4.9.1: CLUSTER-MEAN ANNUAL VALUES OF MAXIMUM TEMPERATURE (T; °C), RAINFALL (R; MM), DROUGHT FACTOR (DF; NO UNITS), THE NUMBER OF SEVERE FIRE DANGER DAYS (SEV; FFDI > 50 DAYS PER YEAR) AND CUMULATIVE FFDI (Σ FFDI; NO UNITS) FOR THE 1995 BASELINE AND PROJECTIONS FOR 2030 AND 2090 UNDER RCP4.5 AND RCP8.5 SCENARIOS. AVERAGES ARE COMPUTED ACROSS ALL STATIONS AND MODELS IN EACH SCENARIO. FOUR STATIONS ARE USED IN THE AVERAGING: DARWIN, BROOME, MT ISA AND TOWNSVILLE.

VARIABLE	1995 BASELINE	2030 RCP4.5	2030 RCP8.5	2090 RCP4.5	2090 RCP8.5
T	31.4	32.5	32.8	33.6	35.2
R	965	958	978	1014	979
DF	7.7	7.8	7.7	7.7	7.8
SEV	3.7	4.7	5.1	5.4	8.0
Σ FFDI	4590	4799	4837	4940	5391



4.9 MARINE PROJECTIONS

Changes in mean sea levels and their extremes, as well as sea surface temperatures (SSTs) and ocean pH (acidity) have the potential to affect both the coastal terrestrial and marine environments. This is discussed at length in Chapter 8 of the Technical Report. Of particular significance for the terrestrial environment is the impact of sea level rise and changes to the frequency of extreme sea levels. Impacts will be felt through coastal flooding and erosion and changes in coastal vegetation. For the adjacent marine environment, increases in ocean temperatures and acidity may alter the distribution and composition of marine vegetation, increase coral bleaching and mortality and impact fisheries.

4.9.1 SEA LEVEL

Changes in sea level are caused primarily by changes in ocean density ('thermal expansion') and changes in ocean mass due to the exchange of water with the terrestrial environment including melting from glaciers and ice sheets (*e.g.* Church *et al.*, 2014; also see Technical Report, Section 8.1 for details). Over 1966 to 2009, the average of the relative tide gauge trends around Australia is a rise of 1.4 ± 0.2 mm/yr. After the influence of the El Niño Southern Oscillation (ENSO) on sea level is removed, the average trend is 1.6 ± 0.2 mm/yr. After accounting for and removing the effects of vertical land movements due to glacial rebound and the effects of natural climate variability and changes in atmospheric pressure, sea levels have risen around the Australian coastline at an average rate of 2.1 mm/yr over 1966 to 2009 and 3.1 mm/yr over 1993 to 2009. These observed rates of rise for Australia are consistent with global average values (White *et al.*, 2014).

Projections of future sea level changes are shown for Townsville and Darwin (Figure 4.10.1) and selected values are given in Table 3 (in Appendix). Continued increase in sea level for the Monsoonal North cluster is projected with *very high confidence*. The rate of sea level rise during the 21st century will be larger than the average rate during the 20th century as greenhouse gas emissions grow (Figure 4.10.1). For the first decades of the 21st century the projections are almost independent of the emission scenario, but they begin to separate significantly from about 2050. For higher greenhouse gas emissions, particularly for RCP8.5, the rate of rise continues to increase through the 21st century and results in sea level rise about 30 % higher than the RCP4.5 level by 2100. Significant interannual variability will likely continue through the 21st century; an indication of its expected magnitude is given by the dotted lines in Figure 4.10.1. In the near future (2030), the projected range of sea level rise for the Monsoonal North cluster coastline is 0.06 to 0.17 m above 1986–2005, with only minor differences

between RCPs, and for late in the century (2090) it is in the range 0.28 to 0.64m for RCP4.5 and 0.38 to 0.85 m for RCP8.5. These ranges of sea level rise are considered *likely* (at least 66% probability), however, if a collapse in the marine based sectors of the Antarctic ice sheet were initiated, these projections could be several tenths of a metre higher by late in the century (Church *et al.*, 2014).

Extreme coastal sea levels are caused by a combination of factors including astronomical tides, storm surges and wind-waves, exacerbated by rising sea levels. Storm surges arise from the passage of weather systems and their associated strong surface winds and falling atmospheric pressure. In the Monsoonal North, tropical cyclones are a major cause of severe storm surges. The impact of a storm surge is influenced by the magnitude of the tides at the time of the surge with the resultant sea levels referred to as a storm-tide. For example, Cyclone Tracy in 1975 produced a storm surge of 1.55 m and coincided with high tides. However, the storm-tide impacts would have been worse had the surge not occurred during a neap tidal period when the tidal range is smaller (Harper, 2010). The tidal range along the north-west coast is the largest in Australia with the tidal range at Broome and Darwin typically around 8.2 and 5.5 m respectively. In addition to tropical cyclones, other weather conditions can also contribute to elevated sea levels on shorter time scales. For example, in the Gulf of Carpentaria, north-westerly winds associated with the evolution of the Madden-Julian Oscillation (MJO) during the north-west monsoon produce wind setup and elevated sea levels within the Gulf on intraseasonal time scales (Oliver and Thompson, 2011).

Using the method of Hunter (2012), an allowance has been calculated based on the mean sea level rise, the uncertainty around the rise, and taking into account the nature of extreme sea levels along the Monsoonal coastline (Haigh *et al.*, 2014). The allowance is the minimum distance required to raise an asset to maintain current frequency of breaches under projected sea level rise. When uncertainty in mean sea level rise is high (*e.g.* in 2090), this allowance approaches the upper end of the range of projected mean sea level rise. For the Monsoonal North in 2030 the vertical allowances along the cluster coastline are in the range of 0.11 to 0.14 m for all RCPs; and 0.46 to 0.54 for RCP4.5 by 2090; and 0.63 to 0.75 m for RCP8.5 by 2090 (see Table 3 in the Appendix).



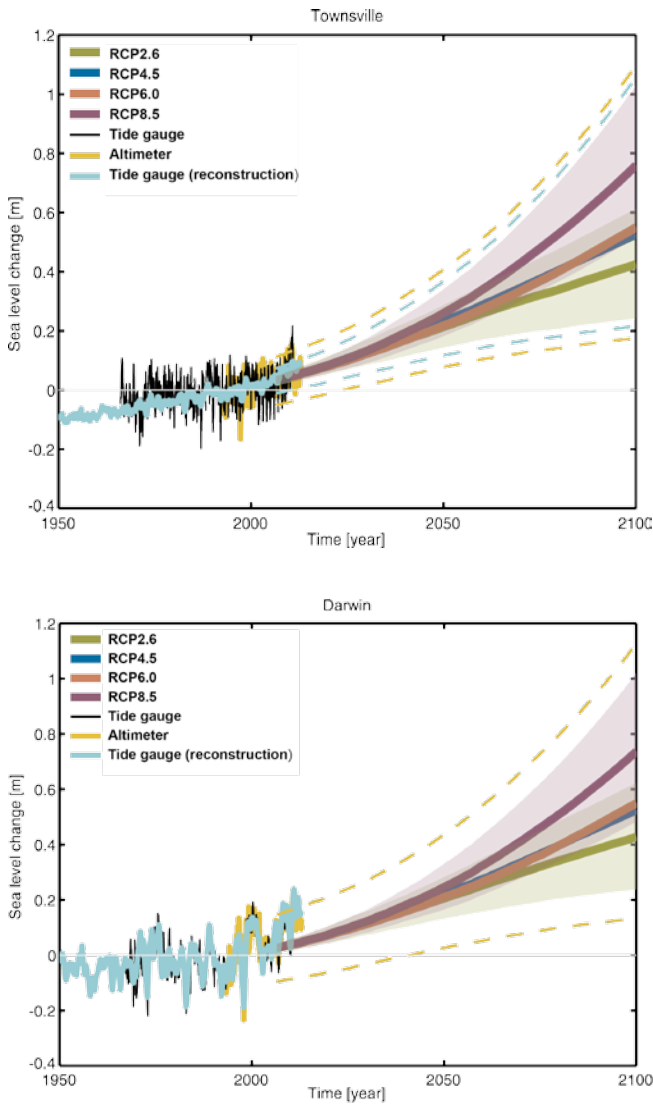


FIGURE 4.10.1: OBSERVED AND PROJECTED RELATIVE SEA LEVEL CHANGE IN METRES FOR TOWNSVILLE (TOP) AND DARWIN (BOTTOM), WHERE THERE ARE CONTINUOUS RECORDS AVAILABLE FOR THE PERIOD 1966 TO 2010. THE OBSERVED TIDE GAUGE RELATIVE SEA LEVEL RECORDS ARE INDICATED IN BLACK, WITH THE SATELLITE RECORD (SINCE 1993) IN MUSTARD AND TIDE GAUGE RECONSTRUCTION (WHICH HAS LOWER VARIABILITY) IN CYAN. MULTI-MODEL MEAN PROJECTIONS (THICK PURPLE AND OLIVE LINES) FOR THE RCP8.5 AND RCP2.6 SCENARIOS WITH LIKELY UNCERTAINTY RANGE ARE SHOWN BY THE PURPLE AND OLIVE SHADED REGIONS FROM 2006 TO 2100. THE MUSTARD AND CYAN DASHED LINES ARE ESTIMATES OF INTERANNUAL VARIABILITY IN SEA LEVEL (UNCERTAINTY RANGE ABOUT THE PROJECTIONS) AND INDICATE THAT INDIVIDUAL MONTHLY AVERAGES OF SEA LEVEL CAN BE ABOVE OR BELOW LONGER TERM AVERAGES. NOTE THAT THE RANGES OF SEA LEVEL RISE SHOULD BE CONSIDERED *LIKELY* (AT LEAST 66 % PROBABILITY) AND THAT IF A COLLAPSE IN THE MARINE BASED SECTORS OF THE ANTARCTIC ICE SHEET WERE INITIATED, THESE PROJECTIONS COULD BE SEVERAL TENTHS OF A METRE HIGHER BY LATE IN THE CENTURY.

4.9.2 SEA SURFACE TEMPERATURES, SALINITY AND ACIDIFICATION

Sea surface temperature (SST) has increased significantly across the globe over recent decades (IPCC, 2013). Along the Western Australian coast, temperatures of up to 5 °C above average were recorded during the 2010/2011 summer. These record temperatures are associated with a warming of the Leeuwin Current over recent decades. Increases in SST pose a significant threat to the marine environment through biological changes in marine species, including in local abundance, community structure, and increased coral bleaching risk. The future projected warming is generally largest over the north-west shelf and smallest in the Gulf of Carpentaria. For 2030, the range of projected SST increase for Broome is 0.6 to 1.1 °C across all RCPs and for Darwin it is 0.4 to 1.1 °C (see Table 3 in Appendix). For 2090, there is a much larger range of warming between the different emissions scenarios and sites. Across the sites in the Monsoonal North the range of increase is projected to be 0.3 to 1.6 °C for RCP2.6 and 2.2 to 4.1 °C for RCP8.5.

Ocean salinity in coastal waters will be affected by changes to rainfall and evaporation and this in turn can affect stratification and mixing, and potentially nutrient supply. Changes to salinity across the coastal waters of the Monsoonal North cluster span a large range that includes possible increases and decreases, particularly over the longer term and higher emission scenarios as indicated in Table 3 (in Appendix). The relatively shallow Gulf of Carpentaria reveals a larger sensitivity to such projected changes (see Table 3 in Appendix). Locally, salinity can also be affected by riverine input.

About 30 % of the anthropogenic carbon dioxide emitted into the atmosphere over the past 200 years has been absorbed by the oceans (Ciais *et al.*, 2014) and this has led to a 0.1 unit decrease in the ocean’s surface water pH, which represents a 26 % increase in the concentration of hydrogen ions in seawater (Raven *et al.*, 2005). As the CO₂ enters the ocean it reacts with the seawater to cause a decrease in pH and carbonate concentration, collectively known as ocean acidification. Carbonate is used in conjunction with calcium as aragonite by many marine organisms such as corals, oysters, clams and some plankton such as foraminifera and pteropods, to form their hard skeletons or shells. A reduction in shell mass has already been detected in foraminifera and pteropods in the Southern Ocean (Moy *et al.*, 2009; Bednaršek *et al.*, 2012). Ocean acidification lowers the temperature at which corals bleach, reducing resilience to natural variability. Ocean acidification can

affect fin and shellfish fisheries, aquaculture, tourism and coastal protection. In 2030, pH change is projected to be another 0.07 units lower. By 2090 it is projected to be up to 0.14 units lower under RCP4.5 and up to 0.3 units lower for RCP8.5, which represents additional increases in hydrogen ion concentration of 40 and 100 % respectively. These changes are also accompanied by reductions in aragonite saturation state (see Table 3 in Appendix) and together with SST changes will affect all levels of the marine food web, and make it harder for calcifying marine organisms to build their hard shells, potentially affecting resilience and viability of marine ecosystems.

In summary, there is *very high confidence* that sea surface temperatures will continue to rise along the Monsoonal North coastline, with the magnitude of the warming dependent on emission scenarios. Changes in salinity are related to changes in the hydrological cycle and are of *low confidence*. There is *very high confidence* that around Australia the ocean will get more acidic, showing a net reduction in pH. There is also *high confidence* that the rate of ocean acidification will be proportional to carbon dioxide emissions.

4.10 OTHER PROJECTION MATERIAL FOR THE CLUSTER

For the Monsoonal North area, previous projection products comprise the nationwide *Climate Change in Australia* projections, produced by the CSIRO and BOM in 2007 (CSIRO and BOM, 2007); regional projections derived for the Northern Territory based on these 2007 results; Western Australia³ (produced through the Indian Ocean Climate Initiative, IOCI) and projections presented in the *Climate Q* document⁴, delivered as part of the Queensland state Government's Climate Smart Strategy and based on the CSIRO and BOM 2007 projections. These previous projections build on climate change information derived from the previous generation of GCMs included in the CMIP3 archive. A very brief comparison of the projections with regard to temperature and rainfall follow below.

In comparison to the 2007 projections (that also formed the projections presented in the *Climate Q* document for Queensland) the warming patterns suggested by the CMIP5 models are somewhat more uniform, with a somewhat less pronounced north-south gradient in warming (Figure A.1 of the Technical Report). With regard to rainfall, the CMIP5 projections appear to give a slightly wetter projection for Australia as a whole but no significant difference in the projections for the Monsoonal North cluster (Figure A.2 of the Technical Report).

Despite the use of previous generation models, these projections are still relevant, particularly if placed in the context of the latest modelling results (see Appendix A in the Technical Report for a discussion on CMIP3 and CMIP5 model-based projections).

3 <http://www.ioici.org.au/our-climate.html?start=1>

4 <http://www.agdf.org.au/information/sustainable-development/climate-q>

5 APPLYING THE REGIONAL PROJECTIONS IN ADAPTATION PLANNING

The fundamental role of adaptation is to reduce the adverse impacts of climate change on vulnerable systems, using a wide range of actions directed by the needs of the vulnerable system. Adaptation also identifies and incorporates new opportunities that become feasible under climate change. For adaptation actions to be effective, all stakeholders need to be engaged, resources must be available and planners must have information on ‘what to adapt to’ and ‘how to adapt’ (Füssel and Klein, 2006).

This report presents information about ‘what to adapt to’ by describing how future climate may respond to increasing concentrations of greenhouse gas. This chapter gives guidance on how climate projections can be framed in the context of climate scenarios (Section 5.1) using tools such as the Climate Futures web tool, available on the Climate Change in Australia website (Box 5.1). The examples of its use presented here are not exhaustive, but rather an illustration of what can be done.

BOX 5.1: USER RESOURCES ON THE CLIMATE CHANGE IN AUSTRALIA WEBSITE

The Climate Change in Australia website provides information on the science of climate change in a global and Australian context with material supporting regional planning activities. For example, whilst this report focuses on a selected set of emission scenarios, time horizons and variables, the website enables generation of graphs tailored to specific needs, such as a different time period or emission scenario.

The website includes a decision tree yielding application-relevant information, report-ready projected change information and the web tool Climate Futures (Whetton et al., 2012).

The web tool facilitates the visualisation and categorisation of model results and selection of data sets that are of interest to the user. These products are described in detail in Chapter 9 of the Technical Report.

www.climatechangeinaustralia.gov.au

5.1 IDENTIFYING FUTURE CLIMATE SCENARIOS

In Chapter 4 of this report, projected changes are expressed as a range of plausible change for individual variables as simulated by CMIP5 models or derived from their outputs. However, many practitioners are interested in information on how the climate may change, not just change in one variable. To consider how several climate variables may change in the future, data from individual models should be considered because each model simulates changes that are internally consistent across many variables. For example, one should not combine the projected rainfall from one model with the projected temperature from another, as these would represent the climate responses of unrelated simulations.

The challenge for practitioners lies in selecting which models to look at – an important decision, since models can vary in their simulated climate response to increasing greenhouse gas emissions. Climate models can be organised according to their simulated climate response to assist with this selection. For example, sorting according to rainfall and temperature responses would give an immediate feel for how models fall into a set of discrete climate scenarios framed in terms such as: *much drier and slightly warmer*, *much wetter and slightly warmer*, *much drier and much hotter*, and *much wetter and much hotter*.

The Climate Futures web tool described in Box 9.1 of the Technical Report presents a scenario approach to investigate the range of climate model simulations for projected future periods. The following Section describes how this tool can facilitate the use of model output in impact and adaptation work.

5.2 DEVELOPING CLIMATE SCENARIOS USING THE CLIMATE FUTURES TOOL

The example presented in Figure 5.1 represents the changes, as simulated by CMIP5 models, in temperature and rainfall in the Monsoonal North cluster for 2090 (2080–2099) under the RCP4.5 scenario. The table organises CMIP5 models into groupings according to their simulated summer rainfall (rows) and summer temperatures (columns).

Rainfall models simulate increases and decreases from *much drier* (less than -15 %) to *much wetter* (greater than 15 %), with 14 of 34 models showing drying conditions (less than -5 %) compared to ten models showing rainfall increases (greater than 5 %) and ten models showing little change (-5 to 5 % change).

With regard to temperature, models show results ranging from *warmer* (0.5 to 1.5 °C warmer) to *hotter* (1.5 to 3 °C warmer) to *much hotter* (greater than 3.0 °C warmer), with no models falling into the lowest category ‘slightly warmer’ (0 to 0.5 °C warmer). The largest number of models falls in the *hotter* category (23 of 34 models). When considering the two variables together we see that the most commonly simulated climate for the 2090 period under RCP4.5 is a *hotter and little change to drier* climate (16 of 34 models).

In viewing the projection data in this way, the user can gain an overview of what responses are possible when considering the CMIP5 model archive for a given set of constraints. In a risk assessment context, a user may want to consider not only the maximum consensus climate (simulated by most models) but also the best case and worst case scenarios. Their nature will depend on the application. A water-supply manager, for example, is likely to determine from Figure 5.1 that the best case scenario would be a *wetter and warmer* climate and the worst case the *much hotter and much drier* scenario.

Assuming that the user has identified which futures are likely to be of most concern for the system of interest, Climate Futures allows exploration of the numerical values for each of the models that populates the futures. Further, it provides a function for choosing a single model that most closely represents the particular future climate of interest, but also takes into account models that have been identified as sub-optimal for particular regions based on model evaluation information (as described in Chapter 5 of the Technical Report). Through this approach users can select a small set of models to provide scenarios for their application, taking into consideration model spread and the sensitivity of their application to climate change.

		Dec - Feb temperature (°C)			
		Slightly warmer 0 to +0.5	Warmer +0.5 to 1.5	Hotter +1.5 to +3.0	Much hotter > +3.0
Dec - Feb rainfall (%)	Much wetter > +15.0				
	Wetter +5.0 to +15.0		4 of 34 models	6 of 34 models	
	Little change -5.0 to +5.0		2 of 34 models	8 of 34 models	
	Drier -15.0 to -5.0		2 of 34 models	8 of 34 GCMs	1 of 34 models
	Much drier < -15.0			1 of 34 models	2 of 34 models

FIGURE 5.1: AN EXAMPLE TABLE FROM THE CLIMATE FUTURES WEB TOOL SHOWING RESULTS FOR THE MONSOONAL NORTH WHEN ASSESSING PLAUSIBLE CLIMATE FUTURES FOR 2090 UNDER RCP4.5, AS DEFINED BY GCM SIMULATED SUMMER RAINFALL (% CHANGE) AND TEMPERATURE (°C WARMING).



Alternatively, the user may wish to consider a small set of scenarios defined irrespective of emission scenario or date (but with their likelihood of occurrence being time and emission scenario sensitive). This may be in circumstances where the focus is on critical climate change thresholds. An example of using this strategy for the Monsoonal North cluster is illustrated in Box 5.2 where results are produced in Climate Futures by comparing model simulations from separate time slices and emission scenarios. This box also illustrates each of these scenarios with current climate analogues (comparable climates) for selected sites.

Another user case could be the desire to compare simulations from different climate model ensembles (such as the earlier CMIP3 ensemble, or ensembles of downscaled results). Comparing model spread simulated by different generations of GCMs in Climate Futures allows an assessment of the ongoing relevance of existing impact studies based on selected CMIP3 models, as well as comparison of scenarios developed using downscaled and GCM results.

BOX 5.2: INDICATIVE CLIMATE SCENARIOS FOR THE MONSOONAL NORTH AND ANALOGUE FUTURE CLIMATES

Users may wish to consider the future climate of their region in terms of a small set of scenarios defined irrespective of emission scenario or date (but with their likelihood of occurrence being time and emission scenario sensitive). An example of using this strategy for the Monsoonal North is illustrated here. Combining the results in Climate Futures for 2030, 2050, and 2090, under RCP2.6, RCP4.5, and RCP8.5, gives a set of future climate scenarios (see Figure B5.2). From these, five highlighted scenarios are considered representative of the spread of results. Other potential scenarios are excluded as generally less likely than the selected cases or because they lie within the range of climates specified by the selected cases. For each case, when available, the current climate analogue for the future climate of Darwin is given as an example. These were generated using the method described in Chapter 9.3.5 of the Technical Report and are based on matching annual average rainfall (within +/- 5 %) and maximum temperature (within +/- 1 °C). Other potentially important aspects of local climate, such as rainfall seasonality, are not matched. Thus the analogues should not be used directly for adaptation planning without considering more detailed information.

- *Warmer* (0.5 to 1.5 °C warmer) with *little change in rainfall* (-5 to +5 %). This could occur by 2030 under any emission scenario, but may persist through to late in the 21st century under RCP2.6. In this case, Darwin's future climate would be more like the current climate of Nguiu (Bathurst Island (NT)).
- *Hotter* (1.5 to 3.0 °C warmer) with *little change in rainfall* (-5 to +5 %). This may occur by 2090 under RCP4.5. In this case, Darwin's future climate has no analogue in Australia.
- *Warmer* (0.5 to 1.5 °C warmer), but *wetter* (5 to 15 % increase). This is also possible by 2030 under any emission scenario, and again may persist through to late in the 21st century under RCP2.6. In this case Darwin's climate would be more like that of Weipa (QLD).
- *Hotter* (1.5 to 3.0 °C warmer), and *drier* (5 to 15 % reduction). This is possible mid-century under lower emission scenarios but may persist through to late in the 21st century under RCP2.6. In this case, Darwin's future climate would be more like Jabiru (NT).
- *Much hotter* (greater than 3.0 °C warmer) and *little change in rainfall* (-5 to +5 %). This is possible late in the century and especially under RCP8.5.

Future Realisations for the Monsoonal North cluster

		Annual Surface Temperature (°C)													
		Slightly Warmer 0 to +0.5				Warmer +0.5 to +1.5			Hotter +1.5 to +3.0			Much Hotter > +3.0			
Annual Rainfall (%)	Much Wetter > +15.0	RCP	2030	2050	2090	2030	2050	2090	2030	2050	2090	2030	2050	2090	
		2.6													
		4.5													
	8.5										2			1	
	Wetter +5.0 to +15.0	2.6				3	6	1							
		4.5				7	5	2		2	6				
		8.5				5									7
	Little Change -5.0 to +5.0	2.6				11	5	8							
		4.5				13	9			6	12				
		8.5				18			1						9
	Drier -15.0 to -5.0	2.6				3	2	3		4	4				
		4.5				6				2	4				1
		8.5				1			2						5
	Much Drier < -15.0	2.6				1		1		1	1				
		4.5				1	1			2	1				1
8.5					1			1						5	

By when and under what greenhouse gas pathway could this occur (colour code=% of models for that period/RCP)?	Not projected	<10%	10-33%	33-66%	RCP2.6-18 models RCP4.5-27 models RCP8.5-29 models
---	---------------	------	--------	--------	--

FIGURE 5.2: A TABLE SHOWING CATEGORIES OF FUTURE CLIMATE PROJECTIONS FOR THE MONSOONAL NORTH CLUSTER, AS DEFINED BY CHANGE IN ANNUAL TEMPERATURE (COLUMN) AND CHANGE IN RAINFALL (ROWS). WITHIN EACH FUTURE CLIMATE CATEGORY, MODEL SIMULATIONS ARE SORTED ACCORDING TO TIME (2030, 2050 AND 2090) AND CONCENTRATION PATHWAY (RCP2.6, RCP4.5 AND RCP8.5); THE NUMBER INDICATING HOW MANY MODEL SIMULATIONS OF THAT PARTICULAR SUB-CATEGORY FALL INTO THE CLIMATE CATEGORY OF THE TABLE (THE NUMBER OF MODELS VARIES FOR DIFFERENT CONCENTRATION PATHWAYS). A COLOUR CODE INDICATES HOW OFTEN A PARTICULAR CLIMATE IS SIMULATED AMONGST THE CONSIDERED MODELS (PER CENT OCCURRENCE). CLIMATE FUTURES DESCRIBED IN THE TEXT ABOVE ARE HIGHLIGHTED.



REFERENCES

- ALLEN, R. J., NORRIS, J. R. & WILD, M. 2013. Evaluation of multidecadal variability in CMIP5 surface solar radiation and inferred underestimation of aerosol direct effects over Europe, China, Japan, and India. *Journal of Geophysical Research-Atmospheres*, 118, 6311-6336.
- BEDNARŠEK, N., TARLING, G., BAKKER, D., FIELDING, S., JONES, E., VENABLES, H., WARD, P., KUZIRIAN, A., LEZE, B. & FEELY, R. 2012. Extensive dissolution of live pteropods in the Southern Ocean. *Nature Geoscience*, 5, 881-885.
- BLANCHI, R., LUCAS, C., LEONARD, J. & FINKELE, K. 2010. Meteorological conditions and wildfire-related house loss in Australia. *International Journal of Wildland Fire*, 19, 914-926.
- BRADSTOCK, R. A. 2010. A biogeographic model of fire regimes in Australia: current and future implications. *Global Ecology and Biogeography*, 19, 145-158.
- BROHAN, P., KENNEDY, J. J., HARRIS, I., TETT, S. F. & JONES, P. D. 2006. Uncertainty estimates in regional and global observed temperature changes: A new data set from 1850. *Journal of Geophysical Research: Atmospheres* (1984–2012), 111, D12, 1-21.
- CHIEW, F., KIRONO, D., KENT, D. & VAZE, J. 2009. Assessment of rainfall simulations from global climate models and implications for climate change impact on runoff studies. *18th World Imacs Congress and Modsim09 International Congress on Modelling and Simulation: Interfacing Modelling and Simulation with Mathematical and Computational Sciences*. 3907-3913
- CHURCH, J. A., CLARK, P. U., CAZENAIVE, A., GREGORY, J. M., JEVREJEVA, S., LEVERMANN, A., MERRIFIELD, M. A., MILNE, G. A., NEREM, R. S., NUNN, P. D., PAYNE, A. J., PFEFFER, W. T., STAMMER, D. & UNNIKRIISHNAN, A. S. 2014. Sea Level Change. In: STOCKER, T. F., D. QIN, G.-K. PLATTNER, M. TIGNOR, S. K. ALLEN, J. BOSCHUNG, A. NAUELS, Y. XIA, V. BEX AND P. M. MIDGLEY (ed.) *Climate Change 2013: The Physical Science Basis. Contribution of Working Group I to the Fifth Assessment Report of the Intergovernmental Panel on Climate Change*.
- CIAIS, P., SABINE, C., BALA, G., BOPP, L., BROVKIN, V., CANADELL, J., CHHABRA, A., DEFRIES, R., GALLOWAY, J., HEIMANN, M., JONES, C., LE QUÉRE, C., MYNENI, R. B., PIAO, S. & THORNTON, P. 2013. Carbon and Other Biogeochemical Cycles. Contribution of Working Group I to the *Fifth Assessment Report* of the Intergovernmental Panel on Climate Change. In: STOCKER, T. F., D. QIN, G.-K. PLATTNER, M. TIGNOR, S.K. ALLEN, J. BOSCHUNG, A. NAUELS, Y. XIA, BEX, V. & MIDGLEY, P. M. (eds.) *Climate Change 2013: The Physical Science Basis*. Cambridge, United Kingdom and New York, NY, USA: Cambridge University Press.
- CLARKE, H., LUCAS, C. & SMITH, P. 2013. Changes in Australian fire weather between 1973 and 2010. *International Journal of Climatology*, 33, 931-944.
- CLARKE, H. G., SMITH, P. L. & PITMAN, A. J. 2011. Regional signatures of future fire weather over eastern Australia from global climate models. *International Journal of Wildland Fire*, 20, 550-562.
- CSIRO AND BOM 2007. Climate change in Australia: Technical Report. Aspendale, Australia: CSIRO Marine and Atmospheric Research. URL http://www.climatechangeinaustralia.gov.au/technical_report.php Accessed 19/8/2014
- FAWCETT, R., DAY, K. A., TREWIN, B., BRAGANZA, K., SMALLEY, R., JOVANOVIĆ, B. & JONES, D. 2012. On the sensitivity of Australian temperature trends and variability to analysis methods and observation networks, Centre for Australian Weather and Climate Research Technical Report No.050.
- FOWLER, H. & EKSTRÖM, M. 2009. Multi-model ensemble estimates of climate change impacts on UK seasonal precipitation extremes. *International Journal of Climatology*, 29, 385-416.
- FÜSSEL, H.-M. & KLEIN, R. J. 2006. Climate change vulnerability assessments: an evolution of conceptual thinking. *Climatic Change*, 75, 301-329.
- GREEN, D., ALEXANDER, L., MCLNNE, K., CHURCH, J., NICHOLLS, N. & WHITE, N. 2010. An assessment of climate change impacts and adaptation for the Torres Strait Islands, Australia. *Climatic Change*, 102, 405-433.
- GROSE, M. R., FOX-HUGHES, P., HARRIS, R. M. & BINDOFF, N. L. 2014. Changes to the drivers of fire weather with a warming climate—a case study of south-east Tasmania. *Climatic Change*, 124, 255-269.
- HAIGH, I. D., WIJERATNE, E., MACPHERSON, L. R., PATTIARATCHI, C. B., MASON, M. S., CROMPTON, R. P. & GEORGE, S. 2014. Estimating present day extreme water level exceedance probabilities around the coastline of Australia: tides, extra-tropical storm surges and mean sea level. *Climate Dynamics*, 42, 121-138.
- HENNESSY, K., LUCAS, C., NICHOLLS, N., BATHOLS, J., SUPPIAH, R. & RICKETTS, J. 2005. Climate change impacts on fire-weather in south-east Australia. Melbourne, Australia: Consultancy report for the New South Wales Greenhouse Office, Victorian Department of Sustainability and Environment, Tasmanian Department of Primary Industries, Water and Environment, and the Australian Greenhouse Office. CSIRO Atmospheric Research and Australian Government Bureau of Meteorology 78pp. URL http://laptop.deh.gov.au/soe/2006/publications/drs/pubs/334/lnd/lnd_24_climate_change_impacts_on_fire_weather.pdf Accessed 18/8/2014

- HILBERT, D. W., HILL, R., MORAN, C., TURTON, S. M., BOHNET, I. C., MARSHALL, N. A., PERT, P. L., STOECKL, N., MURPHY, H. T., RESIDE, A. E., LAURANCE, S. G. W., ALAMGIR, M., COLES, R., CROWLEY, G., CURNOCK, M., DALE, A., DUKE, N. C., ESPARON, M., FARR, M., GILLET, S., GOOCH, M., FUENTES, M., HAMMAN, M., JAMES, C. S., KROON, F. J., LARSON, S., LYONS, P., MARSH, H., MEYER STEIGER, D., SHEAVES, M. & WESTCO, D. A. 2014. Climate Change Issues and Impacts in the Wet Tropics NRM Cluster Region [Online]. Cairns, Australia: James Cook University. URL: http://www.academia.edu/7772712/Climate_Change_Issues_and_Impacts_in_the_Wet_Tropics_NRM_Cluster_Region Accessed 19/8/2014
- HUNTER, J. 2012. A simple technique for estimating an allowance for uncertain sea-level rise. *Climatic Change*, 113, 239-252.
- HUNTINGTON, T. G. 2006. Evidence for intensification of the global water cycle: Review and synthesis. *Journal of Hydrology*, 319, 83-95.
- IPCC 2013. Climate Change 2013: The Physical Science Basis. In: STOCKER, T. F., D. QIN, G.-K. PLATTNER, M. TIGNOR, S. K. ALLEN, J. BOSCHUNG, A. NAUELS, Y. XIA, V. BEX & P. M. MIDGLEY (eds.) *Contribution of Working Group I to the Fifth Assessment Report of the Intergovernmental Panel on Climate Change*. Cambridge, UK, and New York, NY, USA: Cambridge University Press.
- JAKOB, D. 2010. Challenges in developing a high-quality surface wind-speed data-set for Australia. *Australian Meteorological Magazine*, 60, 227-236.
- JONES, D. A., WANG, W. & FAWCETT, R. 2009. High-quality spatial climate data-sets for Australia. *Australian Meteorological and Oceanographic Journal*, 58, 233-248.
- KIRONO, D. G. C. & KENT, D. M. 2011. Assessment of rainfall and potential evaporation from global climate models and its implications for Australian regional drought projection. *International Journal of Climatology*, 31, 1295-1308.
- LEVITUS, S., ANTONOV, J. I., BOYER, T. P. & STEPHENS, C. 2000. Warming of the world ocean. *Science*, 287, 2225-2229.
- LUCAS, C. 2010. On developing a historical fire weather data-set for Australia. *Australian Meteorological Magazine*, 60, 1-13.
- LUCAS, C., HENNESSY, K., MILLS, G. & BATHOLS, J. 2007. Bushfire Weather in Southeast Australia: Recent Trends and Projected Climate Change Impacts. Consultancy Report prepared for The Climate Institute of Australia. Bushfire CRC and Australian Bureau of Meteorology CSIRO Marine and Atmospheric Research. URL <http://www.royalcommission.vic.gov.au/getdoc/c71b6858-c387-41c0-8a89-b351460eba68/TEN.056.001.0001.pdf> Accessed 18/8/2014
- MASTRANDREA, M. D., FIELD, C. B., STOCKER, T. F., EDENHOFER, O., EBI, K. L., FRAME, D. J., HELD, H., KRIEGLER, E., MACH, K. J. & MATSCHOSS, P. R. 2010. Guidance note for lead authors of the IPCC *Fifth Assessment Report* on consistent treatment of uncertainties. *Intergovernmental Panel on Climate Change (IPCC)*. URL <http://www.ipcc.ch/pdf/supporting-material/uncertainty-guidance-note.pdf> Accessed 18/8/2014
- MCARTHUR, A. G. 1967. Fire behaviour in Eucalypt forests. Leaflet. Forestry Timber Bureau Australia, 35-35.
- MCBRIDE, J. L. & NICHOLLS, N. 1983. Seasonal relationships between Australian rainfall and the Southern Oscillation. *Monthly Weather Review*, 111, 1998-2004.
- MCGREGOR, J. & DIX, M. 2008. An updated description of the conformal-cubic atmospheric model. In: HAMILTON, K. & OHFUCHI, W. (eds.) *High Resolution Numerical Modelling of the Atmosphere and Ocean*. Springer New York.
- MCMAHON, T. A., PEEL, M. C., LOWE, L., SRIKANTHAN, R. & MCVICAR, T. R. 2013. Estimating actual, potential, reference crop and pan evaporation using standard meteorological data: a pragmatic synthesis. *Hydrology and Earth System Sciences*, 17, 1331-1363.
- MCVICAR, T. R., RODERICK, M. L., DONOHUE, R. J., LI, L. T., VAN NIEL, T. G., THOMAS, A., GRIESER, J., JHAJHARIA, D., HIMRI, Y. & MAHOWALD, N. M. 2012. Global review and synthesis of trends in observed terrestrial near-surface wind speeds: Implications for evaporation. *Journal of Hydrology*, 416, 182-205.
- MOSS, R. H., EDMONDS, J. A., HIBBARD, K. A., MANNING, M. R., ROSE, S. K., VAN VUUREN, D. P., CARTER, T. R., EMORI, S., KAINUMA, M., KRAM, T., MEEHL, G. A., MITCHELL, J. F. B., NAKICENOVIC, N., RIAHI, K., SMITH, S. J., STOUFFER, R. J., THOMSON, A. M., WEYANT, J. P. & WILBANKS, T. J. 2010. The next generation of scenarios for climate change research and assessment. *Nature*, 463, 747-756.
- MOY, A. D., HOWARD, W. R., BRAY, S. G. & TRULL, T. W. 2009. Reduced calcification in modern Southern Ocean planktonic foraminifera. *Nature Geoscience*, 2, 276-280.
- NAKIĆENOVIC, N. & SWART, R. (eds.) 2000. *Special Report on Emissions Scenarios. A Special Report of Working Group III of the Intergovernmental Panel on Climate Change*, Cambridge, United Kingdom and New York, NY, USA: Cambridge University Press.
- OLIVER, E. & THOMPSON, K. 2011. Sea level and circulation variability of the Gulf of Carpentaria: Influence of the Madden-Julian Oscillation and the adjacent deep ocean. *Journal of Geophysical Research: Oceans* (1978-2012), 116, C02019.
- RAVEN, J., CALDEIRA, K., ELDERFIELD, H., HOEGH-GULDBERG, O., LISS, P., RIEBESELL, U., SHEPHERD, J., TURLEY, C. & WATSON, A. 2005. Ocean acidification due to increasing atmospheric carbon dioxide. *The Royal Society* 68pp.

- SHERWOOD, S. C., ROCA, R., WECKWERTH, T. M. & ANDRONOVA, N. G. 2010. Tropospheric water vapor, convection, and climate. *Reviews of Geophysics*, 48, RG2001.
- TAYLOR, K. E., STOUFFER, R. J. & MEEHL, G. A. 2012. An overview of CMIP5 and the experiment design. *Bulletin of the American Meteorological Society*, 93, 485-498.
- TENG, J., CHIEW, F., VAZE, J., MARVANEK, S. & KIRONO, D. 2012. Estimation of climate change impact on mean annual runoff across continental Australia using Budyko and Fu equations and hydrological models. *Journal of Hydrometeorology*, 13, 1094-1106.
- TIMBAL, B. & MCAVANEY, B. J. 2001. An analogue-based method to downscale surface air temperature: Application for Australia. *Climate Dynamics*, 17, 947-963.
- TROCCOLI, A., MULLER, K., COPPIN, P., DAVY, R., RUSSELL, C. & HIRSCH, A. L. 2012. Long-term wind speed trends over Australia. *Journal of Climate*, 25, 170-183.
- VAN VUUREN, D. P., EDMONDS, J., KAINUMA, M., RIAHI, K., THOMSON, A., HIBBARD, K., HURTT, G. C., KRAM, T., KREY, V. & LAMARQUE, J.-F. 2011. The representative concentration pathways: an overview. *Climatic Change*, 109, 5-31.
- WATTERSON, I. G., HIRST, A. C. & ROTSTAYN, L. D. 2013. A skill score based evaluation of simulated Australian climate. *Australian Meteorological and Oceanographic Journal*, 63, 181-190.
- WHETTON, P., HENNESSY, K., CLARKE, J., MCINNES, K. & KENT, D. 2012. Use of Representative Climate Futures in impact and adaptation assessment. *Climatic Change*, 115, 433-442.
- WHITE, N. J., HAIGH, I. D., CHURCH, J. A., KEON, T., WATSON, C. S., PRITCHARD, T., WATSON, P. J., BURGETTE, R. J., ELIOT, M., MCINNES, K. L., YOU, B., ZHANG, X. & TREGONING, P. 2014. Australian Sea Levels - Trends, regional variability and Influencing factors. *Earth-Science Reviews*, 136, 155-174.
- WILLIAMS, R. J., BRADSTOCK, R. A., CARY, G. J., ENRIGHT, N., GILL, A., LIEDLOFF, A., LUCAS, C., WHELAN, R., ANDERSEN, A. & BOWMAN, D. 2009. Interactions between climate change, fire regimes and biodiversity in Australia- A preliminary assessment. Canberra: Department of Climate Change and Department of the Environment, Water, Heritage and the Arts. URL http://climatechange.gov.au/sites/climatechange/files/documents/04_2013/20100630-climate-fire-biodiversity-PDF.pdf Accessed 18/8/2014
- ZHANG, L., POTTER, N., HICKEL, K., ZHANG, Y. & SHAO, Q. 2008. Water balance modeling over variable time scales based on the Budyko framework – Model development and testing. *Journal of Hydrology* 360, 117-131.

APPENDIX

TABLE 1: GCM SIMULATED CHANGES IN A RANGE OF CLIMATE VARIABLES FOR THE 2020–2039 (2030) AND 2080–2099 (2090) PERIODS RELATIVE TO THE 1986–2005 PERIOD FOR THE MONSOONAL NORTH CLUSTER. THE TABLE GIVES THE MEDIAN (50TH PERCENTILE) CHANGE, AS PROJECTED BY THE CMIP5 MODEL ARCHIVE, WITH 10TH TO 90TH PERCENTILE RANGE GIVEN WITHIN BRACKETS. RESULTS ARE GIVEN FOR RCP2.6, RCP4.5, AND RCP8.5 FOR ANNUAL AND SEASONAL AVERAGES. ‘DJF’ REFERS TO SUMMER (DECEMBER TO FEBRUARY), ‘MAM’ TO AUTUMN (MARCH TO MAY), ‘JJA’ TO WINTER (JUNE TO AUGUST) AND ‘SON’ TO SPRING (SEPTEMBER TO NOVEMBER). THE PROJECTIONS ARE PRESENTED AS EITHER PERCENTAGE OR ABSOLUTE CHANGES. THE COLOURING (SEE LEGEND) INDICATES CMIP5 MODEL AGREEMENT, WITH ‘MEDIUM’ BEING MORE THAN 60 % OF MODELS, ‘HIGH’ MORE THAN 75 %, ‘VERY HIGH’ MORE THAN 90 %, AND ‘SUBSTANTIAL’ AGREEMENT ON A CHANGE OUTSIDE THE 10TH TO 90TH PERCENTILE RANGE OF MODEL NATURAL VARIABILITY. NOTE THAT ‘VERY HIGH AGREEMENT’ CATEGORIES ARE RARELY OCCUPIED EXCEPT FOR ‘VERY HIGH AGREEMENT ON SUBSTANTIAL INCREASE’, AND SO TO REDUCE COMPLEXITY THE OTHER CASES ARE INCLUDED WITHIN THE RELEVANT ‘HIGH AGREEMENT’ CATEGORY.

VARIABLE	SEASON	2030, RCP26	2030, RCP45	2030, RCP85	2090, RCP26	2090, RCP45	2090, RCP85
Temperature mean (°C)	Annual	0.8 (0.5 to 1.2)	0.9 (0.6 to 1.3)	1 (0.7 to 1.3)	0.9 (0.5 to 1.6)	1.8 (1.3 to 2.7)	3.8 (2.8 to 5.1)
	DJF	0.7 (0.5 to 1.3)	0.8 (0.5 to 1.3)	0.8 (0.6 to 1.3)	0.9 (0.6 to 1.9)	1.7 (1.1 to 3)	3.5 (2.3 to 5.1)
	MAM	0.8 (0.5 to 1.2)	0.9 (0.5 to 1.4)	1 (0.6 to 1.4)	1 (0.5 to 1.7)	1.9 (1.2 to 2.9)	3.9 (2.6 to 5.2)
	JJA	0.9 (0.4 to 1.3)	1 (0.5 to 1.4)	1.1 (0.7 to 1.4)	1 (0.5 to 1.6)	2 (1.5 to 2.7)	4.2 (3.2 to 5.3)
	SON	0.8 (0.5 to 1.3)	0.9 (0.6 to 1.3)	1 (0.7 to 1.4)	0.9 (0.4 to 1.7)	1.8 (1.2 to 2.7)	3.7 (2.7 to 4.9)
Temperature maximum (°C)	Annual	0.9 (0.5 to 1.3)	1 (0.6 to 1.3)	1 (0.7 to 1.3)	1 (0.5 to 1.8)	1.9 (1.3 to 2.9)	3.7 (2.7 to 5)
	DJF	0.8 (0.5 to 1.3)	0.9 (0.5 to 1.4)	0.9 (0.6 to 1.4)	1 (0.4 to 2.3)	1.8 (1.1 to 3.5)	3.6 (2.2 to 5.1)
	MAM	0.8 (0.4 to 1.3)	1 (0.5 to 1.5)	1 (0.6 to 1.5)	1.1 (0.5 to 1.8)	1.8 (1.1 to 3)	3.8 (2.6 to 5.1)
	JJA	0.9 (0.3 to 1.3)	1 (0.5 to 1.4)	1.1 (0.7 to 1.4)	1.1 (0.4 to 1.6)	2 (1.3 to 2.7)	3.9 (2.9 to 4.9)
	SON	0.8 (0.4 to 1.5)	1 (0.6 to 1.4)	1.1 (0.7 to 1.4)	1 (0.4 to 1.8)	1.8 (1.2 to 2.8)	3.7 (2.8 to 4.8)
Temperature minimum (°C)	Annual	0.7 (0.5 to 1.2)	0.9 (0.6 to 1.3)	1 (0.8 to 1.3)	0.9 (0.5 to 1.5)	1.9 (1.3 to 2.7)	3.9 (2.9 to 5.2)
	DJF	0.7 (0.5 to 1.1)	0.9 (0.5 to 1.2)	0.9 (0.6 to 1.4)	0.9 (0.5 to 1.5)	1.8 (1.1 to 2.6)	3.7 (2.4 to 4.8)
	MAM	0.8 (0.4 to 1.2)	0.9 (0.6 to 1.2)	1.1 (0.7 to 1.4)	1 (0.5 to 1.6)	2 (1.3 to 2.8)	3.8 (2.8 to 5.3)
	JJA	0.8 (0.2 to 1.2)	1 (0.6 to 1.4)	1.1 (0.7 to 1.4)	1.1 (0.4 to 1.6)	2.1 (1.4 to 2.8)	4.2 (3.4 to 5.5)
	SON	0.7 (0.4 to 1.3)	1 (0.6 to 1.4)	1 (0.7 to 1.4)	0.9 (0.4 to 1.6)	1.8 (1.3 to 2.8)	3.9 (2.9 to 5.1)
Rainfall (%)	Annual	-3 (-11 to +8)	0 (-10 to +5)	-2 (-7 to +6)	-4 (-14 to +4)	-1 (-15 to +7)	+0 (-24 to +24)
	DJF	0 (-9 to +7)	-1 (-7 to +9)	0 (-7 to +9)	-3 (-14 to +4)	0 (-17 to +9)	+3 (-24 to +20)
	MAM	-2 (-15 to +15)	+0 (-19 to +9)	-3 (-18 to +10)	-5 (-20 to +13)	-1 (-19 to +15)	+0 (-31 to +32)
	JJA	-8 (-36 to +20)	-7 (-31 to +19)	-11 (-33 to +19)	-8 (-45 to +19)	-18 (-39 to +19)	-15 (-53 to +44)
	SON	-5 (-25 to +17)	-4 (-26 to +18)	-6 (-23 to +14)	-8 (-31 to +14)	-8 (-30 to +29)	-14 (-46 to +30)
Solar radiation (%)	Annual	+0.3 (-0.4 to +1.3)	-0.1 (-0.8 to +1.1)	+0 (-0.9 to +0.9)	+0.5 (-0.3 to +2.4)	+0.1 (-1.5 to +2)	-0.4 (-3.1 to +1.8)
	DJF	+0.3 (-1.2 to +2.5)	+0.2 (-1.8 to +1.7)	-0.3 (-1.9 to +1.6)	+1.2 (-1.1 to +4.6)	-0.1 (-2.3 to +3.7)	-1.1 (-5 to +4.3)
	MAM	+0 (-1.8 to +2.3)	-0.4 (-2 to +2.4)	+0 (-1.7 to +2.4)	+0.7 (-1.5 to +3.5)	+0 (-2.7 to +2.9)	-0.8 (-5.1 to +2.7)
	JJA	+0.2 (-0.5 to +1.9)	+0.2 (-1.1 to +1.5)	+0.3 (-1 to +2)	+0.4 (-0.9 to +2.3)	-0.3 (-1.6 to +2.1)	-0.9 (-3.4 to +1.7)
	SON	+0.5 (-0.4 to +1.8)	+0.3 (-0.9 to +1.1)	+0 (-0.8 to +1.4)	+0.5 (-1.1 to +2.2)	-0.2 (-1.4 to +1.4)	-0.5 (-2.6 to +2)
Relative humidity (% absolute)	Annual	-0.4 (-1.7 to +0.6)	-0.2 (-1.6 to +0.6)	-0.5 (-1.5 to +0.5)	-0.8 (-3.5 to +0.3)	-0.7 (-3.4 to +0.5)	-1.1 (-5.5 to +1.4)
	DJF	-0.7 (-2.7 to +0.9)	-0.2 (-2.3 to +1)	-0.6 (-2.4 to +0.6)	-1.6 (-4.8 to +1)	-1 (-6.2 to +1.5)	-1.6 (-5 to +1.9)
	MAM	-0.4 (-2.3 to +1.8)	-0.4 (-2.7 to +1.5)	-0.7 (-3.1 to +1.3)	-1.3 (-4.2 to +0.6)	-0.4 (-5.7 to +1.1)	-0.9 (-8.3 to +2.8)
	JJA	-0.3 (-2.7 to +0.3)	-0.3 (-1.5 to +0.6)	-0.8 (-2.2 to +0.5)	-0.6 (-3 to +0.5)	-0.8 (-3.9 to +1)	-1.3 (-5.2 to +2.1)
	SON	-0.4 (-1.6 to +1)	+0 (-1.9 to +1.4)	-0.3 (-1.6 to +0.7)	-0.7 (-2.9 to +1)	-0.2 (-1.9 to +1.2)	-0.5 (-2.9 to +1.7)

-20° -10° 0° 10° 20° 30° 40° 50°



VARIABLE	SEASON	2030, RCP26	2030, RCP45	2030, RCP85	2090, RCP26	2090, RCP45	2090, RCP85
Evapo-transpiration (%)	Annual	2.5 (1.4 to 3.7)	2.9 (1.6 to 4.3)	3.1 (2.3 to 5.1)	3.4 (2.1 to 6)	6.5 (3.9 to 8.6)	12.4 (8.3 to 16.7)
	DJF	2.6 (1.2 to 4.4)	3.2 (0.6 to 4.4)	3 (1 to 5.4)	4.3 (2.7 to 6.8)	5.8 (2 to 9.4)	11.5 (3.1 to 15.7)
	MAM	2.3 (1 to 4)	2.4 (1.5 to 4.3)	3.3 (2 to 5.7)	3.1 (0.7 to 5.7)	5.9 (4 to 10.3)	12.6 (9.2 to 19.7)
	JJA	2.6 (1.2 to 3.8)	3.3 (1 to 5.4)	3.7 (1.2 to 5.6)	3.3 (0.8 to 6.9)	7.3 (4.7 to 9.4)	15.3 (8.4 to 19.5)
	SON	2.7 (1 to 4.7)	3.1 (1.7 to 5)	3.3 (2 to 4.8)	3.4 (1.5 to 4.7)	6.2 (4.2 to 7.9)	11.7 (8.5 to 16.2)
Soil moisture (Budyko) (%)	Annual	NA	-0.7 (-3.7 to +3.3)	-0.8 (-3.6 to +1.8)	NA	-0.9 (-7.6 to +1.4)	-2.6 (-13.1 to +4)
	DJF	NA	-0.6 (-5.7 to +5.4)	-0.2 (-5.5 to +3.6)	NA	-0.6 (-13.9 to +4.2)	-1.9 (-22.4 to +7.1)
	MAM	NA	-1.1 (-8.1 to +5.5)	-1.6 (-7.1 to +4.9)	NA	-1.9 (-10.3 to +1.5)	-5.4 (-20.8 to +3.9)
	JJA	NA	-0.2 (-3.3 to +2)	-0.3 (-2.1 to +1.3)	NA	-0.7 (-4.8 to +0.3)	-1.5 (-6.3 to +0.8)
	SON	NA	-0.2 (-1.3 to +0.6)	-0.1 (-1.1 to +0.7)	NA	-0.1 (-1.4 to +1.7)	-0.1 (-3.8 to +4.9)
Wind speed (%)	Annual	0.5 (-1.2 to 2)	-0.1 (-2.4 to 0.7)	0.2 (-0.9 to 1.4)	1.1 (-1.7 to 4.9)	-0.4 (-3.4 to 2.6)	0.8 (-3.7 to 5.1)
	DJF	0.2 (-2.4 to 4.7)	0 (-3.7 to 2.6)	1 (-1.1 to 2.8)	1.6 (-1.7 to 6)	0 (-3.3 to 4.6)	1.9 (-3.9 to 8.3)
	MAM	-0.2 (-2.6 to 1.7)	-0.6 (-3.4 to 1.7)	-0.6 (-2.9 to 1)	1.1 (-3.4 to 4.2)	-1.6 (-4.6 to 0.7)	-3.3 (-7.6 to 2.5)
	JJA	0 (-2.7 to 2.9)	-0.3 (-4.2 to 2.7)	-0.2 (-1.5 to 3.1)	0.3 (-1.4 to 5.6)	-0.6 (-5 to 3.8)	0.4 (-2.6 to 6)
	SON	0.9 (-1.2 to 3.3)	0.6 (-2 to 2.6)	0.6 (-1.1 to 2.4)	1.3 (0.1 to 6.6)	1 (-2.7 to 4.9)	2.1 (-0.5 to 8.4)

LEGEND

	Very high model agreement on substantial increase
	High model agreement on substantial increase
	Medium model agreement on substantial increase
	High model agreement on increase
	Medium model agreement on increase
	High model agreement on little change
	Medium model agreement on little change
	Low model agreement on the direction of change
	High model agreement on substantial decrease
	Medium model agreement on substantial decrease
	High model agreement on decrease
	Medium model agreement on decrease



TABLE 2: ANNUAL VALUES OF MAXIMUM TEMPERATURE (T; °C), RAINFALL (R; MM), DROUGHT FACTOR (DF; NO UNITS), THE NUMBER OF SEVERE FIRE DANGER DAYS (SEV: FFDI GREATER THAN 50 DAYS PER YEAR) AND CUMULATIVE FFDI (Σ FFDI; NO UNITS) FOR THE 1995 BASELINE AND PROJECTIONS FOR 2030 AND 2090 UNDER RCP4.5 AND RCP8.5. VALUES WERE CALCULATED FROM THREE CLIMATE MODELS AND FOR SEVEN STATIONS.

STATION	VARIABLE	1995 BASELINE	2030 RCP4.5			2030 RCP8.5			2090 RCP4.5			2090 RCP8.5		
			CESM	GFDL	MIROC	CESM	GFDL	MIROC	CESM	GFDL	MIROC	CESM	GFDL	MIROC
Darwin (MNW)	T	32.2	33.1	33.7	33.1	33.4	33.7	33.2	34.5	34.2	34.1	36.3	36.2	35.2
	R	1702	1805	1525	1842	1764	1670	1964	1849	1798	1936	1898	1561	1967
	DF	6.4	6.4	6.8	6.3	6.4	6.5	6.3	6.4	6.5	6.4	6.4	6.8	6.3
	SEV	0.4	0.4	0.6	0.5	0.4	0.5	0.5	0.4	0.6	0.6	0.9	1.1	0.6
	Σ FFDI	3186	3048	3910	3220	3128	3623	3160	3202	3727	3365	3568	4407	3350
Broome (MNW)	T	32.2	33.1	33.6	33.1	33.4	33.6	33.1	34.4	34.2	34.1	36.2	36.2	35.1
	R	600	652	563	637	648	599	695	678	646	690	693	568	685
	DF	8.3	8.3	8.5	8.3	8.3	8.4	8.3	8.3	8.4	8.3	8.3	8.5	8.3
	SEV	1.5	1.5	2.4	2.0	1.7	2.1	2.0	2.2	2.4	2.6	4.2	5.8	3.0
	Σ FFDI	4352	4220	5107	4422	4323	4843	4364	4443	4927	4594	4915	5704	4632
Townsville (MNW)	T	29.3	30.1	30.6	30.2	30.4	30.9	30.7	31.4	31.6	31.6	33.2	33.7	32.5
	R	1111	1122	926	1085	1155	907	1005	1141	1083	951	1178	788	1093
	DF	7.7	7.6	7.9	7.6	7.5	7.9	7.7	7.6	7.8	7.8	7.6	8.2	7.7
	SEV	0.2	0.2	0.3	0.2	0.2	0.3	0.3	0.3	0.3	0.3	0.4	0.4	0.3
	Σ FFDI	2704	2576	3299	2728	2609	3338	2999	2685	3194	3144	3022	4017	2920
Mt Isa (MNW)	T	32.1	32.9	33.5	33.0	33.2	33.7	33.6	34.2	34.4	34.4	36.0	36.5	35.3
	R	452	475	405	471	495	404	440	494	489	420	505	344	478
	DF	8.4	8.4	8.6	8.4	8.3	8.6	8.5	8.4	8.4	8.6	8.4	8.8	8.5
	SEV	12.9	12.5	18.9	16.7	14.0	19.0	20.2	16.9	16.3	22.1	25.5	31.6	22.2
	Σ FFDI	8118	7935	8917	8211	8035	8993	8633	8295	8730	8974	9055	10270	8833

TABLE 3: PROJECTED ANNUAL CHANGE IN SIMULATED MARINE CLIMATE VARIABLES FOR THE 2020–2039 (2030) AND 2080–2099 (2090) PERIODS RELATIVE TO 1986–2005 PERIOD FOR MONSOONAL NORTH, WHERE SEA ALLOWANCE IS THE MINIMUM DISTANCE REQUIRED TO RAISE AN ASSET TO MAINTAIN CURRENT FREQUENCY OF BREACHES UNDER PROJECTED SEA LEVEL RISE. FOR SEA LEVEL RISE, THE RANGE WITHIN THE BRACKETS REPRESENTS THE 5TH AND 95TH PERCENTILE CHANGE, AS PROJECTED BY THE CMIP5 MODEL ARCHIVE WHEREAS FOR SEA SURFACE TEMPERATURE, SALINITY, OCEAN PH AND ARAGONITE CONCENTRATION THE RANGE REPRESENTS THE 10TH TO 90TH PERCENTILE RANGE. ANNUAL RESULTS ARE GIVEN FOR RCP2.6, RCP4.5, AND RCP8.5. NOTE THAT THE RANGES OF SEA LEVEL RISE SHOULD BE CONSIDERED *LIKELY* (AT LEAST 66 % PROBABILITY), AND THAT IF A COLLAPSE IN THE MARINE BASED SECTORS OF THE ANTARCTIC ICE SHEET WERE INITIATED, THESE PROJECTIONS COULD BE SEVERAL TENTHS OF A METRE HIGHER BY LATE IN THE CENTURY.

VARIABLE	LOCATION (°E, °S)	2030, RCP2.6	2030, RCP4.5	2030, RCP8.5	2090, RCP2.6	2090, RCP4.5	2090, RCP8.5
Sea level rise (m)	Broome (122.22, 18.00)	0.12 (0.07-0.16)	0.12 (0.07-0.16)	0.12 (0.08-0.17)	0.38 (0.22-0.55)	0.46 (0.30-0.64)	0.61 (0.40-0.84)
	Wyndham (128.10, 15.45)	0.11 (0.07-0.16)	0.12 (0.07-0.16)	0.12 (0.08-0.17)	0.37 (0.21-0.54)	0.46 (0.29-0.63)	0.60 (0.40-0.83)
	Darwin (130.85, 12.47)	0.12 (0.07-0.16)	0.12 (0.08-0.16)	0.13 (0.08-0.17)	0.38 (0.22-0.55)	0.47 (0.30-0.65)	0.62 (0.41-0.85)
	Groote Eylandt (136.42, 13.86)	0.10 (0.06-0.15)	0.11 (0.07-0.15)	0.11 (0.07-0.16)	0.35 (0.19-0.51)	0.44 (0.28-0.62)	0.59 (0.38-0.81)
	Karumba (140.83, -17.5)	0.11 (0.06-0.15)	0.11 (0.07-0.15)	0.11 (0.07-0.16)	0.35 (0.19-0.51)	0.44 (0.28-0.61)	0.59 (0.38-0.81)
Sea allowance (m)	Broome (122.22, 18.00)	0.12	0.12	0.13	0.42	0.51	0.68
	Wyndham (128.10, 15.45)	0.12	0.12	0.13	0.45	0.54	0.75
	Darwin (130.85, 12.47)	0.12	0.12	0.13	0.43	0.52	0.71
	Groote Eylandt (136.42, 13.86)	0.11	0.11	0.12	0.37	0.46	0.63
	Karumba (140.83, -17.5)	0.13	0.13	0.14	0.44	0.53	0.74
Sea surface temperature (°C)	Broome (122.22, -18.00)	0.7 (0.6 to 1.0)	0.7 (0.6 to 1.1)	0.9 (0.7 to 1.0)	0.8 (0.6 to 1.4)	1.4 (1.3 to 2.3)	3.1 (2.6 to 4.0)
	Wyndham (128.10, -15.45)	0.6 (0.5 to 1.0)	0.7 (0.5 to 1.1)	0.9 (0.7 to 1.1)	0.7 (0.5 to 1.6)	1.5 (1.2 to 2.4)	3.0 (2.6 to 4.1)
	Darwin (130.85E, -12.47)	0.6 (0.4 to 0.8)	0.7 (0.5 to 1.0)	0.8 (0.6 to 1.1)	0.6 (0.4 to 1.3)	1.5 (1.1 to 2.0)	3.0 (2.5 to 3.9)
	Karumba (140.83, -17.5)	0.6 (0.4 to 0.9)	0.7 (0.6 to 1.1)	0.8 (0.6 to 1.1)	0.6 (0.4 to 1.5)	1.4 (1.1 to 2.3)	2.9 (2.4 to 3.9)
	Townsville (146.83, -19.25)	0.6 (0.4 to 0.8)	0.7 (0.4 to 0.9)	0.8 (0.5 to 1.0)	0.6 (0.3 to 1.2)	1.3 (1.0 to 1.8)	2.6 (2.2 to 3.4)
Sea surface salinity	Broome (122.22, -18.00)	-0.03 (-0.11 to 0.44)	-0.07 (-0.29 to 0.55)	0.02 (-0.22 to 0.26)	0.04 (-0.17 to 0.47)	-0.10 (-0.29 to 0.44)	-0.04 (-0.92 to 0.80)
	Wyndham (128.10, -15.45)	-0.05 (-0.18 to 0.34)	-0.06 (-0.43 to 0.39)	-0.04 (-0.29 to 0.26)	0.13 (-0.28 to 0.66)	-0.21 (-0.69 to 0.54)	-0.36 (-2.10 to 1.36)
	Darwin (130.85, -12.47)	-0.01 (-0.20 to 0.28)	-0.08 (-0.29 to 0.11)	-0.08 (-0.17 to 0.15)	-0.12 (-0.32 to 0.41)	-0.27 (-0.81 to 0.20)	-0.49 (-1.68 to 0.55)
	Karumba (140.83, -17.5)	0.25 (-0.19 to 0.62)	0.09 (-0.24 to 0.74)	0.17 (-0.09 to 0.57)	0.24 (-0.17 to 1.16)	-0.12 (-1.61 to 1.56)	-0.20 (-3.16 to 2.34)

VARIABLE	LOCATION (°E, °S)	2030, RCP2.6	2030, RCP4.5	2030, RCP8.5	2090, RCP2.6	2090, RCP4.5	2090, RCP8.5
Ocean pH	Townsville (146.83, -19.25)	-0.06 (-0.14 to 0.14)	-0.09 (-0.34 to 0.04)	-0.03 (-0.11 to 0.10)	-0.15 (-0.29 to 0.21)	-0.16 (-0.62 to 0.28)	-0.20 (-0.97 to 0.35)
	Broome (122.22, -18.00)	-0.06 (-0.06 to -0.06)	-0.07 (-0.07 to -0.06)	-0.07 (-0.08 to -0.07)	-0.06 (-0.07 to -0.06)	-0.14 (-0.15 to -0.14)	-0.30 (-0.31 to -0.28)
	Wyndham (128.10, -15.45)	-0.06 (-0.06 to -0.06)	-0.06 (-0.07 to -0.06)	-0.07 (-0.08 to -0.07)	-0.06 (-0.07 to -0.06)	-0.14 (-0.14 to -0.14)	-0.30 (-0.31 to -0.29)
	Darwin (130.85E, -12.47)	-0.06 (-0.06 to -0.06)	-0.06 (-0.07 to -0.06)	-0.07 (-0.08 to -0.07)	-0.06 (-0.06 to -0.06)	-0.14 (-0.14 to -0.14)	-0.30 (-0.31 to -0.29)
	Karumba (140.83, -17.5)	-0.06 (-0.06 to -0.06)	-0.06 (-0.07 to -0.06)	-0.07 (-0.07 to -0.07)	-0.06 (-0.07 to -0.05)	-0.14 (-0.14 to -0.13)	-0.30 (-0.32 to -0.29)
	Townsville (146.83, -19.25)	-0.06 (-0.06 to -0.06)	-0.07 (-0.07 to -0.06)	-0.08 (-0.08 to -0.07)	-0.06 (-0.07 to -0.06)	-0.14 (-0.15 to -0.14)	-0.32 (-0.32 to -0.31)
Aragonite saturation	Broome (122.22, -18.00)	-0.30 (-0.34 to -0.20)	-0.31 (-0.35 to -0.19)	-0.35 (-0.45 to -0.27)	-0.31 (-0.32 to -0.26)	-0.68 (-0.76 to -0.64)	-1.35 (-1.50 to -1.24)
	Wyndham (128.10, -15.45)	-0.32 (-0.34 to -0.27)	-0.34 (-0.35 to -0.28)	-0.39 (-0.45 to -0.31)	-0.33 (-0.34 to -0.27)	-0.72 (-0.74 to -0.67)	-1.44 (-1.55 to -1.31)
	Darwin (130.85E, -12.47)	-0.31 (-0.34 to -0.25)	-0.34 (-0.36 to -0.27)	-0.40 (-0.45 to -0.30)	-0.32 (-0.35 to -0.29)	-0.72 (-0.74 to -0.66)	-1.45 (-1.55 to -1.29)
	Karumba (140.83, -17.5)	-0.31 (-0.38 to -0.28)	-0.33 (-0.37 to -0.22)	-0.42 (-0.43 to -0.19)	-0.30 (-0.36 to -0.15)	-0.75 (-0.86 to -0.56)	-1.54 (-1.64 to -1.42)
	Townsville (146.83, -19.25)	-0.34 (-0.36 to -0.29)	-0.36 (-0.40 to -0.35)	-0.41 (-0.46 to -0.38)	-0.35 (-0.38 to -0.30)	-0.76 (-0.79 to -0.73)	-1.53 (-1.62 to -1.47)

For sea level rise and sea allowance, the future averaging periods are 2020–2040 and 2080–2100. In the report, these are referred to as 2030 and 2090 respectively.



ABBREVIATIONS

ACORN-SAT	Australian Climate Observations Reference Network – Surface Air Temperature
AWAP	Australian Water Availability Project
BOM	Bureau of Meteorology
CCAM	Conformal Cubic Atmospheric Model
CCIA	Climate Change in Australia
CMIP5	Coupled Model Intercomparison Project (Phase 5)
CSIRO	Commonwealth Scientific and Industrial Research Organisation
ENSO	El Niño Southern Oscillation
FFDI	Forest Fire Danger Index
GCMs	General Circulation Models or Global Climate Models
IOCI	Indian Ocean Climate Initiative
IOD	Indian Ocean Dipole
IPCC	Intergovernmental Panel on Climate Change
MJO	Madden Julian Oscillation
MN	Monsoonal North
MNE	Monsoonal North sub-cluster East
MNW	Monsoonal North sub-cluster West
NRM	Natural Resource Management
RCP	Representative Concentration Pathway
SAM	Southern Annular Mode
SDM	Statistical Downscaling Model
SPI	Standardised Precipitation Index
SRES	Special Report on Emissions Scenarios
SST	Sea Surface Temperature
STR	Sub-tropical ridge

NRM GLOSSARY OF TERMS

Adaptation	<p>The process of adjustment to actual or expected climate and its effects. Adaptation can be autonomous or planned.</p> <p><i>Incremental adaptation</i></p> <p>Adaptation actions where the central aim is to maintain the essence and integrity of a system or process at a given scale.</p> <p><i>Transformational adaptation</i></p> <p>Adaptation that changes the fundamental attributes of a system in response to climate and its effects.</p>
Aerosol	A suspension of very small solid or liquid particles in the air, residing in the atmosphere for at least several hours.
Aragonite saturation state	The saturation state of seawater with respect to aragonite (Ω) is the product of the concentrations of dissolved calcium and carbonate ions in seawater divided by their product at equilibrium: $([Ca^{2+}] \times [CO_3^{2-}]) / [CaCO_3] = \Omega$
Atmosphere	The gaseous envelope surrounding the Earth. The dry atmosphere consists almost entirely of nitrogen and oxygen, together with a number of trace gases (e.g. argon, helium) and greenhouse gases (e.g. carbon dioxide, methane, nitrous oxide). The atmosphere also contains aerosols and clouds.
Carbon dioxide	A naturally occurring gas, also a by-product of burning fossil fuels from fossil carbon deposits, such as oil, gas and coal, of burning biomass, of land use changes and of industrial processes (e.g. cement production). It is the principle anthropogenic greenhouse gas that affects the Earth's radiative balance.
Climate	The average weather experienced at a site or region over a period of many years, ranging from months to many thousands of years. The relevant measured quantities are most often surface variables such as temperature, rainfall and wind.
Climate change	A change in the state of the climate that can be identified (e.g. by statistical tests) by changes in the mean and/or variability of its properties, and that persists for an extended period of time, typically decades or longer.
Climate feedback	An interaction in which a perturbation in one climate quantity causes a change in a second, and that change ultimately leads to an additional (positive or negative) change in the first.
Climate projection	A climate projection is the simulated response of the climate system to a scenario of future emission or concentration of greenhouse gases and aerosols, generally derived using climate models. Climate projections are distinguished from climate predictions by their dependence on the emission/concentration/radiative forcing scenario used, which in turn is based on assumptions concerning, for example, future socioeconomic and technological developments that may or may not be realised.
Climate scenario	A plausible and often simplified representation of the future climate, based on an internally consistent set of climatological relationships that has been constructed for explicit use in investigating the potential consequences of anthropogenic climate change, often serving as input to impact models.
Climate sensitivity	The effective climate sensitivity (units; °C) is an estimate of the global mean surface temperature response to doubled carbon dioxide concentration that is evaluated from model output or observations for evolving non-equilibrium conditions.
Climate variability	Climate variability refers to variations in the mean state and other statistics (such as standard deviations, the occurrence of extremes, etc.) of the climate on all spatial and temporal scales beyond that of individual weather events. Variability may be due to natural internal processes within the climate system (internal variability), or to variations in natural or anthropogenic external forcing (external variability).
Cloud condensation nuclei	Airborne particles that serve as an initial site for the condensation of liquid water, which can lead to the formation of cloud droplets. A subset of aerosols that are of a particular size.

CMIP3 and CMIP5	Phases three and five of the Coupled Model Intercomparison Project (CMIP3 and CMIP5), which coordinated and archived climate model simulations based on shared model inputs by modelling groups from around the world. The CMIP3 multi-model dataset includes projections using SRES emission scenarios. The CMIP5 dataset includes projections using the Representative Concentration Pathways (RCPs).
Confidence	The validity of a finding based on the type, amount, quality, and consistency of evidence (<i>e.g.</i> mechanistic understanding, theory, data, models, expert judgment) and on the degree of agreement.
Decadal variability	Fluctuations, or ups-and-downs of a climate feature or variable at the scale of approximately a decade (typically taken as longer than a few years such as ENSO, but shorter than the 20–30 years of the IPO).
Detection and attribution	Detection of change is defined as the process of demonstrating that climate or a system affected by climate has changed in some defined statistical sense, without providing a reason for that change. An identified change is detected in observations if its likelihood of occurrence by chance due to internal variability alone is determined to be small, for example, less than 10 per cent. Attribution is defined as the process of evaluating the relative contributions of multiple causal factors to a change or event with an assignment of statistical confidence.
Downscaling	Downscaling is a method that derives local to regional-scale information from larger-scale models or data analyses. Different methods exist <i>e.g.</i> dynamical, statistical and empirical downscaling.
El Niño Southern Oscillation (ENSO)	A fluctuation in global scale tropical and subtropical surface pressure, wind, sea surface temperature, and rainfall, and an exchange of air between the south-east Pacific subtropical high and the Indonesian equatorial low. Often measured by the surface pressure anomaly difference between Tahiti and Darwin or the sea surface temperatures in the central and eastern equatorial Pacific. There are three phases: neutral, El Niño and La Niña. During an El Niño event the prevailing trade winds weaken, reducing upwelling and altering ocean currents such that the eastern tropical surface temperatures warm, further weakening the trade winds. The opposite occurs during a La Niña event.
Emissions scenario	A plausible representation of the future development of emissions of substances that are potentially radiatively active (<i>e.g.</i> greenhouse gases, aerosols) based on a coherent and internally consistent set of assumptions about driving forces (such as demographic and socioeconomic development, technological change) and their key relationships.
Extreme weather	An extreme weather event is an event that is rare at a particular place and time of year. Definitions of rare vary, but an extreme weather event would normally be as rare as or rarer than the 10th or 90th percentile of a probability density function estimated from observations.
Fire weather	Weather conditions conducive to triggering and sustaining wild fires, usually based on a set of indicators and combinations of indicators including temperature, soil moisture, humidity, and wind. Fire weather does not include the presence or absence of fuel load.
Global Climate Model or General Circulation Model (GCM)	A numerical representation of the climate system that is based on the physical, chemical and biological properties of its components, their interactions and feedback processes. The climate system can be represented by models of varying complexity and differ in such aspects as the spatial resolution (size of grid-cells), the extent to which physical, chemical, or biological processes are explicitly represented, or the level at which empirical parameterisations are involved.
Greenhouse gas	Greenhouse gases are those gaseous constituents of the atmosphere, both natural and anthropogenic, that absorb and emit radiation at specific wavelengths within the spectrum of terrestrial radiation emitted by the Earth's surface, the atmosphere itself, and by clouds. Water vapour (H ₂ O), carbon dioxide (CO ₂), nitrous oxide (N ₂ O), methane (CH ₄) and ozone (O ₃) are the primary greenhouse gases in the Earth's atmosphere.

Hadley Cell/Circulation	A direct, thermally driven circulation in the atmosphere consisting of poleward flow in the upper troposphere, descending air into the subtropical high-pressure cells, return flow as part of the trade winds near the surface, and with rising air near the equator in the so-called Inter-Tropical Convergence zone.
Indian Ocean Dipole (IOD)	Large-scale mode of interannual variability of sea surface temperature in the Indian Ocean. This pattern manifests through a zonal gradient of tropical sea surface temperature, which in its positive phase in September to November shows cooling off Sumatra and warming off Somalia in the west, combined with anomalous easterlies along the equator.
Inter-decadal Pacific Oscillation	A fluctuation in the sea surface temperature (SST) and mean sea level pressure (MSLP) of both the north and south Pacific Ocean with a cycle of 15–30 years. Unlike ENSO, the IPO may not be a single physical ‘mode’ of variability, but be the result of a few processes with different origins. The IPO interacts with the ENSO to affect the climate variability over Australia. A related phenomena, the Pacific Decadal Oscillation (PDO), is also an oscillation of SST that primarily affects the northern Pacific.
Jet stream	A narrow and fast-moving westerly air current that circles the globe near the top of the troposphere. The jet streams are related to the global Hadley circulation. In the southern hemisphere the two main jet streams are the polar jet that circles Antarctica at around 60 °S and 7–12 km above sea level, and the subtropical jet that passes through the mid-latitudes at around 30 °S and 10–16 km above sea level.
Madden Julian Oscillation (MJO)	The largest single component of tropical atmospheric intra-seasonal variability (periods from 30 to 90 days). The MJO propagates eastwards at around 5 m s ⁻¹ in the form of a large-scale coupling between atmospheric circulation and deep convection. As it progresses, it is associated with large regions of both enhanced and suppressed rainfall, mainly over the Indian and western Pacific Oceans.
Monsoon	A monsoon is a tropical and subtropical seasonal reversal in both the surface winds and associated rainfall, caused by differential heating between a continental-scale land mass and the adjacent ocean. Monsoon rains occur mainly over land in summer.
Percentile	A percentile is a value on a scale of one hundred that indicates the percentage of the data set values that is equal to, or below it. The percentile is often used to estimate the extremes of a distribution. For example, the 90th (or 10th) percentile may be used to refer to the threshold for the upper (or lower) extremes.
Radiative forcing	Radiative forcing is the change in the net, downward minus upward, radiative flux (expressed in W m ⁻²) at the tropopause or top of atmosphere due to a change in an external driver of climate change, such as a change in the concentration of carbon dioxide or the output of the Sun.
Representative Concentration Pathways (RCPs)	Representative Concentration Pathways follow a set of greenhouse gas, air pollution (<i>e.g.</i> aerosols) and land-use scenarios that are consistent with certain socio-economic assumptions of how the future may evolve over time. The well mixed concentrations of greenhouse gases and aerosols in the atmosphere are affected by emissions as well as absorption through land and ocean sinks. There are four Representative Concentration Pathways (RCPs) that represent the range of plausible futures from the published literature.
Return period	An estimate of the average time interval between occurrences of an event (<i>e.g.</i> flood or extreme rainfall) of a defined size or intensity.
Risk	The potential for consequences where something of value is at stake and where the outcome is uncertain. Risk is often represented as a probability of occurrence of hazardous events or trends multiplied by the consequences if these events occur.
Risk assessment	The qualitative and/or quantitative scientific estimation of risks.
Risk management	The plans, actions, or policies implemented to reduce the likelihood and/or consequences of risks or to respond to consequences.

Sub-tropical ridge (STR)	The sub-tropical ridge runs across a belt of high pressure that encircles the globe in the middle latitudes. It is part of the global circulation of the atmosphere. The position of the sub-tropical ridge plays an important part in the way the weather in Australia varies from season to season.
Southern Annular Mode (SAM)	The leading mode of variability of Southern Hemisphere geopotential height, which is associated with shifts in the latitude of the mid-latitude jet.
SAM index	The SAM Index, otherwise known as the Antarctic Oscillation Index (AOI) is a measure of the strength of SAM. The index is based on mean sea level pressure (MSLP) around the whole hemisphere at 40 °S compared to 65 °S. A positive index means a positive or high phase of the SAM, while a negative index means a negative or low SAM. This index shows a relationship to rainfall variability in some parts of Australia in some seasons.
SRES scenarios	SRES scenarios are emissions scenarios developed by Nakićenović and Swart (2000) and used, among others, as a basis for some of the climate projections shown in Chapters 9 to 11 of IPCC (2001) and Chapters 10 and 11 of IPCC (2007).
Uncertainty	A state of incomplete knowledge that can result from a lack of information or from disagreement about what is known or even knowable. It may have many types of sources, from imprecision in the data to ambiguously defined concepts or terminology, or uncertain projections of human behaviour. Uncertainty can therefore be represented by quantitative measures (e.g. a probability density function) or by qualitative statements (e.g. reflecting the judgment of a team of experts).
Walker Circulation	An east-west circulation of the atmosphere above the tropical Pacific, with air rising above warmer ocean regions (normally in the west), and descending over the cooler ocean areas (normally in the east). Its strength fluctuates with that of the Southern Oscillation.

GLOSSARY REFERENCES

- AUSTRALIAN BUREAU OF METEOROLOGY - <http://www.bom.gov.au/watl/about-weather-and-climate/australian-climate-influences.shtml> (cited August 2014)
- INTERGOVERNMENTAL PANEL ON CLIMATE CHANGE - <http://www.ipcc.ch/pdf/glossary/ar4-wg1.pdf> (cited August 2014)
- INTERGOVERNMENTAL PANEL ON CLIMATE CHANGE - http://ipcc-wg2.gov/AR5/images/uploads/WGIIAR5-Glossary_FGD.pdf (cited August 2014)
- MUCCI, A. 1983. The solubility of calcite and aragonite in seawater at various salinities, temperatures, and one atmosphere total pressure *American Journal of Science*, 283 (7), 780-799.
- NAKIĆENOVIĆ, N. & SWART, R. (eds.) 2000. *Special Report on Emissions Scenarios. A Special Report of Working Group III of the Intergovernmental Panel on Climate Change*, Cambridge, United Kingdom and New York, NY, USA: Cambridge University Press.
- STURMAN, A.P. & TAPPER, N.J. 2006. *The Weather and Climate of Australia and New Zealand*, 2nd ed., Melbourne, Oxford University Press.



PHOTO: MICHAEL DOUGLAS

-20° -10° 0° 10° 20° 30° 40° 50°

